Title
STRUCTURE AND BONDING IN ORGANO-LANTHANIDE AND -ACTINIDE COMPOUNDS

Author
Eigenbrot, C.W.

Publication Date
1981-02-01

LBL-12401

Lawrence Berkeley Laboratory
UNIVERSITY OF CALIFORNIA

Materials & Molecular Research Division

STRUCTURE AND BONDING IN ORGANO-LANTHANIDE AND -ACTINIDE COMPOUNDS

Charles Weaver Eigenbrot, Jr.
(Ph.D. thesis)

February 1981

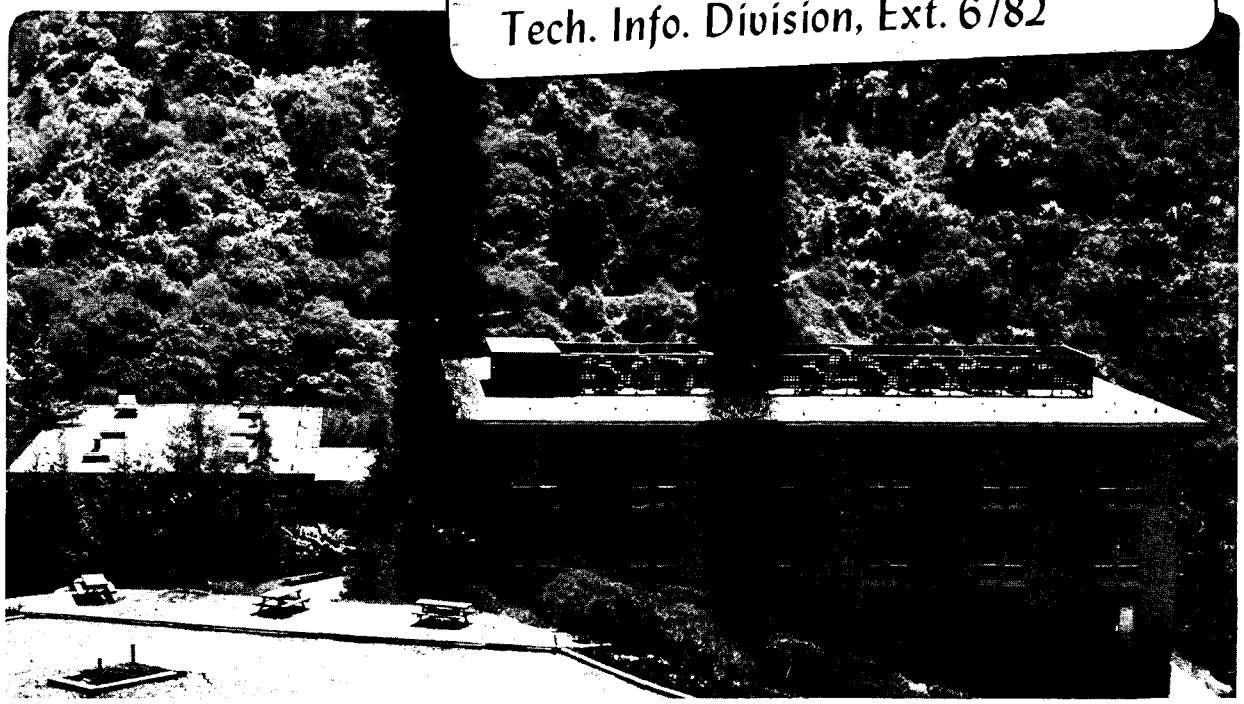

Prepared for the U.S. Department of Energy under Contract W-7405-ENG-48

LBL-12401

DISCLAIMER

LBL-12401

STRUCTURE AND BONDING IN ORGANO-LANTHANIDE

AND

-ACTINIDE COMPOUNDS

Charles Weaver Eigenbrot, Jr.
Ph.D. thesis

February 1981

Materials and Molecular Research Division
Lawrence Berkeley Laboratory
University of California
Berkeley, CA 94720

This work was supported by the Director, Office of Energy Research, Office of Basic Energy Sciences, Chemical Sciences Division of the U.S. Department of Energy under Contract Number W-7405-ENG-48.

Structure and Bonding in Organo-Lanthanide and -Actinide Compounds

Charles Weaver Eigenbrot, Jr.

ABSTRACT

The reactions of $U(C_5H_5)_3(THF)$ and $U(C_5H_4CH_3)_3(THF)$ with pyrazine lead to the formation of dimeric, μ-bridged species of U^{3+} of formulae $[U(C_5H_5)_3]_2(C_4H_4N_2)$ and $[U(C_5H_4CH_3)_3]_2(C_4H_4N_2)$. The dimeric formulation of the two compounds is indicated by the X-ray powder pattern of $[U(C_5H_5)_3]_2(C_4H_4N_2)$, the mass spectra of both compounds, and the pmr spectrum of $[U(C_5H_4CH_3)_3]_2(C_4H_4N_2)$. Preliminary results indicate unusual magnetic behavior at low temperature.

New compounds have been prepared and characterized by their infra-red, visible-near IR, pmr, and mass spectra; and by single crystal X-ray diffraction.

The compound $U(C_5H_5)_3(C_3H_3N_2)$ has been prepared by the reaction between $U(C_5H_5)_3Cl$ and $Na(C_3H_3N_2)$ in THF. The molecular structure consists of discrete $U(C_5H_5)_3(C_3H_3N_2)$ molecules in which the U^{4+} ion is coordinated by three η^5-cyclopentadienide rings in a nearly trigonal array. Two additional coordination sites are occupied by the two nitrogen atoms of the pyrazolate anion, for a total coordination number of 11. This is the first example of an endo-bidentate

η^2 coordination for the pyrazolate anion. Red-brown crystals from toluene conform to space group $P2_1/a$, with a=14.295(1), b=8.383(1), c=14.282(1)Å, β=112.80(1) degrees, and 4 molecules per unit cell. The model refined to final weighted and unweighted R factors both of 3.14%. The U-N bond distances are 2.36(1)Å and 2.40(1)Å. The average U-C bond distance of 2.76Å is consistent with that predicted for an 11-coordinate U^{4+} cyclopentadienide complex.

The reactions between $U(C_5Me_5)_2Cl_2$ and $C_3H_4N_2$ and $Na(C_3H_3N_2)$ in THF have led to the isolation of three new compounds of formulae $U(C_5Me_5)_2Cl_2(C_3H_4N_2)$, $U(C_5Me_5)_2Cl(C_3H_3N_2)$, and $U(C_5Me_5)_2(C_3H_3N_2)_2$.

The crystal structure of $U(C_5Me_5)_2Cl_2(C_3H_4N_2)$ consists of discrete molecular units at positions of mm symmetry. The U^{4+} ion is coordinated by two η^5-pentamethylcyclopentadienide rings, two chloride ions, and one nitrogen from the neutral pyrazole ring, for a total coordination number of 9. Red-brown crystals from hexane conform to space group Cmcm with a=13.697(4), b=11.496(2), c=15.555(2)Å, and 4 molecules per unit cell. The model refined to final weighted and unweighted R factors of 3.48% and 2.45% respectively. The average U-C bond distance is 2.74(2)Å, the U-N bond distance is 2.607(8)Å, and the U-Cl bond distance is 2.696(2)Å.

The crystal structure of $U(C_5Me_5)_2Cl(C_3H_3N_2)$ consists of discrete U^{4+} ions coordinated by two η^5-pentamethylcyclo-

pentadienide rings, one chloride ion, and both nitrogen atoms from the pyrazolate anion, for a total coordination number of 9. Red-brown crystals from hexane conform to space group $P2_1/n$ with a=8.737(1), b=18.068(1), c=15.229(1)Å, β=92.38(1) degrees, and 4 molecules per unit cell. The model refined to final weighted and unweighted R factors of 4.50% and 3.27% respectively. The average U-C bond distance is 2.73(3)Å, the U-N bond distances are 2.351(5)Å and 2.349(5)Å, and the U-Cl bond distance is 2.611(2)Å.

The crystal structure of $U(C_5Me_5)_2(C_3H_3N_2)_2$ consists of discrete U^{4+} ions coordinated by two η^5-pentamethylcyclopentadienide rings and four nitrogen atoms from the two pyrazolate anions, for a total coordination number of 10. Red-brown crystals from hexane conform to space group C2/c with a=33.326(2), b=10.450(2), c=16.646(1)Å, β=117.09(1) degrees, and 8 molecules per unit cell. The model refined to final weighted and unweighted R factors of 3.31% and 2.43% respectively. The U-C bond distances average 2.75(2)Å, and the U-N bond distances are 2.403(4)Å, 2.360(5)Å, 2.363(5)Å, and 2.405(5)Å.

The crystal and molecular structure of the known complex $[Nd(N(C_2H_5NH_2)_3)_2(CH_3CN)](ClO_4)_3$ has been determined by single crystal X-ray diffraction. Clear pink crystals from a mixture of acetonitrile and benzene conform to space group Cc, with a=15.044(1), b=17.729(1), c=11.088(1)Å, β=95.079(5)

degrees, and 4 formula weights per unit cell. The structure of the molecular cation consists of a Nd^{3+} ion coordinated by two tetradentate $N(C_2H_5NH_2)_3$ ligands and the nitrogen atom from an acetonitrile molecule for a total coordination number of 9. The model refined to final weighted and unweighted R factors of 3.19% and 2.94% respectively. The coordination polyhedron is a tri-capped trigonal prism.

Kenneth N Raymond

For Knox Burger.
Ten days older than I am,
he has been a very good father to me.

Acknowledgement

I wish to thank all the people who helped me in completing this work. Most prominent among them are Andy, Hoy, Sherry, Loc, Al, Cathy, and Lirmar from the shops and storerooms in the College. As Professor Raymond's secretary, June Smith was in charge of everything. Fred Hollander was of invaluable assistance with the crystallography, as was Geoff Wong with the nmr spectra. Out softball team, The Ducks on the Pond, brought me more joy than has even the completion of this dissertation. As for all the others, too numerous to mention, I've got $5 that says if you're reading this before December 1981, then you're among those I wish to thank. And, of course, thanks to Ken Raymond. He paid the bills.

This work was supported by the Director, Office of Energy Research, Office of Basic Energy Sciences, Chemical Sciences Division of the U. S. Department of Energy under Contract Number W-7405-ENG-48.

TABLE OF CONTENTS

Introduction

Organometallic chemistry, while over 100 years old, has experienced fantastic growth since the 1950's. Today it is a large, diverse area of ongoing basic research and industrial application. As the number and types of such compounds has increased, theories have been developed that, by and large, satisfactorily explain the role d-electrons play in the bonding of the predominant members of this group of compounds, those formed by the d-transition metals[1,2].

During this period of expansion, the first organometallic complexes of the f-transition elements were characterized. This subset of organometallic chemistry was largely ignored for its first 10 years or so- in part due to the fact that the addition of f-electrons to the electronic configurations made their interrelationships much more complex, and prevented the satisfying analyses performed on the d-metal organometallic compounds. To many, the predominant ionicity of the earliest compounds, the tris(cyclopentadienide)lanthanides[3], made them less interesting than d-metal metallocenes, where covalent interactions are common. Meanwhile the actinides, because they also possess f-electrons, were probably dismissed in the same breath as the "boring" lanthanides. And, of course, many of the actinides were unknown during this period.(Indeed, all the chemistry of the later (synthetic) actinides has been and probably will continue to be hampered by the time and

expense required in handling them safely.)

However, a resurgence of interest in the organometallic chemistry of the lanthanides and actinides was occasioned by Streitwieser and Muller-Westerhoff's synthesis of uranocene[4] in 1968. The subsequent crystal structure[5] offered initial confirmation of the elegance of Streitwieser's hypothesis -- that the symmetry of the f-orbitals was appropriate for covalent bonding to the cyclooctatetraene dianion (COT) in much the same way that the d-orbitals of other metals bond to the cyclopentadienide (Cp) anion. Almost overnight chemists around the world set to the task of exploiting the apparent covalency of uranocene, and they have been working at it ever since.

During the last 12 or so years, the question of f-electron covalency has been one of intense interest. Some workers have been a little over-enthusiastic in concluding certain properties were the effects of covalency[6], apparently due to the lingering opinion that covalent interactions are philosophically and intellectually more satisfying than ionic ones. Other workers have collected data that leave little doubt that some covalency exists, principally in COT complexes of uranium. These studies include Green's[7] photoelectron spectra of uranocene and thoracene. The intensity variation of the observed peaks in going from He(I) irradiation to He(II) irradiation, and their interpretation based on the most plausible molecular

orbital scheme for the complexes, very strongly suggests that there is mixing of ligand and metal (f) orbitals. This is covalency by any definition. In addition, the nmr[8] and the low temperature magnetic susceptibility[9] of uranocene have been interpreted in terms of some degree of covalency. And, while there is generally less evidence of covalency in Cp complexes, the Mossbauer spectrum of $NpCp_4$[9] indicates the net charge on the metal ion is less than +4.0, consistent with some net donation of ligand electrons to the 4+ metal center.

Because intelligent interpretation of the data obtained in these various physical studies requires a detailed knowledge of the crystal and/or molecular symmetry of the compound in question, X-ray crystal structures have played a central role in bonding studies. In addition, the structures themselves can serve as a useful, albeit insensitive, probe of bonding , once a careful and limited structural definition of covalent/ionic bonding has been drawn.

A Structural Definition of Covalent/Ionic Bonding

For the question of the presence or absence of any property to have meaning, the property itself must be well defined. While there are certainly many definitions of covalent/ionic bonding, and various physical techniques lend themselves to each definition, the following two criteria provide a phenomenological definition based only on structure:

[1] The geometries of ionic compounds tend to be irregular and depend on the steric bulk, number, and charge of the ligands. The coordination number observed is the result of a balance between ionic attractive forces and non-bonded repulsions. This is in marked contrast to the regular, directional bonds which typify covalent compounds.

[2] Bond lengths for a series of structurally related compounds will follow systematically from their "ion size" and coordination number--that is, ionic radii can be used to predict bond lengths. In contrast, the structure of predominantly covalent compounds show pronounced departures from such predictions.

In simple ionic salts it is found that the difference between the cation-anion interatomic distances , R , is constant for a given ion. For example, R equals 2.81 and 2.98 for NaCl and NaBr respectively, and their difference is .17 Å. Likewise for the analogous potassium salts the difference is .15 Å, and for the rubidium salts the difference is .15 Å. Then one can say that the radius of bromide ion is about .15 Å greater than that of chloride ion.

Following Pauling's approach[10] one can write

$$R = r_+ + r_- \qquad (1)$$

where r_+ and r_- are radii of the cation and anion,

respectively, and

$$\frac{r_+}{r_-} = \frac{Z_-^*}{Z_+^*} \tag{2}$$

where Z_+^* and Z_-^* are the effective nuclear charges for the valence electrons of the cation and anion respectively. This gives the so-called "univalent radii", which tacitly assumes a ± 1 charge on each ion. The decrease in effective size that accompanies higher charge for a salt $M^{+i}X_{\frac{i}{j}}^{-j}$ is given by

$$R_{ij} = R_{11} \left|\frac{1}{ij}\right|^{\frac{1}{n-1}} \tag{3}$$

where n is the Born exponent[10] (12 for most of the cations we will consider). In a similar fashion, the increase in effective ion size with coordination number is given by

$$\left|\frac{R_{II}}{R_I}\right| = \left|\frac{CN_{II}}{CN_I}\right|^{\frac{1}{n-1}} \tag{4}$$

where R_{II} and R_I are the interionic distances for coordination II and I respectively.

The most useful and complete tabulation of ionic radii today is that of Shannon[11] who has produced a self-consistent set of ionic radii from over 900 structure reports. These radii will be used in the following discussion, with adjustments applied for changes in coordination number as described in equation (4), when appropriate. The definition of coordination number used here is: the number of electron pairs involved in ligand-to-metal coordination.

Structural Types and Coordination Numbers of Organoactinides and -Lanthanides

MCp_3X and MCp_3

There is a large class of lanthanide and actinide compounds of the general formula MCp_3X,[12] where X is a donor ligand, anion, or η^1 bridging cyclopentadienyl ring. The structure of one such compound, tris(benzylcyclopentadienyl)chlorouranium(IV)[13], provided the first accurate determination of a cyclopentadienyl actinide complex. The cyclopentadienyl rings are pentahapto bound and the chloride anion is coordinated along the trigonal axis of the formally ten coordinate complex. The geometry is that of a trigonally compressed tetrahedron such that the Cl-U-(Cp centroid) bond angle is 100° (Fig.1). This geometry remains remains essentially invariant throughout the class.

An introduction to compounds of the formula MCp_3 is provided by another member of this class. In tris(methyl-

cyclopentadienyl)neodymium(III), $Nd(MeCp)_3$,[14] the metal ion (1.17 Å) is ten-coordinate through formation of a tetramer in which all three Cp rings form η^5 bonds to Nd and one of the rings also bridges to form an η^1 ring bridge to the adjacent metal ion. The smaller (1.13 Å) Sm^{3+} ion in Sm(indenyl)$_3$[15] is 9-coordinate with three η^5 rings providing all of the coordination. The even smaller (.87 Å) Sc^{3+} ion in $ScCp_3$[16] is eight-coordinate in a polymeric structure formed by 2 η^5 Cp rings and a third ring which forms an η^1,η^1 bridge. All of the Cp rings in these three compounds show undistorted pentagonal symmetry with no evidence of double-bond localization. Thus there is a monotonic decrease in coordination number with decreasing ionic radius of the metal ion. It is clear from these examples that the principal determinant of coordination numbers and geometries is the metal size, indicating that an ionic mode of bonding best describes these MCp_3 compounds.

In contrast, the structure of tris(cyclopentadienyl)-indium(III)[17] (Fig. 2) is composed of indium atoms which achieve a relatively regular four-coordinate tetrahedral environment of σ bonds by bonding to 2 η^1 Cp rings with the third ring forming a η^1,η^1 bridge. The C-C bond lengths within the Cp rings show localized double bond character of the type

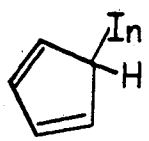

In short, $InCp_3$ provides a classic example of the structural

effects of covalent bonding.

MCp_4

For the series MCp_4 (Fig. 3) there is again a pronounced change in coordination number and structure as the metal ion size changes. In $TiCp_4$[18] the coordination number of the Ti^{4+} ion (.74 Å) is eight, from two η^5 rings and two η^1 rings. For the larger Zr^{4+} ion (.91 Å) in $ZrCp_4$[19] there are three η^5 rings and one η^1 ring to give a total coordination number of ten. In UCp_4[20] all four Cp rings are η^5 bound in a tetrahedral array to give a total coordination number of twelve around the U^{4+} ion (1.17 Å). Thus, these MCp_4 compounds again demonstrate that metal ion size plays the dominant role in determining the coordination number and geometry, indicating an ionic mode of bonding.

$M(COT)_2$

The compounds $Ti(C_8H_8)_2$ and $Ti_2(C_8H_8)_3$ exhibit similar structures,[21,22] involving one symmetrical η^8-coordinated COT ring and one non-planar ring of lower hapticity per titanium. In the analogous zirconium complex,[23] the metal's larger size is manifested in an additional coordination site being occupied by a THF molecule in the otherwise similar structure.

Cyclooctatetraene complexes of larger metal ions such as cerium,[24] thorium[5], and uranium[5] all exhibit two symmetr-

ical η^8-coordinated COT rings. The thorium and uranium compounds exhibit almost exact D_{8h} molecular symmetry while the cerium compound is very close to D_{8d}. Structural parameters of these compounds are collected in Table 1.

The failure of the early metals to accept a uranocene-type structure can be explained in two ways. One way is to note that the lanthanide and actinide ions are substantially larger, thereby requiring more ligands to saturate their coordination sphere. Uranocene is formally ten-coordinate and coordination numbers of nine and ten are quite common for uranium complexes. The early metals cannot accommodate so large a coordination number and so one COT ring slips to the side--providing a total coordination number of seven or eight. This argument rests squarely on an ionic description of the bonding. Alternatively, one may note that two η^8-coordinated COT rings provide 20 π-electrons to the metal center-- in violation of the effective atomic number rule. While actinide and lanthanide complexes do not in general follow this rule, Group IVB organometallic complexes almost invariably have 16 or 18 valence electrons. Thus the second COT ring slips to one side to reduce the number of valence electrons. This argument views the bonding in the early metals as predominantly covalent while recognizing the lack of anything resembling the effective atomic number rule to apply in the case of the lanthanide or actinide analogues. This recognition is tantamount to viewing the bonding in the later metals as ionic.

The Covalent/Ionic Structural Criterion and 3d Metallocenes

Having seen the conclusions drawn by considering the general structural features (i.e. metal coordination number and ligand hapticity) of carbocyclic complexes of the actinides and lanthanides, we now turn to another structural criterion of the mode of bonding--the metal-to-carbon bond distance (R(M-C)). Table 2 contains structural data collected from X-ray and gas phase electron diffraction studies of first row metallocenes[25-36]. If these compounds involved ionic bonding, the metal-to-carbon distances could be predicted as the sum of the ionic radii of the metal ion and the Cp anion. Another way of saying this is that the difference between the metal-to-carbon distance and the ionic radius of the metal (the effective ionic radius of the Cp ligand) would be constant. But in the d-transition metal metallocenes, one cannot assign an effective ionic radius to the Cp anion. If we plot R(M-C) vs. the metal ion radius (Fig. 4) we see that this is not a smooth function.

The predominant covalency of these compounds can be illustrated in a graph of R(M-C) vs. electron imbalance as defined by Haaland[27] (Fig. 5). Haaland's definition is based on a molecular orbital treatment of the bonding in these compounds, considers the effects of electron occupancy of bonding and antibonding orbitals -- and results in a linear correlation of R(M-C) and predicted bond order.

Table 3 collects corresponding structural data for

lanthanide and actinide Cp complexes[37-53]. We can see that the effective ionic radius for the Cp ligand is essentially invariant in structures of 23 complexes, and is 1.64(4) Å. This consistency is illustrated in Figure 6, where the plot of R(M-C) vs. the metal ion radius is presented for the available lanthanide complexes . The relatively high correlation coefficient and near unit slope (equation (1) requires that the slope, $\frac{dR(M-C)}{dr_+}=1.$) shows that R(M-C) varies in direct proportion to metal ion size, a clear indication of ionic bonding.

Bond Lengths in Metal COT Complexes

Of all the lanthanide and actinide organometallic complexes, there is probably the most evidence of covalency in the COT complexes of the actinides (vide supra). For this reason, it is interesting to see how well the purely structural model described here applies to the systematics observed in the geometries of these compounds. Table 4 collects data from X-ray structures of COT complexes of 12 d, f, and s-block metals[54-60]. Subtraction of the metal ionic radii from R(M-C) yields an effective ionic radius for $COT^{=}$, which will be constant if the ionic model is applicable. Indeed, The $COT^{=}$ ionic radius is essentially invariant, averaging 1.56(4) Å. The graph of metal ionic radius vs. R(M-C) for these complexes appears in Figure 6. The slope and correlation coefficient indicate that, despite other evidence suggesting covalency, there is no structural evi-

dence for it.

Statement of Purpose

This analysis of structural data leads us to conclude that within the limited structural definition of covalent/ionic bonding, the bonding in organolanthanides and actinides is predominantly ionic. The usefulness of the analysis can be broadened by examination of new types of compounds; for instance, those with different ligands and/or new coordination numbers. It is possible that the structural definition can become less limited and allow for the consideration of compounds that are not so strictly members of a homologous series.

In addition, we know that other more sensitive techniques have detected some covalency. Among the more sensitive techniques that has not been fully exploited is the measurement of magnetic moments, especially at low temperatures. Such studies are most informative when applied to dimeric species where an opportunity exists for the spins of two paramagnetic metal ions to become coupled, which would result in a pronounced change in the magnetic moment. Few low temperature (below 77K) studies have been performed even on monomeric organolanthanides or actinides. One particularly thorough study has been made, however, on the compound of formula $(YbCp_3)_2(pyrazine)$[38]. The molecular unit of this compound is a dimer located about a crystallographic inversion center. Two ytterbium atoms, each with three

η^5-cyclopentadienide rings, are nearly linearly bridged by a pyrazine ring coordinated through its nitrogens (Fig.7). The magnetic susceptibility of the dinuclear complex exhibits simple Curie-Weiss behavior over the range 4 to 100 K, with $\mu_{eff}=3.48\mu_B$. This result is typical of ionic Yb(III) complexes, and the conclusion can be drawn that the method detects no covalency.

The lack of covalent effects in this study is less than surprising, considering the large amount of evidence indicating that the Ln^{3+} compounds are very ionic in nature. This is attributable to the small radial extension of the 4f orbitals, with the result that they contain what are, chemically, core electrons. However, for the early actinides (before increasing nuclear charge dampens the effect), speculation persists that the greater radial extension of 5f orbitals might be sufficient to allow some 5f participation in covalent bonding.

Thus, this work was undertaken to use the magnetism of appropriate dimeric species of the early actinides as a sensitive probe for covalent effects and to examine novel ligand systems in the light of structural criteria for the mode of bonding. The exclusive use of compounds of uranium in these studies is due to the relative ease with which they can be handled safely.

Table I. Crystal and Molecular Data for COT[a] Complexes

	$U(COT)_2$	$Th((COT)_2$	$[K(d)][Ce(COT)_2]$[b]
space group	$P2_1/n$	$P2_1/n$	Pnma
density, g/cm^3	2.29	2.22	1.56
molecules/cell	2	2	4
site symmetry	Ci	Ci	Cs
mean M-C bond, Å	2.647(4)	2.701(4)	2.742(8)
mean C-C bond, Å	1.392(7)	1.386(9)	1.388(28)
inter-ring dist, Å	3.847(10)	4.007(3)	4.151
reference	5	5	24

[a] COT = $(C_8H_8)^=$

[b] d = $(CH_3OCH_2CH_2)_2O$

Table II.

compound	R(M-C) Å	metal ion radius Å	Cp radius Å	ref
a. Gas-Phase Electron Diffraction Data				
VCp_2	2.280(5)	0.79	1.49	25
$CrCp_2$	2.169(4)	0.73	1.44	25
$MnCp_2$	2.383(3)	0.83	1.55	26
$Mn(MeCp)_2^a$	2.144(12)	0.67	1.47	27
$Mn(MeCp)_2^b$	2.433(8)	0.83	1.60	27
$FeCp_2$	2.064(3)	0.61	1.45	28
$CoCp_2$	2.119(3)	0.65	1.47	29-30
$NiCp_2$	2.196(4)	0.69	1.51	31
b. Single-Crystal X-ray Data				
VCp_2	2.24	0.79	1.45	32
$CrCp_2$	2.14	0.73	1.41	32
$MnCp_2$	2.41	0.83	1.58	33
$FeCp_2$	2.045(4)	0.61	1.44	34
$CoCp_2$	2.096(8)	0.65	1.45	35
$NiCp_2$	2.15	0.69	1.46	32
$[Fe(MeCp)_2]I_3^-$	2.05(2)	0.55	1.50	36

[a] low spin [b] high spin

Table III. Single-Crystal X-ray Diffraction Data

compound	R(M-C) Å	metal ion radius Å	Cp radius Å	ref
$ScCp_3$	2.49(2)	0.87	1.62	16
$Sm(indenyl)_3$	2.75(5)	1.13	1.62	15
$Nd(MeCp)_3$	2.79(5)	1.17	1.62	14
$PrCp_3CNC_6H_{11}$	2.77(2)	1.18	1.59	37
$(YbCp_3)_2(C_4H_4N_2)$	2.68(1)	1.04	1.64	38
$(ScCp_2Cl)_2$	2.46(2)	0.87	1.59	39
$[Yb(MeCp)_2Cl]_2$	2.585(8)	0.985	1.60	40
$(YbCp_2Me)_2$	2.613(13)	0.985	1.63	41
$GdCp_3(THF)$	2.72(6)	1.11	1.61	42
$Yb(Me_5C_5)_2(pyr)_2$	2.741	1.14	1.60	43
UCp_3Cl	2.74	1.06	1.68	44
UCp_3F	2.74	1.06	1.68	45
$U(benzylCp)_3Cl$	2.733(1)	1.06	1.67	13
$U(indenyl)_3Cl$	2.78	1.06	1.72	46
$UCp_3(C_2H)$	2.73(5)	1.06	1.67	47
$UCp_3(C_2\phi)$	2.68	1.06	1.62	48
$UCp_3(p\text{-xylyl})$	2.71(1)	1.06	1.65	49
$UCp_3(n\text{-butyl})$	2.73(1)	1.06	1.67	49
$UCp_3(2\text{-Me-allyl})$	2.74(1)	1.06	1.68	50
UCp_4	2.81(2)	1.17	1.64	20
$(ThCp_2C_5H_4)_2$	2.83	1.13	1.70	51
$UCp_3(NCS)(MeCN)$	2.763	1.08	1.68	52
$U(MeCp)Cl_3(THF)_2$	2.720	1.00	1.72	53

Table IV. X-ray Data for COT^{a} Complexes

compound	R(M-C) Å	metal ion radius Å	net $COT^{=}$ radius Å	ref.
$U(COT)_2$	2.647	1.06	1.59	5
$U(Me_4COT)_2$	2.658	1.06	1.60	54
$Th(COT)_2$	2.701	1.13	1.57	5
$K(dg)[Ce(COT)_2]$	2.742	1.25	1.49	24
$[Ce(COT)Cl(THF)_2]_2$	2.710	1.20	1.51	55
$[Nd(COT)(THF)_2]$	2.68	1.18	1.61	
$[Nd(COT)_2]$	2.79	1.18	1.61	
	2.68	1.16	1.52	56
$Zr(COT)_2(THF)$	2.461	0.89	1.57	23
$Ti(COT)Cp$	2.323	0.76	1.56	57
$[K(dg)]_2(Me_4COT)$	3.003	1.46	1.54	58
$K_2(COT)(dg)$	2.98	1.38	1.60	
	3.05	1.46	1.59	59
$Rb_2(COT)(dg)$	3.10	1.52	1.58	
	3.15	1.56	1.59	60

[a] $COT = C_8H_8^{=}$

[b] $dg = (CH_3OCH_2CH_2)_2O$.

Figure 1. Perspective drawing of U(benzylCp)$_3$Cl from reference 13.

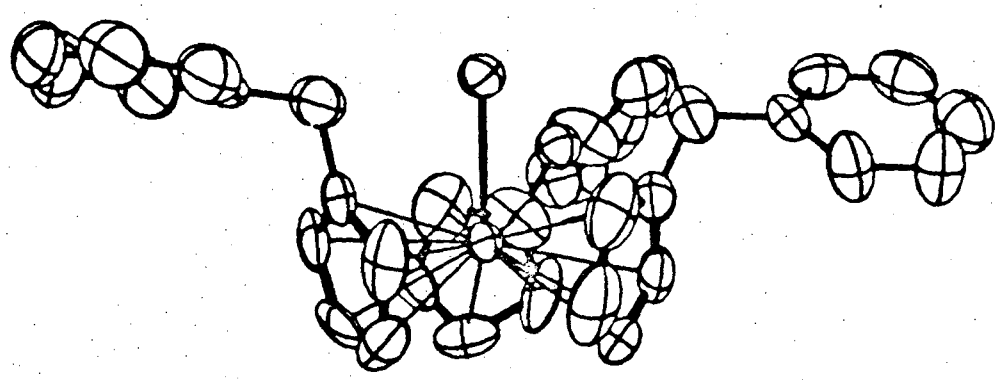

Figure 2. Perspective drawing of $InCp_3$ from reference 17.

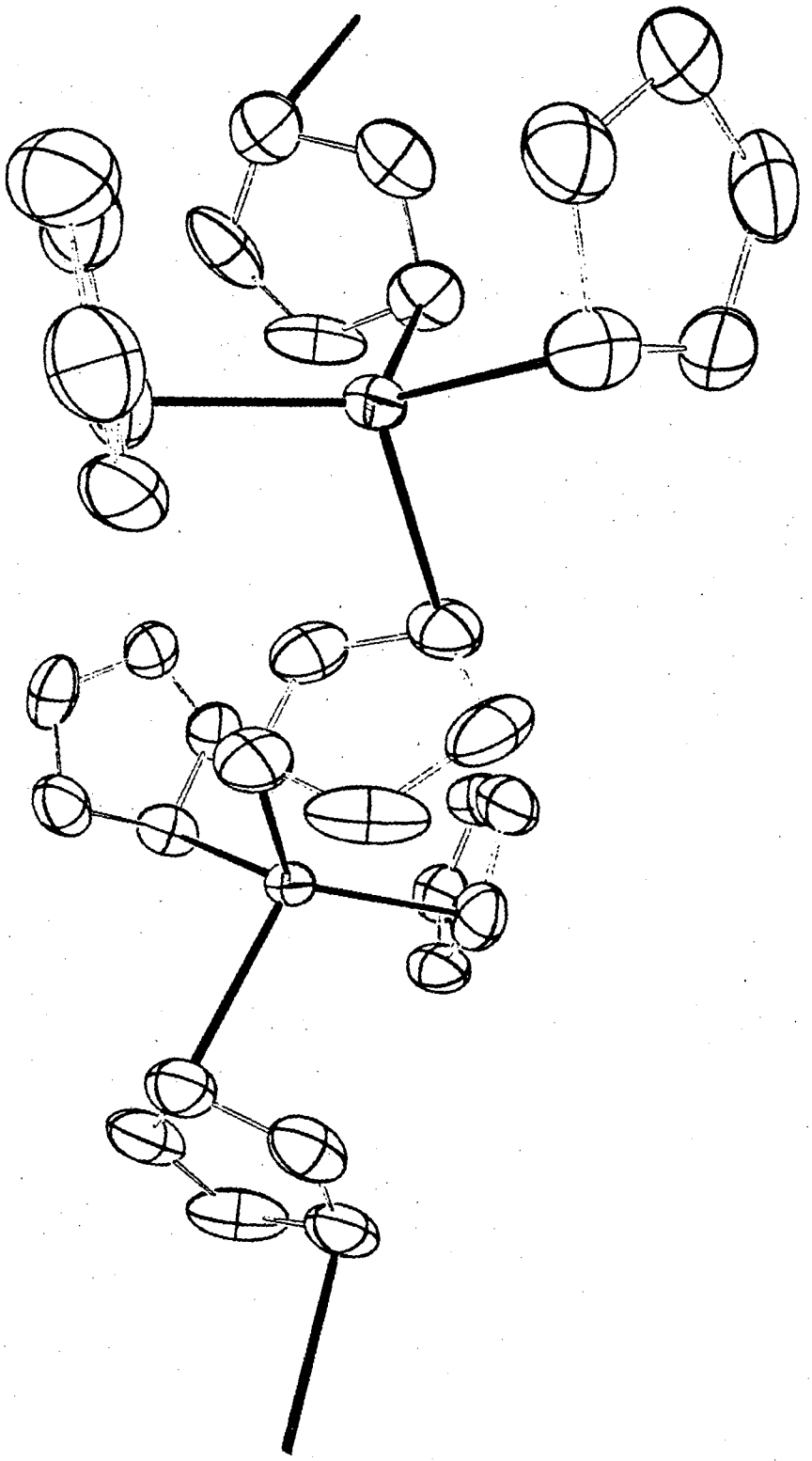

XBL 799-12050

Figure 3. Perspective drawings of tetrakis(Cp) complexes: $TiCp_4$ (left, reference 18), $ZrCp_4$ (middle, reference 19), and UCp_4 (right, reference 20).

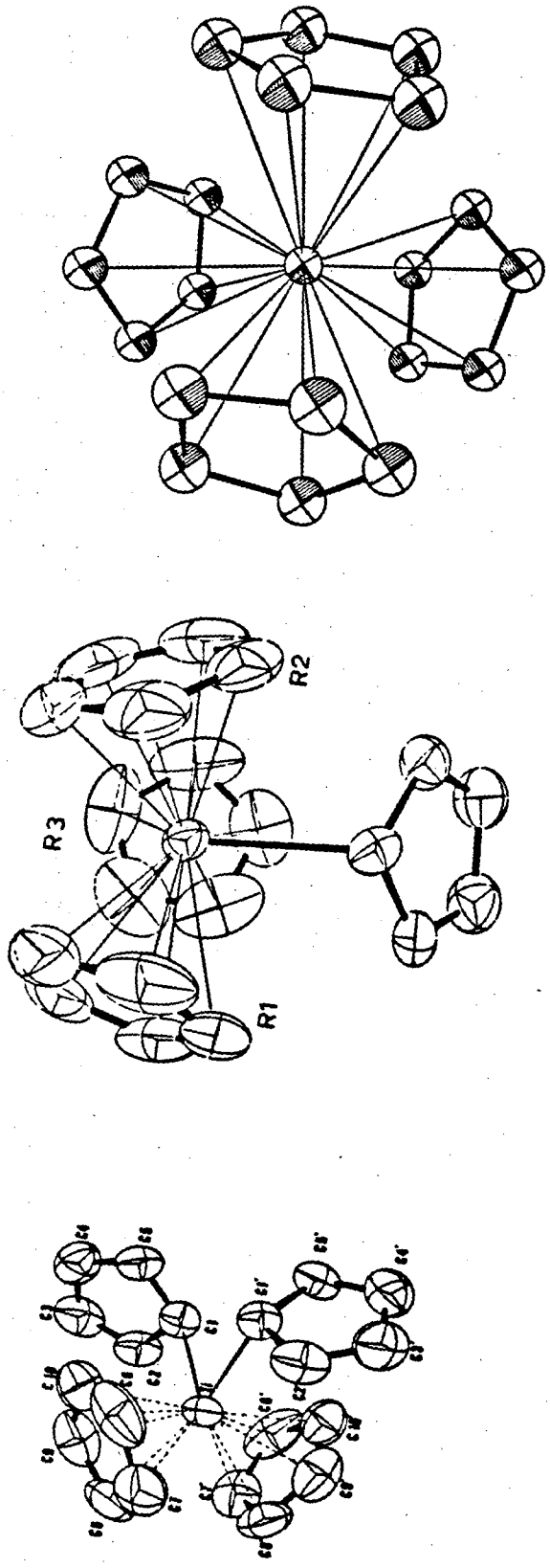

XBL 799-12049

Figure 4. A graph of R(M-C) vs. metal ionic radius for complexes of the type MCp_2.

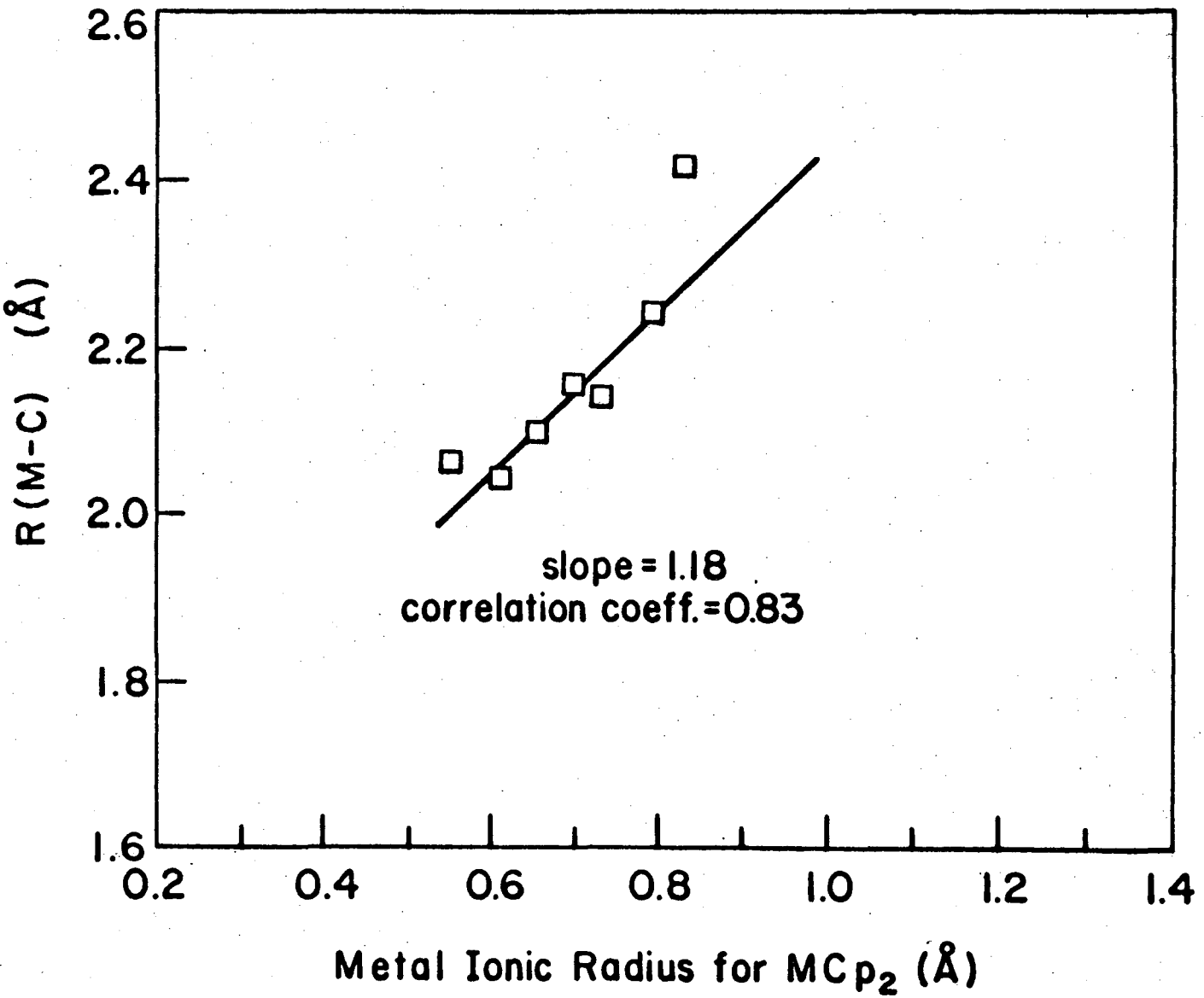
2.6
2.4
2.2
2.0
1.8
1.6
R(M-C) (Å)
slope = 1.18
correlation coeff. = 0.83
0.2
0.4
0.6
0.8
1.0
1.2
1.4
Metal Ionic Radius for MCp_2 (Å)

Figure 5. A graph of R(M-C) vs. "electron imbalance", as defined by Haaland in reference 27.

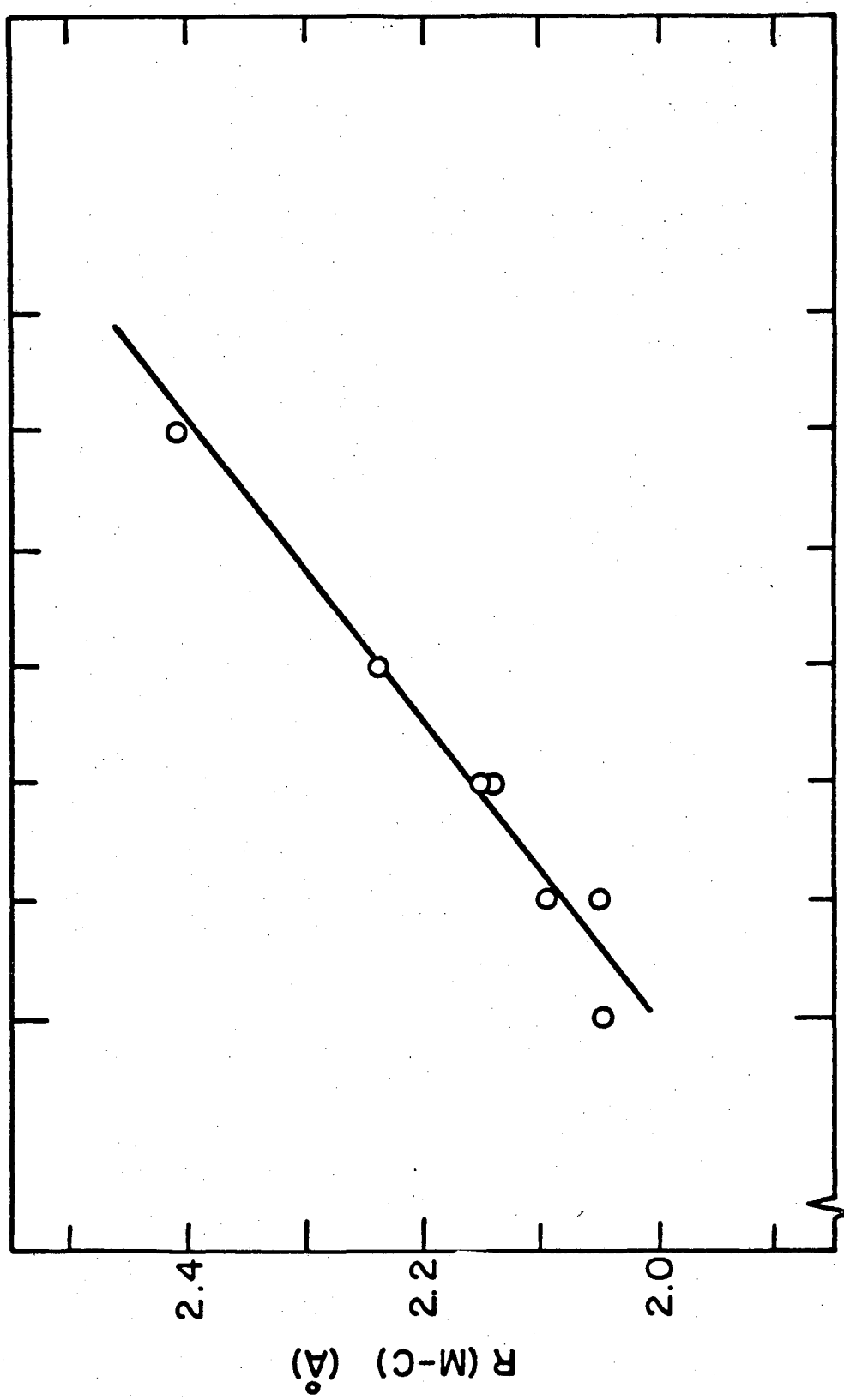

XBL 799-7063

Figure 6. Graphs of R(M-C) vs. metal ionic radius for lanthanide Cp complexes and metal COT complexes.

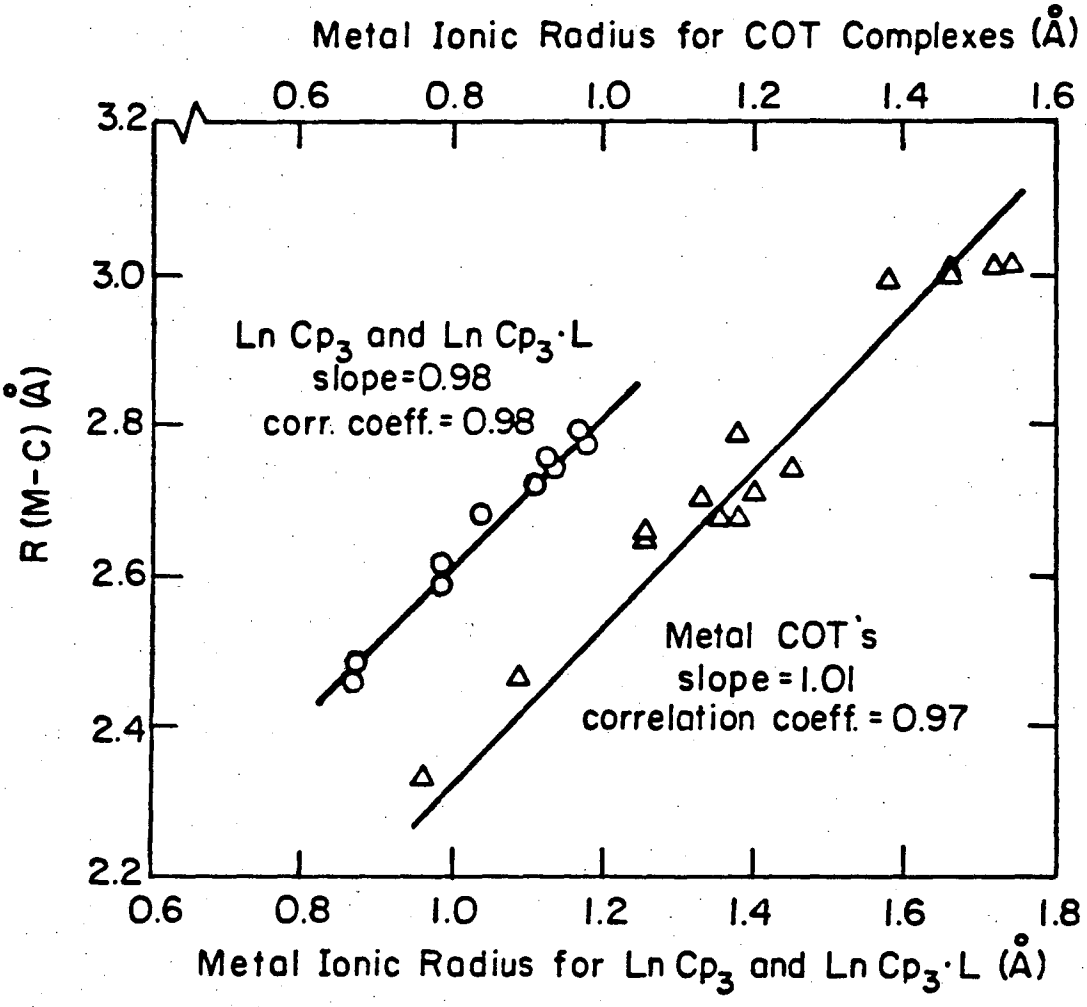

XBL 7911-7288

Figure 7. Perspective drawing of $(YbCp_3)_2$(pyrazine) from reference 38.

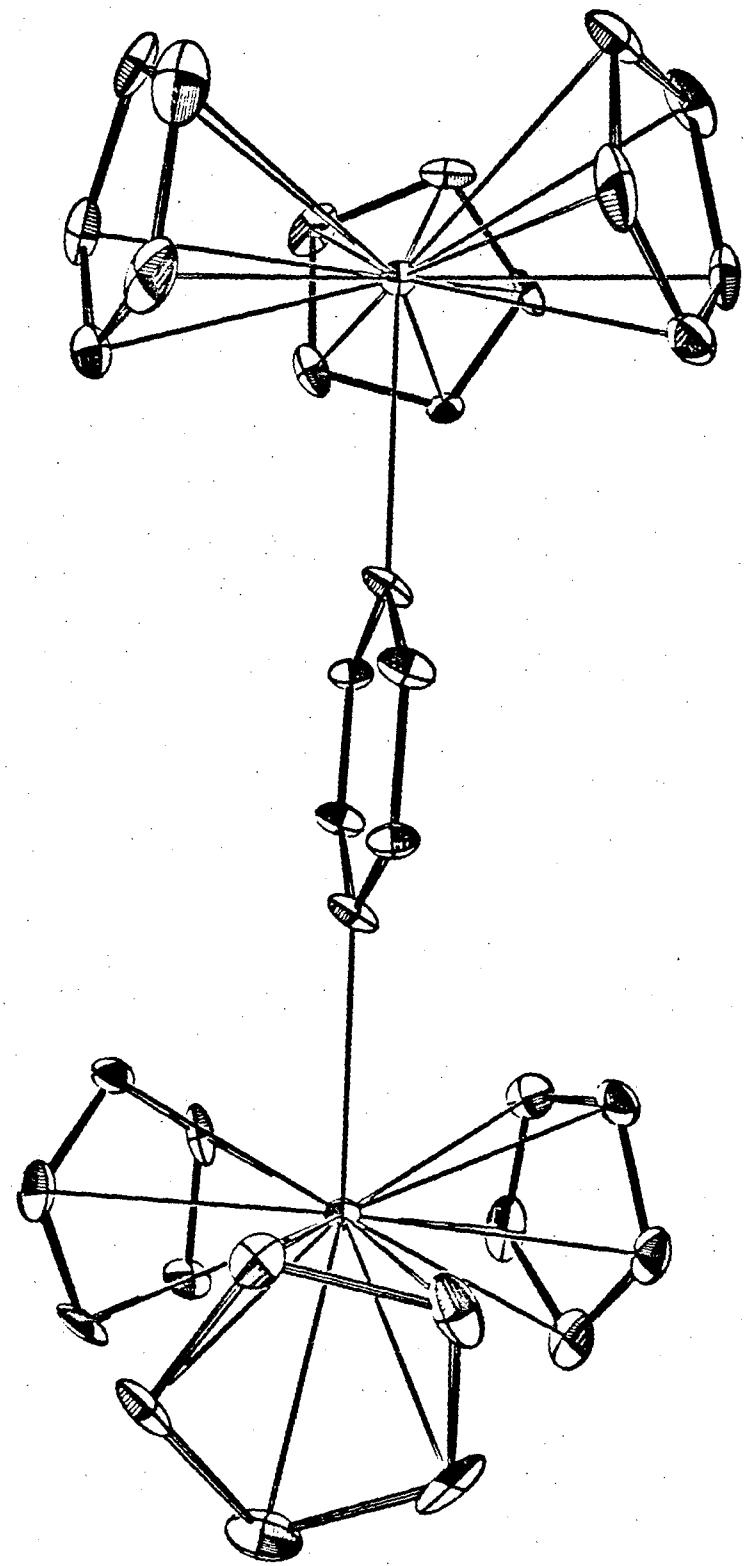

XBL 771-7113

References

1. Cotton,F.A.; Wilkinson,G.; "Advanced Inorganic Chemistry" 4th ed., John Wiley and Sons, N.Y., (1980).

2. Coates,G.E.; Green,M.L.H.; Wade,K.; "Organometallic Compounds" Methuen and Co.,Ltd., London, (1968).

3. Birmingham,J.M.; Wilkinson.G.; J.Amer.Chem.Soc. (1956), 78 , 42.

4. Streitwieser,A.; Mueller-Westerhoff,U.; J.Amer.Chem.Soc. (1968), 90 , 7364.

5. Avdeef,A.; Raymond,K.N.; Hodgson,K.O.; Zalkin,A; Inorg.Chem. (1972), 11 , 1083.

6. Atwood,J.L.; Hains,C.F.; Tsutsui,M.; Gabela,A.E.; J.Chem.Soc.Chem.Commun. (1973), 452.

7. Clark,J.P.; Green,J.C.; J.Chem.Soc.Dalt.Trans. (1977), 505.

8. Streitwieser,A.; Dempf,D.; LaMar,G.N.; Karraker,D.G.; Edelstein,N.; J.Amer.Chem.Soc. (1971), 93 , 7343.

9. Karraker,D.G.; Stone,J.A.; Jones,E.R.,Jr.; Edelstein,N.; J.Amer.Chem.Soc. (1970), 92 , 4841.

10. Pauling,L.; "The Nature of the Chemical Bond" Third Ed., Cornell University Press, Ithaca, N.Y., 1960, pp

505-562.

11. Shannon,R.D.; ActaCrystallogr.A. (1976), 32 , 751.

12. Baker,E.C.; Halstead,G.W.; Raymond,K.N.; Struct.Bonding (1976), 25 , 23.

13. Leong,J.; Hodgson,K.O.; Raymond,K.N.; Inorg.Chem. (1973), 12 , 1329.

14. Burns,J.H.; Baldwin,W.H.; Fink,F.H.; Inorg.Chem. (1974), 13 , 1916.

15. Atwood,J.L.; Burns,J.H.; Laubereau,P.G.; J.Amer.Chem.Soc. (1973), 95 , 1830.

16. Atwood,J.L.; Smith,K.D.; J.Amer.Chem.Soc. (1973), 95 , 1488.

17. Einstein,F.W.B.; Gilbert,M.M.; Tuck,D.G.; Inorg.Chem. (1972), 11 , 2832.

18. Calderon,J.L.; Cotton,F.A.; DeBoer,B.G.; Takats,J.; J.Amer.Chem.Soc. (1971), 93 , 3592.

19. Rogers,R.D.; Bynum,R.V.; Atwood,J.L.; J.Amer.Chem.Soc. (1978), 100 , 5238.

20. Burns,J.H.; J.Organomet.Chem. (1974), 69 , 225.

21. Dietrich,H.; Soltwisch,M.; Angew.Chem.Intern.Ed.Engl. (1969), 8 , 765.

22. Dierks,H.; Dietrich,H.; ActaCrystallogr.B. (1968), 24, 58.

23. Brauer,D.J.; Kruger,C.; J.Organomet.Chem. (1972), 42 , 129.

24. Hodgson,K.O.; Raymond,K.N.; Inorg.Chem. (1972), 11 , 3030.

25. Gard,E.; Haaland,A.; Novak,D.P.; Seip,R.; J.Organomet.Chem. (1972), 88 , 181.

26. Almenningen,A.; Haaland,A.; Motzfeldt,T.; "Selected Topics in Structure Chemistry" Universitetsforlaget, Oslo, (1967), p 105.

27. Almenningen,A.; Haaland,A.; Samdal,S.; J.Organomet.Chem. (1978), 149 , 219.

28. Haaland,A.; Nilsson,J.E.; ActaChem.Scand. (1968), 22 , 2653.

29. Almenningen,A.; Gard,E.; Haaland,A.; Bunvoll,.J.; J.Organomet.Chem. (1976), 107 , 273.

30. Hedberg,A.K.; Hedberg,L.; Hedberg,K.; J.Chem.Phys. (1970), 63 , 1262.

31. Hedberg,L.; Hedberg,K.; J.Chem.Phys. (1970), 53 , 1228.

32. Wheatley,P.J.; "Perspectives in Structural Chemistry" Dunitz,J.D.; Ibers,J.A.; editors, Wiley, N.Y., 1967.

33. Bunder,W.; Weiss,E.; Z.Naturforsch.B:Anorg.Chem.Org.Chem. (1978), 33B , 1235.

34. (a) Dunitz,J.D.; Orgel,L.E.; Rich,A.; ActaCrystallogr. (1956), 9 , 373.

(b) Seiler,P.; Dunitz,J.D.; ActaCrystallogr.B. (1979), 35 , 1068.

35. Bunder,W.; Weiss,E.; J.Organomet.Chem. (1975), 92 , 65.

36. Bats,J.W.; DeBoer,J.J.; Bright,D.; Inorg.Chim.Acta (1971), 5 , 605.

37. Burns,J.H.; Baldwin,W.H.; Laubereau,P.G.; Oak Ridge Chemistry Division Annual Prob. Report, ORNL-4891, 1973, p42.

38. Baker,E.C.; Raymond,K.N.; Inorg.Chem. (1977), 16 , 2710.

39. Atwood,J.L.; Smith,K.D.; J.Chem.Soc.Dalt.Trans. (1973), 2487.

40. Baker,E.C.; Brown,L.D.; Raymond,K.N.; Inorg.Chem. (1975), 14 , 1376.

41. Holton,J.; Lappert,M.F.; Ballard,D.G.H.; Pearce,R.; Atwood,J.L.; Hunter,W.E.; J.Chem.Soc.Chem.Commun. (1976), 480.

42. Rogers,R.D.; Bynum,R.V.; Atwood,J.L.; J.Organomet.Chem. (1980), 192, 65.

43. Zalkin,A.; private communication.

44. Wong,C.; Yen,T.; Lee,.T.; ActaCrystallogr. (1965), 18, 340.

45. Ryan,R.R.; Penneman,R.A.; Kanellakopulos,B.; J.Amer.Chem.Soc. (1975), 97 , 4258.

46. Burns,J.H.; Laubereau,P.G.; Inorg.Chem. (1971), 10 , 2789.

47. Tsutsui,M.; Ely,N.; Dubois,R.; Acc.Chem.Res. (1976), 9, 217.

48. Atwood,J.L.; Hains,C.F.; Tsutsui,M.; Gabela,A.E.; J.Chem.Soc.Chem.Commun. (1973), 452.

49. Parego,G.; Cesari,M.; Farina,F.; Lugli,G.; ActaCrystallogr.B. (1976), 32 , 3034.

50. Halstead,G.W.; Baker,E.C.; Raymond,K.N.; J.Amer.Chem.Soc. (1975), 97 , 3049.

51. Baker,E.C.; Raymond,K.N.; Marks,T.J.; Wachter,W.A.; J.Amer.Chem.Soc. (1974), 96 , 7586.

52. Fischer,R.D.; Klahne,E.; Kopf,J.; Z.Naturforsch.B: Anorg.Chem.Org.Chem. (1978), 33B , 1393.

53. Ernst,R.D.; Kennelly,W.J.; Day,C.S.; Day,V.W.; Marks,T.J.; J.Amer.Chem.Soc. (1979), 101 , 2656.

54. Hodgson,K.O.; Raymond,K.N.; Inorg.Chem. (1973), 12 , 458.

55. Hodgson,K.O.; Raymond,K.N.; Inorg.Chem. (1972), 11 , 171.

56. DeKock,C.W.; Ely,S.R.; Hopkins,T.E.; Brault,M.A.; Inorg.Chem. (1978), 17 , 625.

57. Kroon,P.A.; Helmhodt,R.B.; J.Organomet.Chem. (1970), 25 , 451.

58. Goldberg,S.G.; Raymond,K.N.; Harmon,C.A.; Templeton,D.H.; J.Amer.Chem.Soc. (1974), 96 , 1348.

59. Noordik,J.H.; van den Hark,Th.E.M.; Mooij,J.J.; Klaassen,A.A.K.; ActaCrystallogr.B (1974), 30 , 833.

60. Noordik,J.H.; Degens,H.M.L.; Mooij,J.J.; ActaCrystallogr.B (1975), 31 , 2144.

Chapter One

The Synthesis and Characterization of $(UCp_3)_2$(pyrazine) and $[U(MeCp)_3]_2$(pyrazine): π-Bridged Dimers of U^{3+}.

Introduction

Since the resurgence of interest in the organometallic chemistry of the lanthanide and actinide elements in the late 1960's, occasioned by Streitweiser's synthesis of uranocene[1], many people have investigated the role of f-electrons in the bonding in these compounds[2]. This chapter describes part of our effort[3] to use magnetic studies as a probe for covalency in organouranium compounds. The Introduction summarizes a previous report on the synthesis and characterization of $(YbCp_3)_2$(pyrazine), which led to the conclusion that as low as 4K no spin-pairing took place[4]. The behavior of pyrazine in d-metal dimers has demonstrated that, in the covalent extreme, it can facilitate spin-pairing between the $4f^{13}$ paramagnets. The fact that no pairing was apparent is convincing evidence of the predominantly ionic bonding in this compound. However, since it is well-known that the 4f electrons in the lanthanide elements make very little contribution to the chemical environment, this result was of little surprise.

It is also well-known, however, that early in the actinide series, the 5f shell electrons make a greater

contribution to the chemical environment, and so it was thought some covalency might be involved in compounds of uranium, for instance. Other uranium dimers have been reported[5], but their magnetic characterization has not been complete. This study represents an attempt to completely characterize a π-bridging uranium dimer.

Experimental

All manipulations were accomplished using a Schlenk or vacuum line with high purity Argon or in a Vacuum Atmospheres HE-93 glove box with a recirculating oxygen and moisture-free Argon atmosphere. All solvents were dried by distillation from potassium benzophenone ketyl and were degassed prior to use. Pyrazine (Aldrich 99+%) was dried over BaO at 60°C. Infra-red spectra were recorded on a Perkin-Elmer 597 spectrophotometer, the visible-near IR spectra on a Cary 14M spectrophotometer, nmr spectra on the UCB 250 MHz spectrometer, and mass spectra on an AEI-MS12 spectrometer. The magnetic behavior was measured using a PAR Model 155 vibrating magnetometer equipped with a 12 in. Varian electromagnet capable of producing a homogeneous field between 2.5 and 12.5 kG. A powdered sample was weighed into a calibrated, diamagnetic sample container machined from Kel-F rod. Sample temperatures between 4 and 80 K were measured with a calibrated GaAs diode approximately 12 mm. above the sample in a liquid helium dewar.

Elemental analyses were performed by the

Microanalytical Laboratory at U.C.Berkeley or Mallissa and Reuter Analytische Laboratorien, Engelskirchen, W.Germany. X-ray powder patterns were collected with Cu radiation. $NaCp(DME)$[6] (DME is 1,2-dimethoxyethane) and UCl_4[7] were prepared by the literature techniques. Napthalene was sublimed before use. K(MeCp) was produced by the reaction between the diene (after cracking) and KH in THF (tetrahydrofuran) at 0°C.

$UCp_3(THF)$ and $U(MeCp)_3(THF)$

To small pieces of sodium weighing 0.30 g (13 mmol) in 100 ml THF was added 1.70 g (13 mmol) of napthalene. The resulting dark green mixture was stirred at room temperature overnight. It was then filtered through a glass frit onto 5.00 g (13mmol) of UCl_4 in 150 ml THF. The mixture of green solutions turned immediately to a deep purple. This mixture was stirred at room temperature for one hour. Next, the NaCp(DME) or KMeCp (39.5 mmol) (solution and slurry, respectively) in 100 ml THF was added, the purple changing to brown immediately. This mixture was stirred at room temperature for another hour, at which time the THF was removed under vacuum. Care was taken to retain a slight dampness of THF. The brown residue was soxhlet extracted with benzene overnight. Next the benzene was removed under vacuum and the residue subjected to room temperature vacuum for 12 hours to remove the napthalene. The product thus obtained (90% based on UCl_4) is crystalline. Its composition was con-

firmed by the IR spectrum[8], pmr spectrum (for the methylated compound at 21°C in d^8-toluene, shifts in δ ppm vs. TMS : -8.1 (s,~7H, 102 Hz); -14.5 (s,~12H, 49 Hz); -21.4 (s,~8H, 73 Hz)), and elemental analysis.
$UC_{22}H_{29}O$: calculated-- %C, 48.26 , %H, 5.30 : found-- %C, 48.91 , %H, 5.53 .

$\underline{(UCp_3)_2(pyrazine)}$

This compound can be synthesized by the combination of stoichiometric amounts of $UCp_3(THF)$ and pyrazine in benzene, toluene, DME, or THF. The blue-grey product precipitates immediately upon addition of pyrazine to a brown solution of $UCp_3(THF)$. It is most soluble in THF, but only sparingly so. The supernatant from a THF preparation, if cooled quickly to -78°C and held there for a few days, yields black microcrystalline material. This material was used for the X-ray powder pattern. Analysis $U_2C_{34}H_{34}N_2$. Calculated-- %C,43.13; %H,3.59; %N,2.96 . Found-- %C,43.40; %H,4.07; %N, 2.22 .

Infra-red Spectrum (Nujol mull)($cm.^{-1}$)

3080, 1422, 1279, 1261, 1068,

1018, 960, 809, 782, 737,

619, 602, 470.

Mass spectral data (70 eV) are included in Table Ia.

The low solubility of this compound hampered further characterization.

$\underline{[U(MeCp)_3]_2(pyrazine)}$

To a dark brown solution of $U(MeCp)_3(THF)$ in toluene was added a stoichiometric amount of pyrazine in a small volume of toluene. The color changed immediately to a deep blue-black. Stirring at room temperature for a few minutes, followed by filtration yielded a very strongly colored filtrate. Cooling to -15°C overnight yielded black crystals shaped like needles. Analysis $U_2C_{40}H_{46}N_2$-- calculated: %C, 46.29 , %H, 4.28 , %N, 2.81 ; found: %C, 46.60 , %H 4.47 , %N, 2.72 .

Infra-red spectrum(Nujol mull)($cm.^{-1}$)

1420, 1279, 1057, 1048, 1030,

950, 880, 849, 840, 805, 770,

758, 742, 728, 694, 611, 463.

PMR spectrum (20°C, d^8-toluene , δ ppm vs. TMS)

-2.15 (s, 18H, 9 Hz, Me)

-11.5 (s, 11H, 15 Hz, ring)

-13.4 (s, 12H, 15 Hz, ring)

-67.0 (s, 4H, 15 Hz, pyrazine).

Mass spectral data (70 eV) are in Table Ib.

Electronic spectrum (in toluene vs. toluene)(nm.)

1510, 1360, 1220, 1180, 1020, 910,

680. The maxima are quite broad.

Single crystals suitable for diffraction studies have not been obtained. Both this and the previous compound sublime with some decomposition at 10^{-3} torr and 120°C.

Discussion

The dimeric formulation of these compounds is based primarily on;

(a) the X-ray powder pattern of $(UCp_3)_2$(pyrazine)

(b) the mass spectra of both compounds, and

(c) the pmr of the methylated compound.

The crystal and molecular structure of $(YbCp_3)_2$-(pyrazine) has been determined[4] and is illustrated in Figure 1. It consists of a dimer located about a crystallographic inversion center. Two ytterbium atoms, each with three η^5-Cp rings, are nearly linearly bridged by a pyrazine ring coordinated through its nitrogens. Because $(UCp_3)_2$(pyrazine) exhibits low solubility, and $[U(MeCp)_3]_2$(pyrazine) forms only thin needles during crystal growth, a single crystal X-ray structure of these compounds has eluded us. However, it is reasonable to assume that substitution of U^{3+} for Yb^{3+} would lead to isomorphic structures, and if so, that powder patterns of the two compounds should be quite similar. Indeed this is so, the similarity of the patterns extending to the general pattern of the lines and their relative intensities (Fig 2).

The mass spectra of both compounds reveal the presence of dimeric species (Table I). Both spectra contain several prominent peaks that are not easily assigned, but that are included for completeness. The intensity of the high-mass peaks is rather low, consistent with the decomposition observed during sublimation. In the spectrum of the methylated compound, peaks appear that correspond to $[U_2L_{6-x}(pyrazine) + 15]^+$, which suggests that perhaps uranium-methyl bonds are formed in the spectrometer.

The pmr spectrum of the methylated compound includes one singlet resonance for the four pyrazine protons. In any

reasonable monomeric formulation their chemical shifts would differ. This spectrum also exhibits resonances one expects for the mono-methylCp ligands--the methyl groups shifted the least, while the inequivalent sets of ring protons are shifted more by the uranium ion.

The infra-red spectra also confirm the presence of η^5-Cp rings, the spectrum of the methylated compound being predictably more complex due to the lowered symmetry the methyl groups impart. The electronic spectrum is consistent with the almost indescribable color, consisting as it does of nearly constant absorption throughout the range 1600-450 nm. With the structure thus confidently assigned, we address the magnetic behavior.

Our use of the liquid helium apparatus is predicated on the expectation that any covalent effects would be of particularly low energy and necessitate the use of very low temperatures. For this reason neither the room temperature moment nor the temperature dependence of the nmr spectrum has been determined. The magnetic behavior of the methylated compound has been investigated four times. Three times the data indicate the compound is only weakly paramagnetic, and that the paramagnetism varies slowly with temperature. The fourth investigation produced results that suggest an abrupt spin-state change at very low temperature. The magnetic behavior of this compound remains under investigation.

Acknowledgement

We wish to thank Helena Ruben for her assistance with the X-ray powder patterns.

Table Ia. Mass Spectrum of $(UCp_3)_2$(pyrazine)

RA(%)[a]	$\frac{m}{e}$	assignment[b]
0.8	883	U_2L_5X
1.5	817	U_2L_4X
0.8	620	U_2LX
1.1	514	UL_3X
1.4	512	-
15	433	UL_3
16	403	-
25	387	-
22	368	UL_2
16	338	-
23	322	-
4	303	UL
72	80	X
73	66	L
100	44	-

[a] relative abundance

[b] L = C_5H_5 and X = $C_4H_4N_2$

Table Ib. Mass Spectrum of $[U(MeCp)_3]_2$(pyrazine)

RA(%)[a]	$\frac{m}{e}$	assignment[b]
0.2	966	U_2L_5X + 15
0.1	952	U_2L_5X
0.7	887	U_2L_4X + 15
0.4	873	U_2L_4X
0.3	726	-
0.6	647	-
0.7	602	-
0.7	568	-
2.0	556	UL_3X
1.5	523	-
30	494	-
20	475	UL_3
25	431	-
88	415	-
40	336	-
70	80	X
100	79	L

[a] relative abundance

[b] L = C_6H_7 and X = $C_4H_4N_2$

Figure 1. Perspective drawing of $(YbCp_3)_2$(pyrazine) from reference 4.

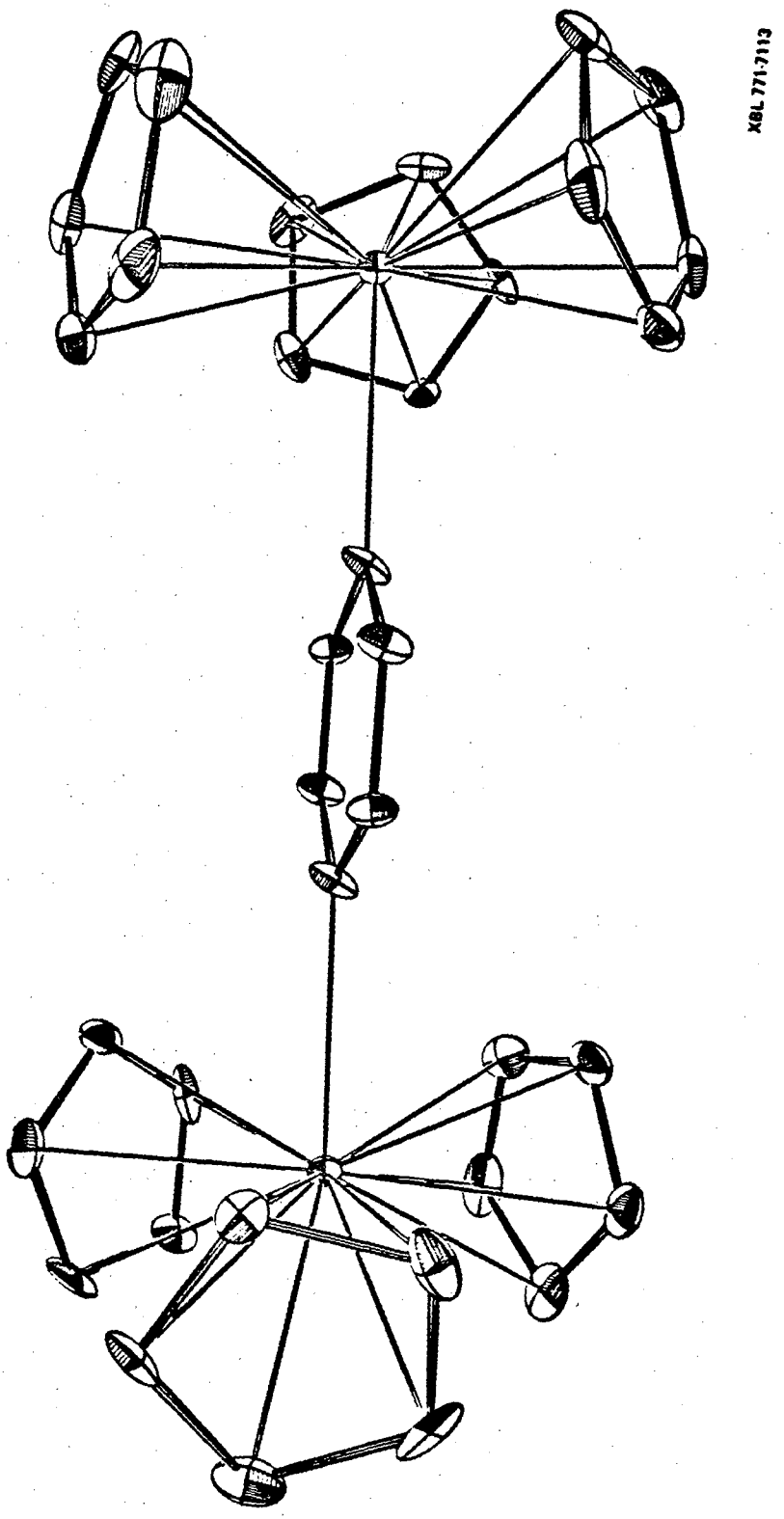
XBL 771-7113

Figure 2. X-ray powder patterns of $(YbCp_3)_2$(pyrazine) (A) and $(UCp_3)_2$(pyrazine) (B) in the forward-scattering region.

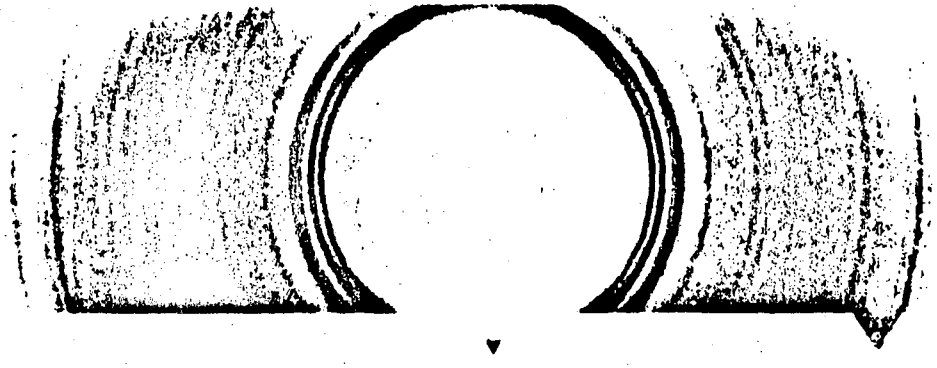

A

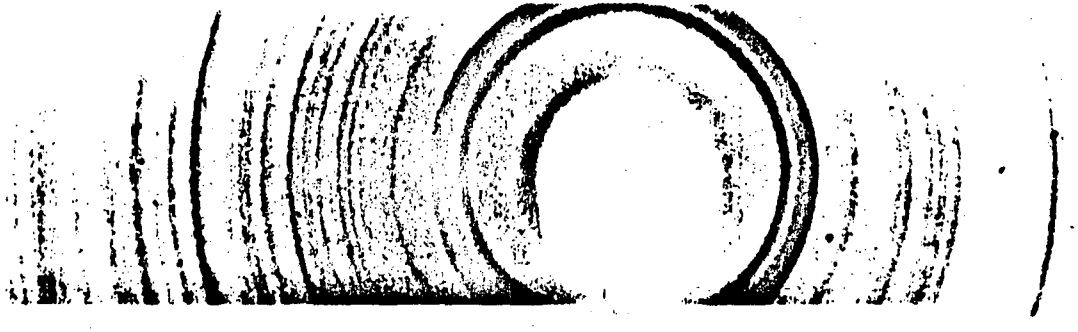

B

References

1. Streitwieser,A.; Mueller-Westerhoff,U.; J.Amer.Chem.Soc. (1968), 90, 7364.

2. Raymond,K.N.; Eigenbrot,C.W.,Jr.; Acc.Chem.Res. (1980), 13, 276., and references therein.

3. Eigenbrot,C.W.,Jr.; Raymond,K.N.; Inorg.Chem. (1981), in press.

4. Baker,E.C.; Raymond,K.N.; Inorg.Chem. (1977), 16, 2710.

5. Tsutsui,M.; Ely,N.; Gebala,A.; Inorg.Chem. (1975), 14, 78.

6. Smart,J.C.; Curtis,C.J.; Inorg.Chem. (1977), 16, 1788.

7. Hermann,J.A.; Suttle,J.F.; Inorg.Syn. (1957), 5, 143.

8. Kanellakopulos,B.; Fischer,E.O.; Dornberger,E.; Baumgartner,F.; J.Organomet.Chem. (1970), 24, 507.

Chapter Two

Synthesis and X-ray Structure of $UCp_3(C_3H_3N_2)$. A New Mode of Pyrazolate Bonding.

Introduction

The search for new organoactinide and -lanthanide compounds for use in structural and magnetic analyses of their mode of bonding[1,2] has led to a new complex of uranium. The pyrazolate anion has been used extensively throughout transition metal chemistry[3], where its coordination is almost always exo-bidentate, i.e. an η^2 bridging ligand. Stucky and Fieselman recently reported that the reaction of $TiCp_2Cl$ with Na(pyrazolate) yields a dimeric compound of formula $[TiCp_2(pyrazolate)]_2$[4]. And, while the large class of MCp_3X compounds (M = lanthanide or actinide) are all formally ten-coordinate, R.D. Fischer and coworkers have reported the eleven-coordinate $UCp_3(NCS)(CH_3CN)$[5]. Thus we anticipated that results similar to those with $TiCp_2Cl$ would be obtained with UCp_3Cl. Instead, we report the first example of an endo-bidentate (η^2 non-bridging) pyrazolate anion in the formally 11-coordinate $UCp_3(C_3H_3N_2)$.

Experimental

All reactions were carried out under an inert atmosphere of argon on a Schlenk or vacuum line. Transfer and some handling were facilitated by a Vacuum Atmospheres HE-

93-A glove box with recirculating moisture and oxygen-free argon atmosphere. Elemental analyses were performed by the U.C.Berkeley Analytical Laboratory . Infra-red spectra were recorded on a Perkin-Elmer Model 597 spectrophotometer (Nujol mull, reported in cm^{-1}), mass spectra were obtained on an AEI-MS12 mass spectrometer (70 eV, reported as m/e(relative abundance)), electronic spectra were recorded on a Cary 14 spectrophotometer, and pmr spectra obtained with a JEOL model FX90Q spectrometer (in d^8-toluene, shifts reported in δ ppm vs. TMS). Crystalline samples for X-ray diffraction were mounted in glass capillaries under a He atmosphere in a horizontal-format inert atmosphere glove box equipped with a binocular microscope.

Materials

Toluene and tetrahydrofuran (THF) were distilled from potassium benzophenone ketyl. Pyrazole was obtained from Aldrich (98%) and recrystallized from toluene at -15°C before use. Sodium pyrazolate was prepared from NaH and pyrazole in THF[6]. UCp_3Cl was prepared by the reaction between UCl_4[7] and NaCp(DME)[8] in 1,2-dimethoxyethane (DME).

$UCp_3(C_3H_3N_2)$

To a clear brown solution of 2.00 g UCp_3Cl (4.27 mmol) dissolved in 100 ml THF was added 0.38 g $Na(C_3H_3N_2)$ (4.22 mmol) in 10 ml THF. A fine precipitate was visible after stirring for a few hours at room temperature. The mixture

was filtered through diatomaceous earth and the THF removed from the filtrate under vacuum. A saturated toluene solution was cooled to -15°C whereupon large crystals formed. Analysis calc.(found) for $UC_{18}H_{18}N_2$; %C,43.20(43.55), %H 3.60(3.62), %N 5.60(5.64).

Infra-red spectrum.

1469(w), 1440(w), 1409(w), 1343(w),
1280(s), 1070(s), 1022(s), 998(s),
970(m), 776(s), 616(m).

Mass spectrum.

500(21.7), 435(86.5), 370(18.7),
343(13.2), 317(28.8), 68(100).

Electronic spectrum (toluene solution, in nm.).

1640, 1600, 1520, 1370, 1325,
1290, 1260, 1230, 1160, 1110,
1080, 980, 892, 790, 760, 738,
690, 662, 587, 548.

Variable temperature pmr.

At 35°C ; -9.51(s,Cp), 10.68(s,pyrazolate), 8.75(s,pyrazolate).
The respective peaks at other temperatures are;
-10°C; -11.59, 11.31, 9.18.
-50°C; -14.22, 12.06, 9.69.
-75°C; -15.84, 12.53, 10.03.

Magnetic susceptibility measurements were made with a PAR model 155 vibrating sample magnetometer used with a homogeneous field produced by a Varian Associates 12 in. electromagnet capable of a maximum field strength of 12.5 kG. A 173 mg sample was weighed and transferred to a diamagnetic , calibrated sample holder machined from Kel-F rod. A variable temperature liquid helium dewar produced sample temperatures in the range 5-80 K which were measured by a calibrated GaAs diode approximately 12 mm above the sample. The magnetometer was calibrated with $HgCo(CNS)_4$. The resulting susceptibilities were corrected for underlying diamagnetism and yield a temperature independent paramagnetism from 7.5 to 37.1 K, above which μ_{eff} calculated from the slope of $\frac{1}{x}$ vs. T is equal to $2.67\mu_B$ (Table I).

Data Collection, Solution and Refinement

Suitable crystals for diffraction were obtained by

cooling an unsaturated toluene solution of $UCp_3(C_3H_3N_2)$ to -75^oC overnight. Several crystals were mounted in .2 mm glass capillaries under He, the capillaries sealed with grease, and later sealed in a flame. The crystal was mounted on a CAD4 automatic diffractometer with graphite monochromator and molybdenum tube. The lattice constants were determined from a least squares refinement on 25 automatically centered reflections with 2θ values between 27 and 38 degrees. Data reduction and processing were carried out as described elsewhere[9]. The intensities were corrected for Lorentz and polarization effects and converted to values of F^2. Crystal faces were identified with the help of the diffractometer, and the dimensions of the 9 faces found were measured at 7X magnification under a binocular microscope. Absorption corrections were then made using an analytical algorithm[10]. Azimuthal scans on 6 reflections revealed an intensity variation of roughly $\pm$10%. Minor adjustments to the observed dimensions of the crystal were made to minimize the variation after the absorption correction was made (μ=97.50cm^{-1}.), and it was thus adjusted to $\pm$4%. The actual data were then subjected to an absorption correction which ranged from 2.76 to 3.84. No crystal decay was observed in the three reflections monitored throughout data collection. The data were averaged to yield the 3631 independent reflections with $F^2>3\sigma(F^2)$ used in the final refinement.

The calculated density agrees well with that observed for Z = 4. The initial Patterson map confirmed the space

group $P2_1/a$[11]. The structure was then solved using heavy atom methods[12-15]. In the final refinement all non-hydrogen atoms were treated anisotropically and hydrogen atoms were fixed in calculated positions with a C-H distance of .95Å[16] and an isotropic temperature factor of 8.0 $Å^2$. The model converged to give weighted and unweighted R factors both of 3.14%. On the final cycle all parameters shifted by less than .10 sigma. The variation of residuals with both $\frac{\sin\theta}{\lambda}$ and F_o showed no abnormalities. In the final difference Fourier, the only peaks of greater than $1.0\frac{e^-}{A^3}$ were within 1.4 Å of the uranium, and the most negative electron density at a grid point was $-.95\frac{e^-}{Å^3}$. Positional and thermal parameters are listed in Table II.

Description of the Structure

The crystal structure consists of discrete mononuclear units at general positions in the unit cell (Figure 1). A perspective drawing of the complex is shown in Fig 2. The molecular structure consists of a uranium ion coordinated by three η^5-coordinated cyclopentadienyl rings and by the two nitrogens of the pyrazolate ion. If the coordination polyhedron is considered to be formed by the centers of the Cp rings and the midpoint of the N-N bond, the coordination about the uranium can be considered roughly C_{3v} in symmetry; with the Cp rings at the base, and the N-N midpoint at the apex of a flattened tetrahedron (Figure 3). The angles for

this polyhedron are [(Cp centroid)-U-(N-N)] 106.3°,108.4°,and 97.1° for rings 1 to 3 respectively. The angles between centroids are 114.2°,115.0°, and 113.8° (1-U-2, 1-U-3, 2-U-3).

The pyrazolate ring exhibits local C_{2v} symmetry as in $[TiCp_2(pyrazolate)]_2^4$. The pyrazolate ring and the Cp rings are planar with average deviations from their least squares planes of 0075, .0055, .0044, and .0134 Å (Cp1,2,3,pyrazolate) (Table III). The angle between the U-N-N plane and the pyrazolate plane is 10.4°. The N-U-N angle is 32.19°. Cp 3 and the pyrazolate are nearly parallel, the angle between their least squares planes being 5.7°. The Cp C-C distances average 1.388(19) Å, and the internal angles average 108.0°(1.0). The Cp's are symmetrically bound to the uranium with average U-C distance of 2.762(12) Å. The U-N distances are 2.40(1) and 2.36(1) Å. The closest intramolecular contact is 2.91 Å between N(2) and C(10), and the closest intermolecular contact is 3.53 Å between C(16) and C(6). Pertinent bond distances are listed in Table IV.

Discussion

The endo-bidentate coordination of the pyrazolate ion in this structure is surprising, and the failure to adopt a bridging geometry is best attributed to the highly ionic character of the U-N bond. In numerous pyrazolate complexes of the d-block transition metals, the pyrazolate bridges two

metal ions. This is the appropriate geometry for directional covalent bonding involving the nitrogen lone pair electrons, and substantial overlap seems to be implied by the observation of magnetic interaction mediated by such bridging pyrazolates[17,18]. In the present compound, the ionic character of the U-N bond dominates , with the coordination being a non-directional association of the N-N bond (the more negative side of the pyrazolate ring) with the uranium cation.

The geometry of the large class of compounds of the type MCp_3X, where X is a monodentate Lewis base, anion or η^1 bridging Cp ring, is best described as a flattened tetrahedron[19]. The Cp rings are shifted towards the sterically less bulky X ligand, decreasing the X-M-Cp(centroid) angles, and increasing the Cp-M-Cp angles. This is also the case with our compound. The Cp-U-Cp angles are nearly identical and greater than 109°, while the Cp-U-(N-N) angles are all less than 109°.

The placement of the pyrazolate ring divides the Cp's into two classes. Cp1 and Cp2 are non-parallel with the pyrazolate, (the angles are 62.0° and 73.2°), while Cp3 is nearly parallel to the pyrazolate. In addition, the angle from the Cp3 centroid to the midpoint of the N-N bond is much less than for the other two Cp rings (vide supra).

The average U-C distance of 2.76 Å is a little longer than those typically found in the 10-coordinate, UCp_3X-type structures, and is a reflection of the increased effective

ionic radius of the uranium[1] in a formally 11-coordinate complex. The compound $UCp_3(NCS)(MeCN)$[5] is also formally 11-coordinate. It exists in a trigonal-bipyramidal geometry with the Cp rings occupying the equatorial sites. Table V contains angles and distances for a comparison of some representative uranium Cp complexes. The compounds $U(benzylCp)_3Cl$[20], $UCp_3(2\text{-Me-allyl})$[21], and $UCp_3(C_4H_9)$[22] all exhibit the flattened tetrahedral geometry described above. In $UCp_3(NCS)(CH_3CN)$ however, the Cp-U-Cp angles are close to 120° and the Cp-U-N angles are close to 90°. Clearly, this represents a unique geometry -- different from the flattened tetrahedron characterizing the MCp_3X compounds including the present one.

While the angles and geometries of the thiocyanato and pyrazolate complexes are distinctly different, there are marked similarities in their bond lengths, which are in turn consistent with the ionic radius calculated for an eleven-coordinate uranium(IV) complex. The average U-C distances (2.76 Å) for both compounds and the U-N distances (2.40 and 2.36 for the pyrazolate versus 2.40 for the thiocyanate) agree well. The reason for the 0.04 Å difference in the U-N distances of the pyrazolate is unclear; the closest intramolecular contact (between N(2) and C(10)) must be expected to make U-N(2) the longer bond, but the opposite is true.

The structure of $Cu(\phi\text{-}N{=}N\text{-}\phi)(CNCMe_3)_2$[23] reveals a

roughly analogous, endo-bidentate coordination of an N_2 moiety. Structural evidence for a covalent σ-bond includes a lengthening of the N-N bond vs. uncoordinated azobenzene (from an average of 1.20 Å to 1.38 Å). However, one can expect the N-N bond in the pyrazolate anion to be less susceptible to such an effect by virtue of its incorporation in an aromatic π-system. In this light, we mention that in $[TiCp_2(pyz)]_2$ the N-N distance (1.312(6) Å) is quite similar to that in our compound (1.318(10) Å).

Table I. Molar Susceptibilities for UCp_3(pyrazolate)	
T(K)	x_m^{corr} (cm^3/mole)[a]
7.5	12.92
10.7	12.80
18.3	12.62
27.2	12.23
37.1	13.14
50.0	11.55
56.7	10.94
77.3	8.57

[a] times 10^3

Table IIa. Positional and Thermal Parameters ($\times 10^4$) for UCp_3(pyrazolate)

	x	y	z	β_{11}	β_{22}	β_{33}	β_{33}	β_{12}	β_{13}
U(1)	.23092(2)	.224422(3)	.24961(2)	42.42(18)	75.5(4)	35.79(17)	4.9(3)	15.33(13)	4.2(3)
C(1)	.3752(8)	.3632(14)	.4215(8)	63.(8)	196.(23)	67.(8)	-18.(10)	16.(6)	-49.(11)
C(2)	.3091(9)	.2799(13)	.4551(7)	101.(9)	149.(18)	37.(6)	-8.(11)	25.(5)	-16.(10)
C(3)	.2171(9)	.3602(15)	.4201(9)	88.(9)	207.(23)	78.(9)	-26.(12)	52.(8)	-52.(12)
C(4)	.2250(10)	.4882(13)	.3624(9)	90.(10)	148.(21)	75.(9)	24.(11)	27.(7)	-32.(11)
C(5)	.3206(11)	.4924(13)	.3634(9)	117.(12)	138.(21)	77.(10)	-34.(12)	42.(8)	-12.(11)
C(6)	.1581(10)	.2577(14)	.0425(7)	110.(11)	190.(26)	49.(7)	-2.(12)	19.(6)	9.(11)
C(7)	.1061(9)	.3735(18)	.0726(9)	70.(9)	305.(33)	73.(9)	51.(14)	11.(7)	69.(14)
C(8)	.1782(12)	.4912(14)	.1243(10)	127.(13)	144.(22)	83.(10)	46.(13)	41.(9)	44.(12)
C(9)	.2702(10)	.4428(18)	.1242(10)	78.(10)	274.(31)	85.(10)	-27.(14)	26.(8)	78.(15)
C(10)	.2568(10)	.3004(18)	.0723(9)	107.(11)	266.(29)	60.(8)	16.(14)	47.(7)	21.(13)
C(11)	.0486(8)	.1293(13)	.2550(9)	56.(7)	200.(20)	86.(9)	-15.(10)	42.(7)	9.(11)
C(12)	.0467(8)	.0751(15)	.1609(9)	66.(9)	225.(25)	75.(9)	-44.(11)	8.(7)	22.(12)
C(13)	.1168(10)	-.0476(15)	.1786(11)	100.(11)	165.(24)	115.(13)	-57.(12)	46.(10)	-36.(14)
C(14)	.1627(9)	-.0720(12)	.2801(12)	73.(9)	100.(19)	144.(14)	-24.(9)	34.(9)	33.(13)
C(15)	.1203(9)	.0357(14)	.3291(9)	91.(10)	176.(22)	83.(9)	-37.(11)	36.(8)	27.(12)
N(1)	.3722(6)	.0455(9)	.3204(6)	62.(6)	140.(15)	58.(6)	18.(7)	19.(5)	-13.(7)
N(2)	.3472(6)	.0497(10)	.2213(6)	69.(6)	175.(16)	52.(6)	21.(7)	20.(5)	-25.(8)
C(16)	.4015(10)	-.0660(16)	.1986(11)	95.(10)	265.(29)	110.(12)	7.(13)	49.(9)	-72.(15)
C(17)	.4575(9)	-.1468(13)	.2826(11)	82.(10)	121.(19)	140.(13)	23.(13)	35.(10)	-26.(14)
C(18)	.4369(9)	-.0777(14)	.3576(10)	95.(10)	185.(24)	88.(10)	45.(12)	14.(8)	34.(12)

Table IIb. Calculated Hydrogen Atom Positions[a] for UCp_3(pyrazolate)

	x	y	z
H(1)	.4439	.3370	.4354
H(2)	.3245	.1854	.4949
H(3)	.1589	.3325	.4334
H(4)	.1718	.5611	.3276
H(5)	.3456	.5697	.3303
H(6)	.1289	.1629	.0067
H(7)	.0359	.3735	.0608
H(8)	.1656	.5863	.1356
H(9)	.3326	.4982	.1547
H(10)	.3078	.2422	.0596
H(11)	.0091	.2131	.2657
H(12)	.0044	.1149	.0960
H(13)	.1308	-.1043	.1276
H(14)	.2143	-.1483	.3128
H(15)	.1378	.0425	.4002
H(16)	.4003	-.0861	.1327
H(17)	.5013	-.2340	.2882
H(18)	.4641	-.1103	.4263

[a] isotropic thermal parameters equal 8.0 $\frac{e^-}{Å^2}$

Table III. Least-Squares Planes for $UCp_3(C_3H_3N_2)$

Cp 1		Cp 2	
atom	dist(Å)	atom	dist(Å)
C1	.006(10)	C6	.005(10)
C2	-.008(9)	C7	-.001(11)
C3	.012(10)	C8	-.004(11)
C4	-.01(1)	C9	.009(10)
C5	.000(11)	C10	-.009(11)
Parameters from Equation of Plane			
A	.140	A	1.58
B	2.59	B	3.23
C	5.93	C	9.52
D	3.39	D	.681
Cp3		pyrazolate	
atom	dist(Å)	atom	dist(Å)
C11	.005(10)	N1	.013(8)
C12	-.001(10)	N2	-.013(8)
C13	-.003(11)	C16	.015(13)
C14	.006(10)	C17	.004(12)
C15	-.007(10)	C18	-.022(13)
Parameters from Equation of Plane			
A	10.5	A	3.83
B	5.52	B	1.87
C	3.32	C	.80
D	.37	D	1.25

Table IV. Bond Distances (Å) for UCp_3(pyrazolate)

U-C(1)	2.78	U-C(6)	2.74	U-C(11)	2.75
U-C(2)	2.75	U-C(7)	2.76	U-C(12)	2.74
U-C(3)	2.76	U-C(8)	2.78	U-C(13)	2.76
U-C(4)	2.76	U-C(9)	2.77	U-C(14)	2.76
U-C(5)	2.78	U-C(10)	2.77	U-C(15)	2.77
ave.U-C	2.76	C(16)-N(2)	1.36	C(18)-N(1)	1.35
U-N(1)	2.40	C(16)-C(17)	1.34	N(1)-N(2)	1.32
U-N(2)	2.36	C(17)-C(18)	1.35		

Table V. Bond Angles(°) and Distances(Å) for Representative Uranium Cp Complexes

formula	Cp-U-Cp	Cp-U-X	ave. U-C(Cp)	ref.
$U(benzylCp)_3Cl$	117,118,116	100,101,99	2.73	18
$UCp_3(2Me\text{-}allyl)$	119,115,118	102,100,98	2.74	19
$UCp_3(n\text{-}but)$	118,116,116	98,102,101	2.74	20
$UCp_3(C_3H_3N_2)$	114,115,114	106,108,97	2.76	herein
$UCp_3(NCS)(MeCN)$	121,119,119	92,95,90 86,89,88	2.76	5

Figure 1. Stereoscopic packing diagram for UCp_3(pyrazolate). The view is down the b axis.

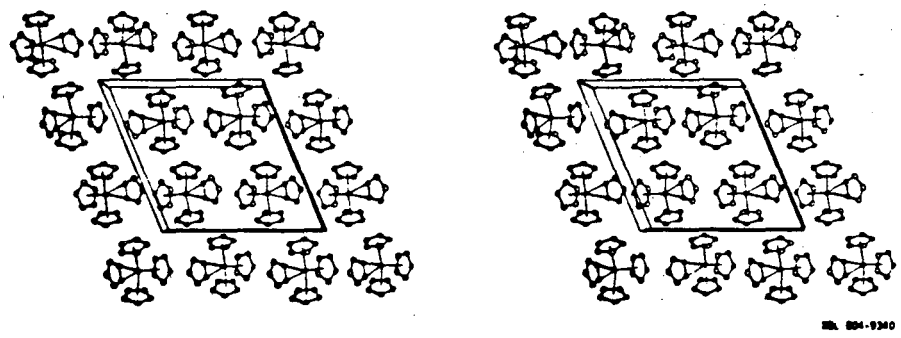

Figure 2. Perspective drawing of UCp_3(pyrazolate).

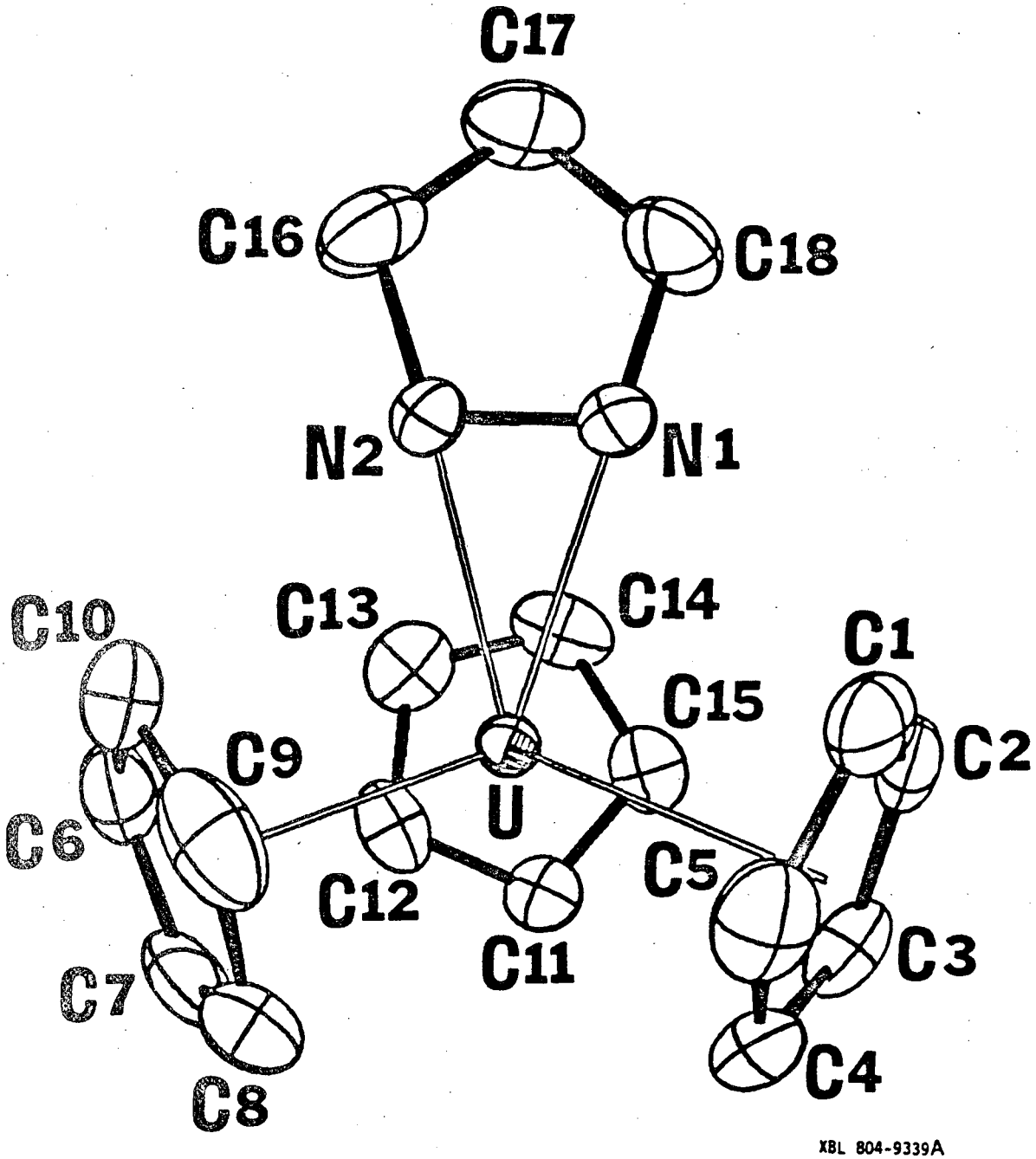

XBL 804-9339A

Figure 3. Perspective drawing of UCp_3(pyrazolate) looking down the pseudo-threefold axis.

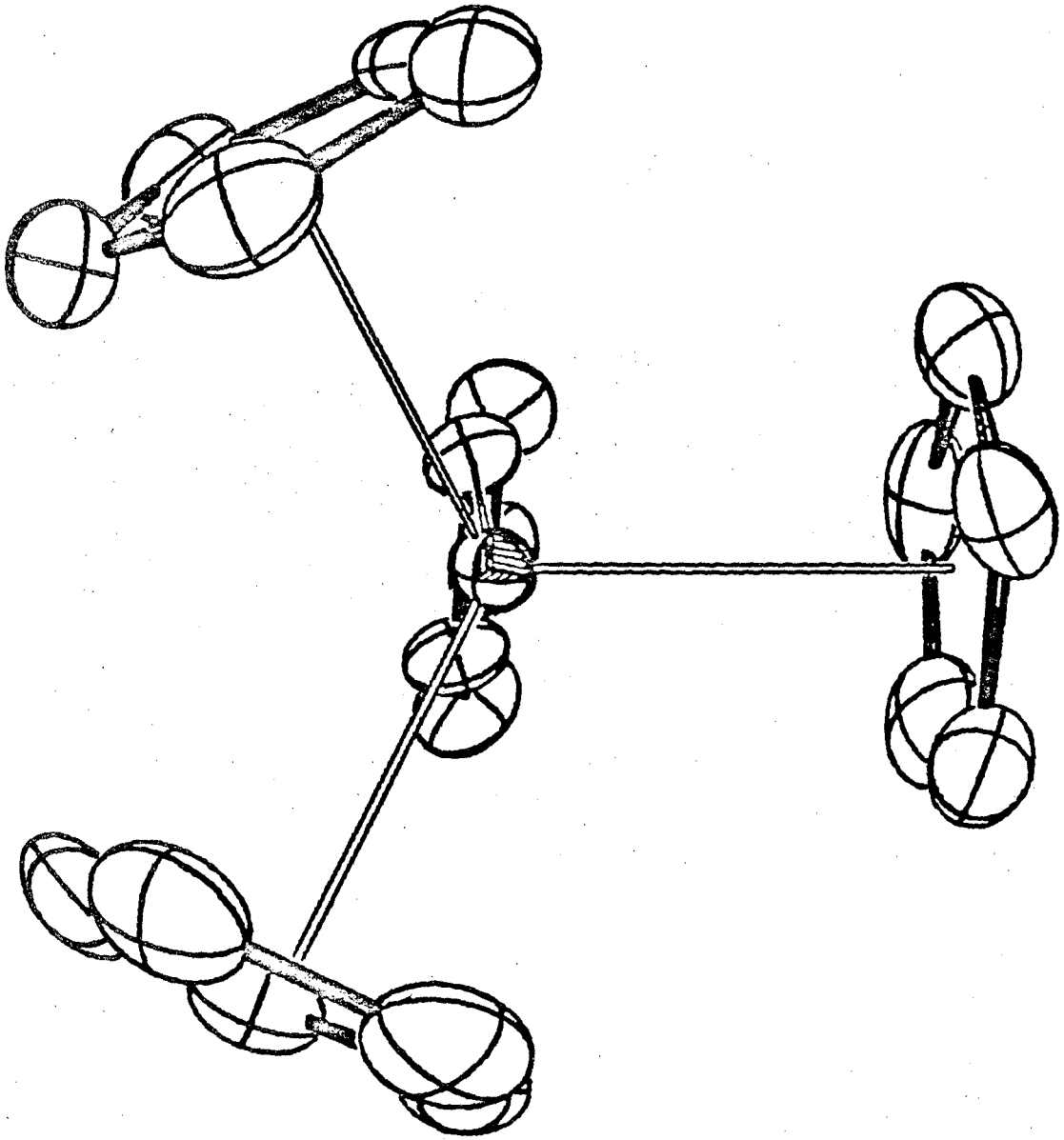

XBL 804-9338

References

1. Raymond,K.N.; Eigenbrot,C.W.,Jr.; Acc.Chem.Res. (1980), 13, 276.

2. Baker,E.C.; Raymond,K.N.; Inorg.Chem. (1977), 16, 2710.

3. Trofimenko,S.; Chem.Rev. (1972), 72, 497.

4. Fieselman,B.F.; Stucky,G.D.; Inorg.Chem. (1978), 17, 2074.

5. Fischer,R.D.; Klahne,E.; Kopf,J.; Zeit.fur Natur. (1978), 33b, 1393.

6. Breakwell,K.R.; Patmore,D.J.; Storr,A.; J.Chem.Soc.Dalt.Trans. (1975), 749.

9. Sofen,S.R.; Abu-Dari,K.; Freyberg,D.P.; Raymond,K.N.; J.Amer.Chem.Soc. (1978), 100, 7882.

10. L.K.Templeton and D.K.Templeton, Abstracts, American Crystallographic Association Proceedings, Series 2, Vol.1, 1973, p.143.

11. The symmetry operations for this non-standard setting of $P2_1/c$ are: x,y,z ; -x,-y,-z ; 1/2+x,1/2-y,z ; 1/2-x,1/2+y,-z.

12. Full matrix least-squares refinement on F was used in which the function minimized was $\Sigma w(|F_o| - |F_c|)^2$,

where F_o and F_c are the observed and calculated structure factors and the weighting factor, w, is $\frac{4F_o^2}{\sigma^2(F_o^2)}$. The atomic scattering factors for neutral U, C, and N were taken from the tables of Cromer and Mann[13], and those for neutral H from Stewart, Davidson, and Simpson[14]. Corrections for anomalous dispersion using both $\Delta f'$ and $\Delta f''$ were included for all atoms except H[15].

13 Cromer,D.T.; Mann,B.; ActaCrystallogr.A (1968), 24, 321.

14. Stewart,R.F.; Davidson,E.R.; Simpson,W.T.; J.Chem.Phys. (1965), 42, 3175.

15. Cromer,D.T.; ActaCrystallogr. (1965), 18, 17.

16. Churchill,M.R.; Inorg.Chem. (1973), 12, 1213.

17. Fieselman,B.J.; Hendrickson,D.N.; Stucky,G.D.; Inorg.Chem. (1978), 17, 2078.

18. Barraclough,C.G.; Brookes,R.W.; Martin,R.L.; Aust.J.Chem. (1974), 27, 1843.

19. Raymond,K.N.; "Organometallics of the f-Elements", Marks,T.J.; Fischer,R.D., eds.; D.Reidel, Dordrecht, Holland, 1979, p249.

20. Leong,J.; Hodgson,K.O.; Raymond,K.N.; Inorg.Chem. (1973), 12, 1329.

21. Halstead,G.W.; Baker,E.C.; Raymond,K.N.; J.Amer.Chem.Soc. (1975), 97, 3049.

22. Perego,G.; Cesari,M.; Farina,F.; Lugli,G.; ActaCrystallogr. (1976), B32, 3034.

23. Dickson,R.S.; Ibers,J.A.; Otsuka,S.; Tatsuno,Y.; J.Amer.Chem.Soc. (1971), 93, 4636.

Chapter Three

Synthesis and X-ray Structures of $U(C_5Me_5)_2Cl_2(pyrazole)$, $U(C_5Me_5)_2Cl(pyrazolate)$, and $U(C_5Me_5)_2(pyrazolate)_2$

Introduction

The synthesis and structure of $UCp_3(pyrazolate)$[1], reported in chapter 2, revealed that our attempt to form a dimer based on a precedent in titanium chemistry, $[TiCp_2(pyrazolate)]_2^2$, resulted instead in the formation of a monomeric species, allowing us to characterize a new mode of pyrazolate bonding. To investigate what role, if any, steric factors played in the formation of the monomeric compound, and to learn more about the pyrazolate ion as a ligand, we have adjusted the size and number of the Cp (C_5H_5) ligands. We anticipated that a reduction in the total steric bulk of the other ligands might lead to the formation of one or more dimeric species. The compound $UCp"_2Cl_2$ ($Cp"=C_5Me_5$) has proven to be a useful starting material for other studies[3,4], and now our own. We have not, however, succeeded in forming dimeric compounds. The compounds $U(C_5Me_5)_2Cl(pyrazolate)$ and $U(C_5Me_5)_2(pyrazolate)_2$ are formed by the reaction between $U(C_5Me_5)_2Cl_2$ and stoichiometric amounts of Na(pyrazolate). In the course of this study, an adduct of neutral pyrazole, $U(C_5Me_5)_2Cl_2(pyrazole)$ was also characterized.

Experimental

All reactions were carried out under an inert atmosphere of argon on a Schlenk or vacuum line. Transfer and some handling were facilitated by a Vacuum Atmospheres HE-93-A glove box with recirculating moisture and oxygen-free argon atmosphere. Elemental analyses were performed by the Microanalytical Laboratory UC Berkeley. Infra-red spectra were recorded on a Perkin-Elmer 597 spectrophotometer (Nujol mulls, reported in cm^{-1}), mass spectra were obtained on an AEI-MS12 mass spectrometer (reported as m/e(relative abundance (%)), electronic spectra were recorded on a Cary 14 spectrophotometer (in toluene vs. toluene reported in nm.), and pmr spectra obtained with the UCB-250 nmr spectrometer (in d^8-toluene, shifts in δ ppm vs. TMS). Magnetic susceptibilities were determined with a PAR 155 vibrating magnetometer equipped with a 12 inch Varian electromagnet capable of producing homogeneous fields up to 12.5 kilogauss. Weighed samples were loaded into calibrated, diamagnetic sample containers machined from Kel-F rod. Sample temperatures between 4 K and 80 K were measured with a GaAs diode approximately 12 mm. above the sample in the variable temperature liquid helium dewar. The instrument was calibrated with $Hg[Co(NCS)_4]$. The reported susceptibilities are the average of those obtained at 5.0, 7.5, 10.0, and 12.5 kG., and are corrected for underlying diamagnetism[5]. Crystalline samples for X-ray diffraction were mounted in glass capillaries under a He atmosphere in a horizontal-format

inert atmosphere glove box equipped with a binocular microscope.

Materials

Toluene and tetrahydrofuran (THF) were distilled from potassium benzophenone ketyl. Pyrazole was obtained from Aldrich (98%) and recrystallized from toluene at -15°C before use. Sodium pyrazolate was prepared from NaH and pyrazole in THF[6]. UCl_4 was prepared by the literature procedure[7].

$UCp"_2Cl_2$

To a green solution of 5.00 g(13.2 mmol) UCl_4 in THF was added 6.87 g(39.5 mmol) $K(C_5Me_5)$ (prepared by the reaction between KH and HC_5Me_5 in THF). The total of 200 ml THF was maintained at reflux under argon for 24 h. After removal of solvent, the residue was extracted several times with a total of 200 ml of toluene. The separation of suspended particulate and solvent was facilitated by centrifugation. The volume of toluene was reduced and cooling overnight to -15°C yielded crystals of $U(C_5Me_5)_2Cl_2$ in moderate yield.

$UCp"_2Cl_2$(pyrazole)

To a red-brown solution of 0.55 g (0.9 mmol) $U(C_5Me_5)_2Cl_2$ in 75 ml THF was added 0.06 g(0.9 mmol) pyrazole. The solution was stirred overnight at room temperature. After solvent removal, the red-brown residue was washed with hexane, then dissolved in toluene and this solution cooled to -15°C. After 12 hours, the large crystals that had formed were filtered and an IR spectrum clearly revealed an N-H stretch at 3100 $cm.^{-1}$ Analysis-- found: %C, 43.26 ; %H, 5.55 ; %N, 4.38 : calculated: %C, 42.66; %H, 5.29; %N, 4.33.

Infra-red spectrum

3265(s), 3115, 2720, 1424(s), 1337(s), 1149(sh), 1132(s), 1052(sh), 1040(s), 1018(s), 930, 910, 776(s), 723(sh), 598.

Mass spectrum

624(9.5), 622(7.4), 578(93.4), 542(34.3), 443(98.6), 407(73.1), 403(79.3), 308(100), 135(37.6), 119(75.1), 105(42.5) .

Electronic spectrum

1607, 1590, 1423, 1400, 1168, 1133, 1118, 1095, 1049, 990, 908, 880, 858, 817, 790, 730, 718, 708, 691, 680 .

PMR spectrum

At 22°C. 11.49 (s, ~40 Hz, 30H, methyl) ; -9.58 (s, ~200 Hz, 2H, pyrazole) ; -28.63 (~1500 Hz, 1H, N-H).

At -10°C. 12.; -16.; -47.; -65.

At -25°C. 13.; -17.; -19.; -52.; -72.

At -40°C. 13.9 (s, ~40 Hz, 30H, methyl) ; -20.0 (s, ~80 Hz, 1H, pyrazole) ; -21.2 (s, ~90 Hz, 1H, pyrazole) ; -58.1 (s, ~205 Hz, 1H, pyrazole) ; -80.2 (s, ~250 Hz, 1H, pyrazole).

Magnetic susceptibility

This compound exhibits Curie-Weiss behavior with C=1.46 and θ = 42.34K. Table Ia includes x_M^{corr} versus T. The slope of $1/x_M^{corr}$ versus T yields $\mu_{eff} = 3.42\mu_B$.

$U(C_5Me_5)_2Cl$(pyrazolate).

About 150 ml THF was vacuum distilled from potassium benzophenone ketyl onto a mixture of 1.00g (1.7 mmol) UCp_2Cl_2 and 0.16g (1.8 mmol) Na(pyrazolate). The reaction was warmed to room temperature and stirred 12 hours. The THF was distilled away under vacuum. A hexane solution was filtered through diatomaceous earth, concentrated, and cooled to -15°C overnight yielding large crystals. Analysis $UC_{23}H_{33}N_2Cl$-- calculated: %C,45.21 ; %H,5.44 ; %N,4.58 ; %Cl,5.80 : found: %C,45.35 ; %H,5.57 ; %N,4.54 ; %Cl,6.06 .

Infra-red spectrum

2730(w), 1418, 1348(w), 1286(s), 1066(w), 1023(w), 968(s), 922, 782(s), 771), 726(w), 609.

Mass spectrum

610(6.8), 542(1.0), 475(38.7), 407(5.6), 403(4.8), 340(7.3), 137(19.6), 121(28.2), 105(63.3), 91(57.0), 77(31.3), 68(100) .

Electronic spectrum

1648, 1635, 1562, 1440, 1290, 1259, 1175, 1122, 1095, 1040, 967, 920, 907, 872, 855, 826, 773, 721, 713, 700, 660, 600.

PMR spectrum

12.956 (s,~84Hz,2H,pyrazolate); 8.098 (s,~30Hz,30H,Me).

Magnetic susceptibility

This compound exhibits Curie-Weiss behavior with C = 0.73 and θ = 5.95K. Table Ib. includes x_M^{corr} versus T. The slope of $1/x_M^{corr}$ versus T yields $\mu_{eff} = 2.42\mu_B$.

$U(C_5Me_5)_2$(pyrazolate)$_2$

Onto a mixture of 1.35g (2.3 mmol) $U(C_5Me_5)_2Cl_2$ and 0.42g (4.7 mmol) Na(pyrazolate) was distilled about 200 ml THF from potassium benzophenone ketyl. The resulting red-brown solution was stirred at room temperature for 24 hours with the development of a fine precipitate. The solvent was removed under vacuum and the residue extracted with a small volume of hexane (ca. 30 ml). The volume was reduced and the solution cooled overnight to -15 °C, whereupon large crystals formed. Analysis: calculated-- %C,48.59; %H,5.65; %N,8.72; found-- %C,48.72; %H,5.71; %N,8.80.

Infra-red spectrum

3125(w), 3100(w), 2720(w), 1731(w), 1696(w), 1590(w), 1410, 1349, 1280(s), 1230(w), 1052, 1018, 985(s), 921(s), 866, 800(w), 759(s), 725(w), 616(s), 591(w), 550(w), 382 .

Mass spectrum

642(67.35), 575(3.13), 508(73.93), 507(91.79), 412(66.92), 372(42.65), 136(34.74), 119(57.09), 105(32.69), 91(27.69), 77(15.02), 68(99.15) .

Electronic spectrum

1464, 1317, 1262, 1183, 1124, 1089, 982, 950, 930, 855, 834, 745, 691, 661 .

PMR spectrum

29.09(s, ~30 Hz, 2H, pyrazolate); 27.44(s, ~200 Hz, 4H, pyrazolate); -0.20(s, 30H, ~7 Hz, methyl).

Magnetic susceptibility

This compound does not exhibit simple behavior. Table Ic includes x_M^{corr} vs. T, and Figure 1 illustrates $1/x_M^{corr}$ vs. T.

Data Collection, Solution, and Refinement[8-16]

UCp''_2Cl_2(pyrazole)

Suitable crystals for diffraction were grown by cooling a saturated hexane solution to -15 °C. Precession photographs revealed mm symmetry, indicating orthorhombic or higher symmetry. For reflections hkl, h + k = 2n indicated a C-centered unit cell. A glide plane was indicated by the condition for h0l, l = 2n. These data left as possible space groups Cmcm, $Cmc2_1$, and Ama2 .

The crystal was oriented and lattice parameters accurately determined by 25 automatically centered reflections with values of 2θ between 26° and 40° (Table II).

One octant (+h+k+l), for a total of 1071 data, was collected between 4° and 52° 2θ by ignoring those reflections not satisfying the C-centering condition. During data collection, one reorientation was required.

Azimuthal scans on 5 reflections with θ between 7° and

21° revealed an intensity variation of ±17%. The crystal faces were identified with the help of the diffractometer, and their dimensions measured at 7X under a binocular microscope. The distances of the 8 planes identified from a common center were adjusted incrementally until the calculated edge lengths agreed most closely with those observed. An absorption correction ranging between 2.15 and 2.67 was then applied (μ = 65.82 cm^{-1}). No crystal decay was observed during data collection.

There were 58 reflections collected that were weak and were excluded from the least squares refinement. Inspection of the 56 reflections of the type hOl that were collected revealed almost all were less than 3σ. Those 9 such reflections for which the intensity exceeded 3σ were finally excluded on the grounds that some of their intensity could be attributed to contamination of the X-ray beam with $\lambda/2$. We therefore were left with the 924 reflections used in the final refinement.

The initail Patterson map confirmed the space group Cmcm, and the structure was solved by heavy-atom techniques (p factor =.03). The pyrazole was found to be lying across the mirror-plane at x = 0, disordering the NH and CH ortho to the metal-bound nitrogen. The structure was refined with only the carbon atom position varied (at .25 occupancy), with the parameters of the mirror-related nitrogen being reset to those of the carbon after each least-squares cycle.

This is a reasonable approximation considering how close to one another these two elements are in the Periodic Chart. The model converged to weighted and unweighted R factors of 3.48% and 2.45% respectively. During the final least-squares cycle the largest parameter shift was .18σ. The largest peak in the final difference Fourier was $.4\frac{e^-}{\text{Å}^3}$ and was less than one Angstrom from the uranium. Hydrogen atoms were not found, nor were calculated positions included in the final calculations. The residuals showed no anomalies. Positional and thermal parameters appear in Table III.

$\underline{UCp"_2Cl(pyrazolate)}$

Crystals suitable for diffraction studies were obtained by cooling a concentrated hexane solution at -15°C overnight. The large polycrystalline solids that formed were fractured into single crystal fragments. Precession photographs revealed systematic absences $\underline{h}0\underline{l}$, $\underline{h} + \underline{l} = 2n$, and $0\underline{k}0$, $\underline{k} = 2n$ indicating space group $P2_1/n$. Cell parameters were determined from 25 automatically centered reflections between 27° and 30° in 2θ (Table II).

A total of 3513 $\underline{hk} \pm \underline{l}$ data were collected between 4° and 45° in 2θ. Azimuthal scans on 6 reflections between 5° and 22° in θ revealed an intensity variation of $\pm$17%. Because the data crystal was of a particularly irregular shape, an empirical absorption correction was applied; it ranged from 1.00 to 1.49 (μ=66.00cm^{-1}). No decay was

observed during data collection.

Of the 138 absent reflections that were collected, 3 had an intensity greater than 3σ ; these were rejected with the rest on the grounds that their intensity resulted from contamination of the X-ray beam with $\lambda/2$ (low θ). The averaging of equivalent reflections left 3134 unique data, 2566 of which were greater than 3σ and were used in the least-squares refinement.

The initial Patterson map confirmed the space group and revealed the positions of the uranium and the chloride ion. The p factor for weighting was set at 0.03. Subsequent difference Fourier-least-squares cycles revealed the pyrazolate and the two Cp" rings. Residual electron density and some poor atomic relationships suggested a second orientation for both the Cp" rings, so primed carbon atom positions and isotropic thermal parameters were refined. The relative occupancy factors of the two orientations refined to about 50/50 for Cp"2 and about 60/40 for Cp"1. Fourier maps showed these ligands consisted of diffuse rings of electron density. This observation led us to conclude that further attempts to improve the moderately poor atomic relationships in the ring were unwarranted. In the final refinements, only the thermal parameters of uranium and chlorine were treated anisotropically.

The model converged to weighted and unweighted R factors of 4.50% and 3.27% respectively. On the final

least-squares cycle, the largest parameter shift was .29σ, while for those 7 atoms not involved in the disorder the largest shift was .02σ. The residual peaks in the final difference Fourier (largest = .525$\frac{e^-}{Å^3}$) were near the methyl carbons of the Cp" rings. Hydrogen atoms were not found, nor were calculated positions included in the final calculations. The residuals showed no anomalies. Positional and thermal parameters appear in Table IV.

$\underline{UCp"_2(pyrazolate)_2}$

Crystals suitable for diffraction experiments were obtained by slow cooling of a hexane solution to -15 °C. Precession photographs revealed systematic absences indicating space groups Cc or C2/c ($\underline{hkl}$, $\underline{h} + \underline{k} = 2n$, and $\underline{hol}$, $\underline{l} = 2n$).

The crystal was oriented and lattice parameters accurately determined by 25 automatically centered reflections with values of 2θ between 26° and 35° (Table II). A total of 3737 $\underline{hk} \pm \underline{l}$ data were collected between 4° and 45° 2θ by ignoring those reflections not satisfying the C-centering condition. Twice during data collection reorientation of the crystal was required.

Azimuthal scans on 7 reflections with θ between 5° and 22° revealed an intensity variation of $\pm$ 10%. The crystal faces were identified with the help of the diffractometer, and their dimensions measured at 7X under a binocular

microscope. The distance of the 8 planes used to approximate the true shape of the crystal from a common center were adjusted incrementally until calculated edge lengths agreed most closely with those observed. The absorption correction applied ranged from 1.91 to 2.77 (μ = 60.52cm^{-1}). No crystal decay was observed during data collection.

Inspection of the 223 reflections of the type hol, l = 2n that were collected revealed 12 reflections where F_{obs} was about or greater than 1σ, but all of these were rather weak and were rejected with the rest of the 223. Symmetry equivalent reflections were averaged leaving 3363 reflections of which 2706 were greater than 3σ and were used in the least-squares refinements.

The initial Patterson map confirmed the space group C2/c, and the structure was solved by heavy-atom techniques. (The p factor for weighting was set to 0.03.) In the final refinements, the temperature factors of all atoms were treated anisotropically, the model converging to weighted and unweighted R factors of 3.31% and 2.43% respectively. On the final cycle, the largest parameter shift was 0.63σ for one of the methyl carbons on Cp"2. This ring has generally greater thermal motion than the other parts of the molecule. In the final difference Fourier map the largest peak at a grid point was 0.36 $\frac{e^-}{Å^3}$, and was more than 1.6 Å from any atom or other peak. Hydrogen atoms were not found, nor were calculated positions included in the final calculations. The

residuals showed no anomalies. Positional and thermal parameters are listed in Table V.

Description of the Structures

UCp''_2Cl_2(pyrazole)

The crystal structure consists of discrete mononuclear units at postions of mm symmetry (Fig 2). The closest intermolecular contact is 3.68(1)A between C(60) and C(71). The molecular structure consists of a uranium ion bound by two η^5-pentamethylcyclopentadienide rings, two chloride ions, and one nitrogen from the pyrazole ring, for a formal coordination number of 9. Both the uranium and the bound nitrogen lie at the intersecton of mirror planes, while the chlorides, C(3), C(6), and the remaining atoms of the pyrazole ring lie in mirror planes. All the other atoms are in general positions. A perspective drawing of the molecular unit is illustrated in Figure 3.

The uranium-carbon distances average 2.74(2)Å, the U-Cl bond is 2.696(2)Å, and the U-N bond is 2.607(8)Å long. The closest intramolecular non-bonded contact is 3.07(1)Å between Cl and C(80). Data on the least-squares planes of the ligand rings appears in Table VI. The Cl-U-Cl angle of 148.29(8)° is by symmetry bisected by the U-N bond. The Cl-U-Cp"(centroid) angle is 95.7°, and the Cp"-U-Cp" angle is 137.1°. The Cp"-U-N angle is 111.4°. Pertinent bond angles and distances are listed in Table VII.

$UCp"_2Cl$(pyrazolate)

The crystal structure consists of discrete mononuclear units at general positions in the unit cell (Fig 4). The closest intermolecular contact is 3.41(3)Å between C(17) and C(20'). The molecular structure consists of a uranium ion coordinated by two η^5-pentamethyl cyclopentadienide rings, one chloride ion, and two nitrogens from the pyrazolate ion for a formal coordination number of 9. The coordination geometry is very roughly tetrahedral when considering the chloride, the Cp" centroids, and the midpoint of the N-N bond as the ligands. The angles from both the N-N midpoint and the chloride to each of the other three ligands are approximately equal; either serves as the apex of a tetrahedron in which the basal angles are distorted by the 136° angle between the Cp" centroids. Figure 5 illustrates the molecular structure utilizing one nominal orientation for each Cp" ring

The uranium-carbon distances range between 2.69(1)Å and 2.78(1)Å, averaging 2.73(3)Å. The U-N distances are 2.351(5)Å and 2.349(5)Å. The U-Cl distance is 2.611(2)Å. Within a molecule, the closest inter-ligand non-bonded contact is 3.00(2)Å between N(1) and C(16'). Selected bond lengths and angles appear in Table VIII.

Least-squares planes for the 4 Cp" rings show all but that of C's 11-15 are planar to about one sigma; C's 13 and 14 are about two sigma from their least-squares plane (Table

IX). The methyl carbons generally are tilted away from the uranium by tenths of an Angstrom (5-15 sigma); one methyl carbon from each ring, however, is much more nearly coplanar with the internal carbons of the ring to which it belongs. The pyrazolate ring is planar to within one sigma, and the three pyrazolate carbon atoms are about one sigma from the UN_2 plane.

$\underline{UCp"_2(pyrazolate)_2}$

The crystal structure consists of discrete mononuclear units at general positions in the unit cell (Fig 6). The closest intermolecular contacts are 3.638(8) and 3.637(9)Å between C(10) and C(2) and C(7) respectively. The molecular structure consists of the uranium ion coordinated by two η^5-pentamethylcyclopentadienide rings and 4 nitrogens from the two pyrazolate rings, for a total formal coordination number of 10. The pyrazolates are adjacent and nearly coplanar while they oppose the two Cp" rings, whose least-squares planes are about 40° from each other (vide infra). A perspective drawing of the molecule appears in Figure 7, where one can see relatively high thermal motion in Cp"2.

The U-carbon distances range from 2.724(6)Å to 2.786(5)Å, averaging 2.75(2)Å. The U-N distances are 2.403(4)Å, 2.360(5)Å, 2.363(5)Å, and 2.405(5)Å. The closest intramolecular non-bonded contact is 3.006(6)Å between N's 2 and 3 . Selected bond lengths and angles appear in Table X.

The internal carbons of both Cp" rings are essentially planar, deviations from the least squares plane being on the order of one sigma. Also, the methyl carbons are all bent out away from the uranium ion by a few tenths of an Angstrom. Both pyrazolates are planar. The average deviation from the UN_4 least squares plane is 0.003 Å (ca. 5 σ). The angles between the least squares planes of the Cp" rings is 41.4°, between the pyrazolates is 5.6°, and between the Cp"s and the pyrazolates 20.2°,25.3°,21.6°,and16.1° (Cp"1-pyz1,2;;Cp"2-pyz1,2). Complete data on the least squares planes appear in Table XI.

Discussion

These structures constitute the first formal reports of bis-pentamethylCp uranium 4+ compounds. Marks has presented unpublished results on the structure of $UCp"_2(CONMe_2)_2$[17] and has published structural results on $[UCp"_2Cl]_3$[4] , $[ThCp"_2H_2]_2$[18], and $[ThCp"_2O_2C_2Me_2]_2$[19]. More unpublished results include the structures of $ThCp"_2Cl(COCH_2CMe_3)$ and $ThCp"_2Cl(CONEt_2)$[17]. In addition, the structures of numerous Ti^{4+} and Zr^{4+} compounds of the type MCp_2X_2 have been reported[20,21].

The larger size of the methylated Cp* rings means fewer of them are able to share a coordination sphere, relative to the numerous compounds with unsubstituted Cp rings of general formula MCp_3X[22]. The Cp-U-Cp angles in these compounds is less than 120°, wereas the present compounds share a

value for this angle of about 137°. All the Cp" ligands characterized here exhibit the bending outward of the methyl groups as is quite common for the ligand. The U-Cl distance in $UCp"_2Cl$(pyrazolate) (2.611 Å) is similar to those found in other U^{4+} organometallics[23-26], but the U-Cl distance in $UCp"_2Cl_2$(pyrazole) (2.696(2)Å) is considerably longer. This is probably best attributed to the relatively greater crowding the chloride in $UCp"_2Cl_2$(pyrazole) experiences.

The average U-C(ring) distances are nearly identical for the three compounds, and the two rings bear a constant relationship to each other of 137°. In $UCp"_2Cl_2$(pyrazole), the two Cp" centroids and N(1) are coplanar by symmetry. The 137° angle between centroids leaves 111.5° between each of the centroids and N(1). We also see that the Cp"-U-Cl angle is 95° (Table XII).

In moving to $UCp"_2Cl$(pyrazolate), the angles from the Cp"'s to the other ligands is raised from 95° by the removal of one ligand. Also as a result of there being fewer ligands, the Cl-U-(N-N) angle relaxes to 103° from the 148° for the Cl-U-Cl angle in $UCp"_2Cl_2$(pyrazole). In going to $UCp"_2(pyrazolate)_2$, substitution of a sterically larger pyrazolate for the remaining chloride results in an increase in the (N-N)-U-(N-N) angle relative to the Cl-U-(N-N) angle in $UCp"_2Cl$(pyrazolate), while also the Cp"-U-(N-N) angles decrease slightly on average. This behavior is the same as that seen in the thorium compounds (Table XIII). The Cp"-

Th-Cp" angle decreases in going from the small bridging hydride ligands to the larger bridging enediolate ligands, and the monomeric species, where crowding is decreased, exhibit the largest angles. We see, then, that the inter-ligand relationships in these compounds can be explained with steric arguments.

In $UCp"_2(pyrazolate)_2$, Cp"(2) exhibits much more thermal motion than Cp"(1). This is probably the result of the fact that Cp"(2) has fewer non-bonded neighbors than Cp"(1). For instance, the closest intermolecular contact in this compound is 3.64 Å and involves atoms of Cp"(1) (vide supra). The closest such contact for Cp"(2) is 3.72 Å (C(19)-C(19)). In addition, Cp"(1) has 33 intermolecular contacts within 4.5 Å, while Cp"(2) has only 29.

The disorder in $UCp"_2Cl(pyrazolate)$ can also be explained in terms of intermolecular contacts. Although the closest intermolecular contact is shorter than in $UCp"_2(pyrazolate)_2$ (3.413(3)Å vs. 3.638(8)Å), in $UCp"_2Cl(pyrazolate)$), Cp"(2) and Cp"(2') have only 34 contacts within 4.5 Å, or 17 contacts per 5 methyl carbons. The occupancy factors for Cp"(1) refined to .62/.38, while for Cp"(2) they refined to .50/.50 . The fact that Cp"(1) has many more contacts (32 per 5 methyl carbons) explains its greater preference for one orientation over the other, inasmuch as the orientation is determined by the intermolecular environment.

The U-N distance in $UCp"_2Cl_2$(pyrazole) is much longer than those reported in UCp_3(pyrazolate)[1], and this is undoubtedly due to the electrical neutrality of the pyrazole ligand. In $UCp"_2$(pyrazolate)$_2$, we see the same U-N distances found in UCp_3(pyrazolate), i.e. 2.36 Å and 2.40 Å. The origin of 0.04 Å difference in UCp_3(pyrazolate) is difficult to explain, but even more mystifying is the pattern of the U-N bond lengths in $UCp"_2$(pyrazolate)$_2$. The shorter bonds are those from uranium to the "internal" nitrogens where the crowding is greatest (vide supra), while the longer bonds are those to the "external" nitrogens where the crowding is less. However, in $UCp"_2Cl$(pyrazolate) the U-N distances are identical, as one would expect by almost any argument.

Of the other physical properties of these compounds, a couple are worthy of mention. The pmr spectrum of $UCp"_2Cl_2$(pyrazole) reveals a fluxionality of the pyrazole ligand. At low temperature, four resonances are resolved that can be assigned to the pyrazole. Those most strongly shifted can be assigned to the C-H and N-H adjacent to the metal-bound nitrogen, while those less strongly shifted are the protons further from the uranium. By room temperature, the four resonances have collapsed into a broad singlet and a very broad resonance, indicative of a fluxional U-N bond that makes all the carbon bound protons nearly equivalent and leaves the remaining proton's resonance quite broad and less strongly shifted than previously.

The magnetic behavior of both $UCp"_2Cl_2$(pyrazole) and $UCp"_2Cl$(pyrazolate) is as one expects for U^{4+} ions. However, $UCp"_2$(pyrazolate)$_2$ does not exhibit similar magnetic behavior. Instead of decreasing with increasing temperature from an initial high value as the others, the susceptibility of $UCp"_2$(pyrazolate)$_2$ has its minimum at low temperature and increases as the temperature increases, until it becomes relatively invariant with temperature. While temperature independent paramagnetism is common in U^{4+} compounds, the behavior seen for $UCp"_2$(pyrazolate)$_2$ remains a matter for conjecture.

Table Ia. Magnetic Susceptibility for $UCp"_2Cl_2$(pyrazole)

T(K)	$x_M^{corr}x10^3$ (cm^3/mol)
5.4	30.26
9.0	27.16
17.9	23.83
27.8	21.46
37.4	52.18
46.4	58.52
60.2	73.69

Table Ib. Magnetic Susceptibility for $UCp"_2Cl$(pyrazolate)

T(K)	$x_M^{corr} x10^3$ (cm^3/mol)
4.2	93.17
9.1	57.89
17.9	31.47
27.8	21.23
37.4	16.20
46.4	12.81
60.2	10.69
77.6	9.34

Table Ic. Magnetic Susceptibility for $UCp''_2(pyrazolate)_2$	
T(K)	$x_M^{corr} x10^3$ (cm^3/mol)
6.1	2.57
8.6	4.37
17.9	7.56
27.5	9.29
37.2	9.42
46.3	8.82
60.2	8.58
77.6	8.73

Table II. Cell Parameters for $UCp"_2Cl_2(pyrazole)$, $UCp"_2Cl(pyrazolate)$, and $UCp"_2(pyrazolate)_2$

	HPYZ	1:1	1:2
space group	Cmcm	$P2_1/n$	C2/c
a(Å)	13.697(4)	8.737(1)	33.326(2)
b(Å)	11.496(2)	18.068(1)	10.450(2)
c(Å)	15.555(2)	15.229(2)	16.646(1)
β(°)	90	92.38(1)	117.09(1)
Vol.($Å^3$)	2449.4(14)	2401.9(6)	5160.8(17)
molecules/cell	4	4	8
$d_{calc}(g/cm^3)$	1.756	1.690	1.654
$d_{obs}(g/cm^3)$	1.77	1.68	1.66
observations	924	2566	2706
parameters	75	201	280
R	2.45%	3.27%	2.43%
R_w	3.48%	4.50%	3.31%

HPYZ is $UCp"_2Cl_2(pyrazole)$

1:1 is $UCp"_2Cl(pyrazolate)$

1:2 is $UCp"_2(pyrazolate)_2$

Table III. UCp''_2Cl_2(pyrazole)

POSITIONAL AND THERMAL PARAMETERS AND THEIR ESTIMATED STANDARD DEVIATIONS.

ATOM	X	Y	Z	B(1,1)	B(2,2)	B(3,3)	B(1,2)	B(1,3)	B(2,3)
U	0.0000(0)	0.22632(3)	0.2500(0)	0.00421(2)	0.00532(3)	0.00358(2)	0.0000(0)	0.0000(0)	0.0000(0)
CL	0.1893(2)	0.2984(2)	0.2500(0)	0.00448(9)	0.0131(3)	0.0087(1)	-0.0004(3)	0.0000(0)	0.0000(0)
N1	0.0000(0)	0.4531(8)	0.2500(0)	0.0089(7)	0.0041(7)	0.0093(7)	0.0000(0)	0.0000(0)	0.0000(0)
N2	0.0776(0)	0.6222(0)	0.2500(0)	0.0066(0)	0.0082(0)	0.0121(0)	-0.0035(0)	0.0000(0)	0.0000(0)
C11	0.0616(6)	0.2273(5)	0.0918(4)	0.0077(4)	0.0114(6)	0.0038(3)	-0.0028(7)	0.0017(6)	0.0018(6)
C21	0.0835(6)	0.1173(6)	0.1119(4)	0.0096(4)	0.0123(6)	0.0042(3)	0.0070(9)	0.0012(6)	-0.0008(7)
C31	0.0000(0)	0.0516(8)	0.1287(5)	0.0160(9)	0.0077(7)	0.0035(3)	0.0000(0)	0.0000(0)	-0.0021(9)
C71	0.4496(8)	0.1397(9)	0.2500(0)	0.0104(7)	0.0069(8)	0.0165(11)	0.0022(14)	0.0000(0)	0.0000(0)
C80	0.0776(12)	0.6222(16)	0.2500(0)	0.0066(10)	0.0082(16)	0.0121(16)	-0.0035(23)	0.0000(0)	0.0000(0)
C41	0.1136(6)	0.3256(9)	0.0442(5)	0.0134(6)	0.0205(9)	0.0067(4)	-0.0120(13)	0.0041(8)	0.0071(10)
C61	0.0000(0)	-0.0791(10)	0.1467(7)	0.0412(25)	0.0063(9)	0.0063(6)	0.0000(0)	0.0000(0)	-0.0035(12)
C51	0.1091(6)	0.0728(9)	0.1145(5)	0.0121(5)	0.0310(12)	0.0088(5)	0.0258(11)	0.0013(9)	-0.0063(13)

THE FORM OF THE ANISOTROPIC THERMAL PARAMETER IS:

EXP[-(B(1,1)*H*H + B(2,2)*K*K + B(3,3)*L*L + B(1,2)*H*K + B(1,3)*H*L + B(2,3)*K*L)].

Table IV. UCp_2^3Cl(pyrazolate)

POSITIONAL AND THERMAL PARAMETERS AND THEIR ESTIMATED STANDARD DEVIATIONS.

ATOM	X	Y	Z	B(1,1) or B_{iso}	B(2,2)	B(3,3)	B(1,2)	B(1,3)	B(2,3)
U	0.40954(3)	0.10361(2)	0.26343(2)	0.00976(4)	0.00221(1)	0.00367(1)	0.00038(4)	0.00044(4)	-0.00008(2)
Cl	0.6845(3)	0.1054(1)	0.3375(2)	0.0123(3)	0.0062(1)	0.0073(1)	-0.0014(3)	-0.0043(4)	0.0024(2)
N1	0.2119(8)	0.0393(4)	0.3387(5)	4.5(1)					
N2	0.3419(8)	0.0261(4)	0.3705(5)	5.2(2)					
C1	0.378(1)	-0.0228(7)	0.1671(9)	4.2(3)					
C2	0.319(2)	0.0352(8)	0.1147(10)	5.6(3)					
C3	0.438(1)	0.0771(7)	0.0882(8)	3.1(2)					
C4	0.569(1)	0.0528(7)	0.1262(9)	4.1(3)					
C5	0.535(2)	-0.0099(8)	0.1766(9)	4.9(3)					
C6	0.258(2)	-0.0826(11)	0.1909(14)	8.3(5)					
C7	0.158(3)	0.0527(13)	0.0789(15)	9.6(6)					
C8	0.458(2)	0.1379(12)	0.0132(14)	8.0(5)					
C9	0.748(3)	0.0655(13)	0.1281(16)	9.9(6)					
C10	0.626(3)	-0.0659(17)	0.2304(16)	11.3(7)					
C11	0.287(2)	0.2118(8)	0.3818(10)	3.6(3)					
C12	0.276(2)	0.2364(9)	0.2198(10)	3.6(3)					
C13	0.438(2)	0.2636(9)	0.2378(10)	3.3(3)					
C14	0.454(2)	0.2453(9)	0.3314(11)	3.9(3)					
C15	0.328(2)	0.2178(9)	0.3657(10)	3.5(3)					
C16	0.021(3)	0.1955(15)	0.2833(18)	9.2(7)					
C17	0.224(3)	0.2589(13)	0.1284(16)	7.6(6)					
C18	0.555(3)	0.2988(12)	0.1984(16)	6.9(5)					
C19	0.576(3)	0.2683(14)	0.3881(17)	8.5(6)					
C20	0.253(4)	0.1938(19)	0.4497(24)	12.7(10)					
C21	0.386(1)	-0.0218(6)	0.4456(7)	7.0(3)					
C22	0.154(1)	-0.0347(6)	0.4421(7)	6.2(2)					
C23	0.102(1)	0.0009(6)	0.3714(7)	7.0(3)					
C1'	0.464(2)	-0.0382(9)	0.1858(11)	2.1(3)					
C2'	0.322(2)	-0.0048(11)	0.1442(13)	3.3(4)					
C3'	0.346(3)	0.0524(12)	0.0942(15)	4.2(5)					
C4'	0.518(2)	0.0665(12)	0.1010(14)	4.0(4)					
C5'	0.561(2)	0.0176(12)	0.1508(14)	4.2(4)					
C11'	0.238(2)	0.2078(9)	0.3468(11)	4.0(3)					
C12'	0.197(1)	0.2142(7)	0.2499(9)	2.7(3)					
C13'	0.326(2)	0.2420(8)	0.2051(10)	3.6(3)					
C14'	0.434(2)	0.2521(10)	0.2705(11)	4.6(4)					
C15'	0.398(2)	0.2320(10)	0.3528(12)	5.2(4)					
C6'	0.475(5)	-0.1019(19)	0.2369(30)	9.0(11)					
C7'	0.157(5)	-0.0395(22)	0.1312(28)	10.0(11)					
C8'	0.327(5)	0.1123(19)	0.0111(30)	10.1(11)					
C9'	0.684(4)	0.1087(15)	0.0852(24)	7.4(8)					
C10'	0.739(4)	-0.0235(20)	0.2027(23)	9.1(9)					
C16'	0.102(3)	0.1020(13)	0.4075(16)	7.9(6)					
C17'	0.031(3)	0.1969(12)	0.2092(14)	6.0(5)					
C18'	0.334(3)	0.2695(13)	0.1140(16)	8.2(6)					
C19'	0.505(3)	0.2934(18)	0.2684(22)	11.7(9)					
C20'	0.466(4)	0.2375(17)	0.4458(20)	11.2(8)					

THE FORM OF THE ANISOTROPIC THERMAL PARAMETER IS:

EXP[-(B(1,1)*H*H + B(2,2)*K*K + B(3,3)*L*L + B(1,2)*H*K + B(1,3)*H*L + B(2,3)*K*L)].

Table V. UCp^{π}_2(pyrazolate)$_2$

POSITIONAL AND THERMAL PARAMETERS AND THEIR ESTIMATED STANDARD DEVIATIONS.

ATOM	X	Y	Z	B(1,1)	B(2,2)	B(3,3)	B(1,2)	B(1,3)	B(2,3)
U	0.12839(1)	0.20541(2)	0.05748(1)	0.00083(0)	0.00684(2)	0.00378(1)	0.00011(1)	0.00147(1)	-0.00022(3)
N1	0.1729(2)	0.4758(5)	0.0819(3)	0.00135(6)	0.0085(6)	0.00556(2)	-0.0007(3)	0.0027(2)	-0.0002(6)
N2	0.1613(2)	0.4332(6)	-0.0023(3)	0.00146(6)	0.0108(6)	0.0047(2)	-0.0015(3)	0.0025(2)	-0.0008(7)
N3	0.1528(2)	0.2849(5)	-0.0984(4)	0.00178(7)	0.0113(7)	0.0048(2)	0.0008(4)	0.0018(2)	-0.0014(7)
N4	0.0884(2)	0.1198(5)	-0.0489(3)	0.00125(6)	0.0099(6)	0.0064(3)	-0.0009(3)	0.0019(2)	-0.0041(7)
C1	0.2168(2)	0.2862(6)	0.1445(4)	0.00083(6	0.0108(7)	0.0043(3)	0.0013(4)	0.0015(2)	0.0021(8)
C2	0.1918(2)	0.0965(6)	0.0991(4)	0.00114(7	0.0108(7)	0.0048(3)	0.0025(4)	0.0015(2)	0.0019(7)
C3	0.1662(2)	0.0588(6)	0.1438(4)	0.00119(7	0.0073(6)	0.0058(3)	0.0006(4)	0.0018(2)	0.0048(8)
C4	0.1749(2)	0.1453(7)	0.2157(4)	0.00115(6	0.0110(7)	0.0047(3)	0.0017(4)	0.0021(2)	0.0036(9)
C5	0.2068(2)	0.2377(7)	0.2149(4)	0.00112(7	0.0108(7)	0.0048(3)	0.0009(4)	0.0018(2)	0.0007(8)
C6	0.2523(2)	0.2739(8)	0.1269(5)	0.00126(7	0.0165(10)	0.0084(3)	0.0004(5)	0.0039(2)	0.0058(11)
C7	0.1941(2)	0.0264(8)	0.0229(4)	0.00198(9	0.0156(10)	0.0055(3)	0.0042(5)	0.0027(2)	-0.0018(10)
C8	0.1393(3)	-0.0648(8)	0.1272(6)	0.00217(11	0.0095(8)	0.0092(5)	-0.0028(5)	0.0026(4)	0.0028(12)
C9	0.1628(2)	0.1232(9)	0.2938(4)	0.00201(8	0.0213(13)	0.0068(3)	0.0028(6)	0.0048(2)	0.0008(11)
C10	0.2259(2)	0.3482(8)	0.2821(4)	0.00168(9	0.0142(9)	0.0048(3)	0.0001(6)	0.0005(3)	-0.0034(11)
C11	0.0645(2)	0.4716(8)	0.1044(5)	0.00154(8	0.0123(9)	0.0106(4)	0.0018(4)	0.0044(3)	-0.0062(10)
C12	0.0668(2)	0.4794(8)	0.0158(6)	0.00158(7	0.0137(9)	0.0084(4)	0.0041(4)	0.0042(2)	0.0073(10)
C13	0.0417(2)	0.3742(10)	-0.0229(5)	0.00078(7	0.0275(13)	0.0066(4)	0.0035(5)	0.0002(3)	-0.0107(12)
C14	0.0453(2)	0.2931(7)	0.0511(7)	0.00142(6	0.0092(8)	0.0210(6)	-0.0006(4)	0.0006(3)	-0.0067(12)
C15	0.0724(2)	0.3621(10)	0.1296(5)	0.00207(8	0.0213(12)	0.0089(3)	0.0057(5)	0.0061(2)	0.0042(12)
C16	0.1134(3)	0.5738(11)	0.1762(7)	0.00241(14	0.0271(14)	0.0178(7)	-0.0003(8)	0.0047(5)	-0.0273(15)
C17	0.0712(3)	0.5965(10)	-0.0339(7)	0.00478(14	0.0238(12)	0.0246(7)	0.0148(7)	0.0159(4)	0.0325(16)
C18	0.0119(3)	0.3494(15)	-0.1238(7)	0.00232(14	0.0661(25)	0.0093(6)	0.0154(9)	-0.0016(5)	-0.0241(19)
C19	0.0202(3)	0.1659(12)	0.0484(11)	0.00393(11	0.0137(12)	0.0633(13)	-0.0034(7)	0.0276(4)	-0.0069(26)
C20	0.0793(3)	0.3277(14)	0.2288(6)	0.00491(14	0.0471(23)	0.0124(4)	0.0108(9)	0.0125(3)	0.0202(10)
C21	0.1991(2)	0.5822(8)	0.0981(5)	0.00164(8	0.0117(8)	0.0091(4)	-0.0018(5)	0.0039(3)	0.0011(11)
C22	0.2038(2)	0.6108(7)	0.0288(5)	0.00213(9	0.0113(9)	0.0099(4)	-0.0015(5)	0.0049(3)	0.0032(11)
C23	0.1798(2)	0.5153(8)	-0.0408(5)	0.00195(9	0.0152(10)	0.0074(4)	-0.0013(5)	0.0035(3)	0.0057(11)
C24	0.0891(3)	0.1678(9)	-0.1766(5)	0.00263(12	0.0166(11)	0.0048(3)	0.0021(6)	0.0027(3)	-0.0029(11)
C25	0.0653(2)	0.0531(9)	-0.1914(5)	0.00176(10	0.0206(12)	0.0076(4)	0.0021(6)	0.0017(3)	-0.0102(12)
C26	0.0654(2)	0.0253(9)	-0.1103(6)	0.00154(10	0.0175(11)	0.0102(5)	-0.0021(6)	0.0021(4)	-0.0115(13)

THE FORM OF THE ANISOTROPIC THERMAL PARAMETER IS:

EXP[-(B(1,1)*H*H + B(2,2)*K*K + B(3,3)*L*L + B(1,2)*H*K + B(1,3)*H*L + B(2,3)*K*L)].

Table VI. Least-Squares Plane for $UCp"_2Cl_2$(pyrazole)

atom	dist(Å)	parameters	
C(11)	.003(6)	A	-.0001
C(21)	-.009(6)	B	-.3480
C(31)	.011(9)	C	-.9375
C(12)	.003(6)	D	-2.0935
C(22)	-.008(6)		

Table VII. Bond Distances (Å) and Angles (°) for $UCp"_2Cl_2$(pyrazole)

U-Cl	2.696(2)	C(11)-C(12)	1.410(11)
U-C(11)	2.722(5)	C(11)-C(21)	1.422(7)
U-C(21)	2.737(5)	C(11)-C(41)	1.525(8)
U-C(31)	2.756(7)	C(21)-C(31)	1.396(7)
U-N(1)	2.607(8)	C(21)-C(51)	1.535(7)
C(31)-C(61)	1.525(12)	Cl-U-Cl	148.29(8)
N(1)-C(80)	1.327(14)	Cl-U-N(1)	74.14(4)
C(80)-C(71)	1.401(17)	Cl-U-Cp	95.73(1)
C(71)-C(72)	1.384(16)	Cp-U-N(1)	111.44(1)
U-C(ave)	2.74(2)	Cp-U-Cp	137.1
C(12)-C(11)-C(21)		108.0(3)	
C(12)-C(11)-C(41)		123.9(4)	
C(41)-C(11)-C(21)		127.8(6)	
C(11)-C(21)-C(51)		126.6(6)	
C(11)-C(21)-C(31)		107.0(5)	
C(51)-C(21)-C(31)		125.9(6)	
C(21)-C(31)-C(61)		124.5(3)	
C(21)-C(31)-C(22)		110.1(7)	
N(2)-N(1)-C(80)		106.(1)	
N(1)-C(80)-C(71)		111.(1)	
C(80)-C(71)-C72)		105.4(6)	

Table VIIIa. Bond Distances (Å) and Angles (°) for $UCp"_2Cl$(pyrazolate)

U-X distances

C(1),C(1')	2.72(1),2.75(1)	C(11),C(11')	2.72(1),2.73(1)
C(2),C(2')	2.69(1),2.75(2)	C(12),C(12')	2.74(1),2.73(1)
C(3),C(3')	2.72(1),2.77(2)	C(13),C(13')	2.75(1),2.74(1)
C(4),C(4')	2.72(1),2.76(2)	C(14),C(14')	2.78(1),2.70(1)
C(5),C(5')	2.70(1),2.73(2)	C(15),C(15')	2.70(1),2.69(2)
N(1),N(2)	2.351(5),2.349(5)	Cl	2.611(2)
U-C(av)	2.73(3)		

pyrazolate distances and angles

N(1)-C(23)	1.354(9)	around N(1)	104.5(5)
C(23)-C(22)	1.318(10)	around N(2)	107.7(5)
C(22)-C(21)	1.343(10)	around C(21)	109.9(7)
C(21)-N(2)	1.367(9)	around C(22)	104.4(7)
N(2)-N(1)	1.348(7)	around C(23)	113.4(7)

interligand angles

Cp"-U-Cp"	136.2
Cp"(1)-U-Cl	102.5
Cp"(1)-U-(N-N)	104.6
Cp"(2)-U-Cl	98.4
Cp"(2)-U-(N-N)	107.4
Cl-U-(N-N)	103.2
N(1)-U-N(2)	33.3(2)

Table VIIIb. Distances (Å) and Angles (°) for Cp"(1) and Cp"(1') in $UCp"_2Cl$(pyrazolate)

C(1)-C(2)	1.39(2)	1.44(2)	C(1)-C(6)	1.57(2)	1.52(3)
C(2)-C(3)	1.37(2)	1.30(3)	C(2)-C(7)	1.55(2)	1.58(3)
C(3)-C(4)	1.40(2)	1.52(3)	C(3)-C(8)	1.61(2)	1.67(4)
C(4)-C(5)	1.41(2)	1.33(3)	C(4)-C(9)	1.52(2)	1.67(3)
C(5)-C(1)	1.46(2)	1.41(3)	C(5)-C(10)	1.51(2)	1.68(3)

C(5)-C(1)-C(2)	107(1)	107(1)
C(1)-C(2)-C(3)	108(1)	91(1)
C(2)-C(3)-C(4)	112(1)	106(2)
C(3)-C(4)-C(5)	106(1)	108(2)
C(4)-C(5)-C(1)	107(1)	108(2)
C(3)-C(4)-C(9)	140(2)	158(3)
C(5)-C(4)-C(9)	113(2)	94(3)
C(4)-C(5)-C(10)	136(2)	149(3)
C(5)-C(1)-C(6)	139(2)	130(2)
C(2)-C(1)-C(6)	114(2)	123(2)
C(1)-C(2)-C(7)	135(2)	133(3)
C(3)-C(2)-C(7)	116(2)	115(3)
C(2)-C(3)-C(8)	137(2)	160(3)
C(4)-C(3)-C(8)	111(1)	91(3)
C(1)-C(5)-C(10)	117(2)	102(2)

Table VIIIc. Distances (Å) and Angles (°) for Cp"(2) and Cp"(2') of $UCp"_2Cl$(pyrazolate)

C(11)-C(12)	1.48(2);1.50(2)	C(11)-C(16)	1.67(2);1.61(2)
C(12)-C(13)	1.40(2);1.44(2)	C(12)-C(17)	1.61(2);1.58(2)
C(13)-C(14)	1.44(2);1.44(2)	C(13)-C(18)	1.49(2);1.48(2)
C(14)-C(15)	1.34(2);1.25(2)	C(14)-C(19)	1.40(2);1.53(3)
C(15)-C(11)	1.41(2);1.40(2)	C(15)-C(20)	1.53(3);1.55(3)

C(15)-C(11)-C(12)	104(1)	103(1)
C(11)-C(12)-C(13)	109(1)	110(1)
C(12)-C(13)-C(14)	106(1)	100(1)
C(13)-C(14)-C(15)	110(1)	116(2)
C(14)-C(15)-C(11)	112(1)	113(2)
C(13)-C(14)-C(19)	131(2)	121(2)
C(15)-C(14)-C(19)	119(2)	122(2)
C(14)-C(15)-C(20)	146(2)	132(2)
C(15)-C(11)-C(16)	146(2)	141(2)
C(12)-C(11)-C(16)	110(2)	116(2)
C(11)-C(12)-C(17)	140(2)	123(1)
C(13)-C(12)-C(17)	111(2)	127(1)
C(12)-C(13)-C(18)	136(2)	129(2)
C(14)-C(13)-C(18)	117(2)	129(2)
C(11)-C(15)-C(20)	103(2)	117(2)

Table IX. Least-Squares Planes for $UCp"_2Cl$(pyrazolate)

Cp"(1)		Cp"(2)	
atom	dist(Å)	atom	dist(Å)
C(1)	.019(13)	C(11)	-.002(15)
C(2)	-.023(15)	C(12)	-.016(16)
C(3)	.019(12)	C(13)	.028(15)
C(4)	-.006(13)	C(14)	-.031(16)
C(5)	-.008(14)	C(15)	.021(15)
A= .15	B= -.58	A=.29	B= -.94
C= -.80	D= -1.34	C= -.17	D= -3.93

pyrazolate

atom	dist(Å)	
C(21)	.010(11)	A= .19
C(22)	-.012(10)	B= -.80
C(23)	.010(11)	C= -.57
N(1)	-.004(7)	D= -3.13
N(2)	-.004(8)	

Table X. Bond Distances (Å) and Angles (°) for $UCp"_2(pyrazolate)_2$

U-X distances

C(1)	2.753(5)	C(11)	2.753(6)	N(1)	2.403(4)
C(2)	2.740(5)	C(12)	2.738(6)	N(2)	2.360(5)
C(3)	2.759(5)	C(13)	2.735(6)	N(3)	2.363(5)
C(4)	2.786(5)	C(14)	2.724(6)	N(4)	2.405(5)
C(5)	2.763(5)	C(15)	2.757(6)	U-C(av)	2.75(2)

Pyrazolate distances

N(1)-N(2)	1.349(6)	N(3)-N(4)	1.348(7)
N(1)-C(21)	1.362(8)	N(3)-C(24)	1.352(8)
C(21)-C(22)	1.411(9)	C(24)-C(25)	1.388(11)
C(22)-C(23)	1.386(10)	C(25)-C(26)	1.380(11)
C(23)-N(2)	1.373(8)	C(26)-N(4)	1.31(8)

Angles of interest

Cp"(1)-U-Cp"(2)	137.2	Cp"(2)-U-N(3,4)	101.7
Cp"(1)-U-N(1,2)	101.2	N(1,2)-U-N(3,4)	112.2
Cp"(1)-U-N(3,4)	103.1	N(1)-U-N(2)	32.9
Cp"(2)-U-N(1,2)	100.9	N(3)-U-N(4)	32.8

Table XI. Least-Squares Planes for $UCp"_2(pyrazolate)_2$

Cp"(1)		Cp"(2)	
atom	dist(Å)	atom	dist(Å)
C(1)	-.008(6)	C(11)	.000(8)
C(2)	.006(6)	C(12)	-.005(8)
C(3)	-.002(7)	C(13)	.009(8)
C(4)	-.004(7)	C(14)	-.009(8)
C(5)	.008(7)	C(15)	.006(9)
A= -.53	B= .57	A= -.89	B= .44
C= -.62	D= -3.32	C= -.03	D= .36
pyrazolate(1)		pyrazolate(2)	
atom	dist(Å)	atom	dist(Å)
N(1)	.005(5)	N(3)	-.001(7)
N(2)	-.004(6)	N(4)	.001(6)
C(21)	-.009(8)	C(24)	.002(10)
C(22)	.003(9)	C(25)	-.001(9)
C(23)	.004(9)	C(26)	-.001(9)
A= -.75	B= .57	A= -.81	B= .52
C= -.35	D= -1.44	C= -.29	D= -1.83

Table XII. Comparisons Between $UCp"_2Cl_2$(pyrazole), $UCp"_2Cl$(pyrazolate), and $UCp"_2$(pyrazolate)$_2$.

	HPYZ	1:1	1:2
coord.number	9	9	10
U-C(ave)(Å)	2.74(2)	2.73(3)	2.75(2)
U-Cl(Å)	2.696(2)	2.611(2)	---
U-N(Å)	2.607(8)	2.351(5)	2.403(4)
		2.349(5)	2.360(5)
			2.363(5)
			2.405(5)
Cp"-U-Cp"(°)	137	136	137
Cp"-U-N(°)	111.4	---	---
Cp"-U-(N-N)(°)	---	107.4	101.2
		104.6	103.1
			100.9
			101.7
X-U-N(-N)(°)	X=Cl	X=Cl	X=(N-N)
	74.14	103.2	112.2
Cp"-U-Cl(°)	95.7	102.5	---
		98.4	

HPYZ is $UCp"_2Cl_2$(pyrazole)

1:1 is $UCp"_2Cl$(pyrazolate)

1:2 is $UCp"_2$(pyrazolate)$_2$

Table XIII. Distances (Å) and Angles (°) from some reported structures

compound	Cp"-M-Cp"	M-C(ring) ave.	coord. number	ref.
$(ThCp"_2H_2)_2$	130	2.83(1)	9	20
$(ThCp"_2O_2C_2Me_2)_2$	129	2.83(6)	8	21
$ThCp"_2Cl(COCH_2CMe_3)$	138	2.80(3)	9	19
$ThCp"_2Cl(CONEt_2)$	138	2.78(4)	9	19
$UCp"_2(CONMe_2)_2$	138	2.79(1)	10	19

Figure 1. Graph of $\frac{1}{x_M^{corr}}$ vs. T for $UCp"_2(pyrazolate)_2$.

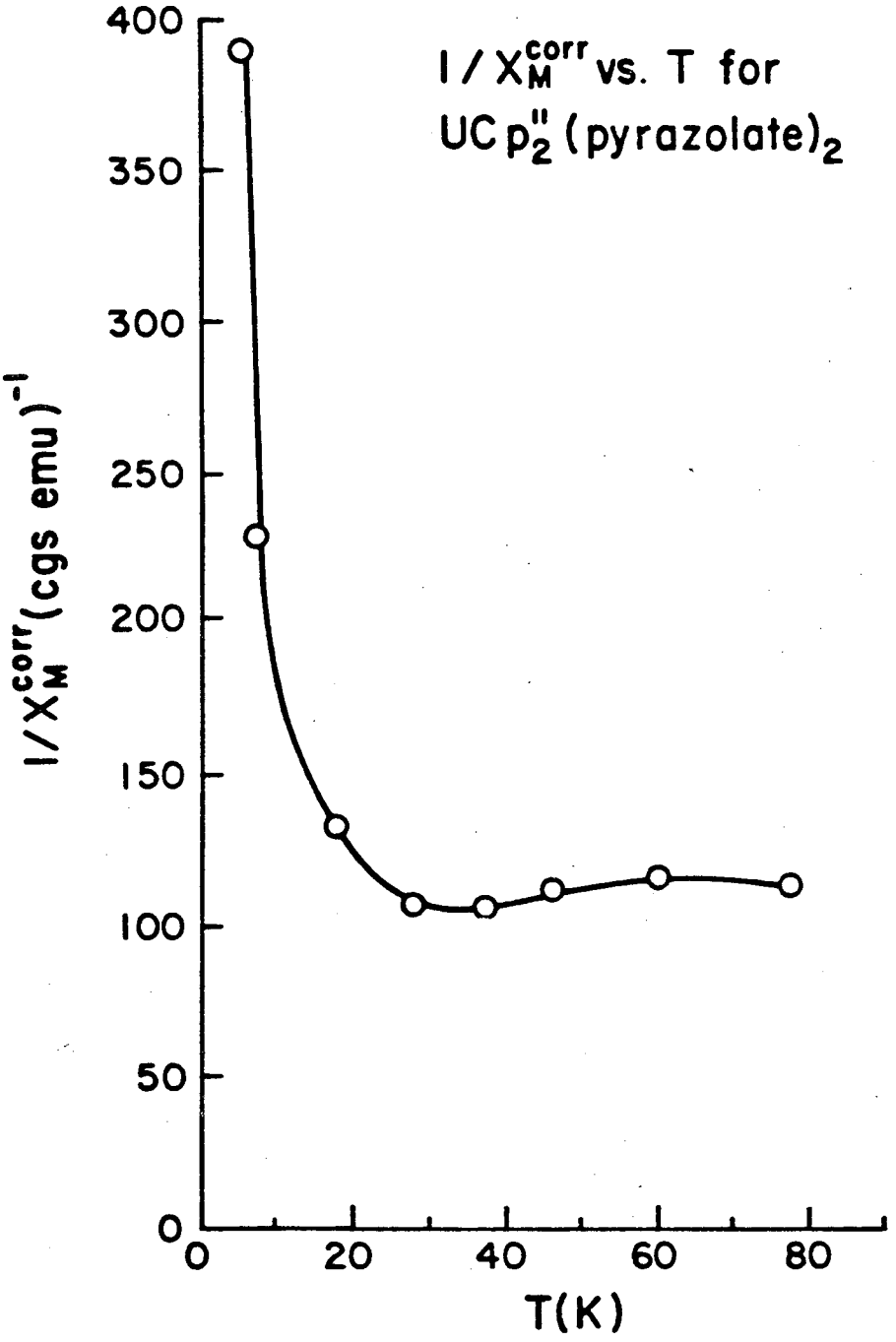
$1/X_M^{corr}$ vs. T for
UCp_2''(pyrazolate)$_2$
$1/X_M^{corr}$(cgs emu)$^{-1}$
400
350
300
250
200
150
100
50
0
0
20
40
60
80
T(K)

XBL 811-7787

Figure 2. Stereoscopic drawing of the unit cell of $UCp"_2Cl_2(pyrazole)$.

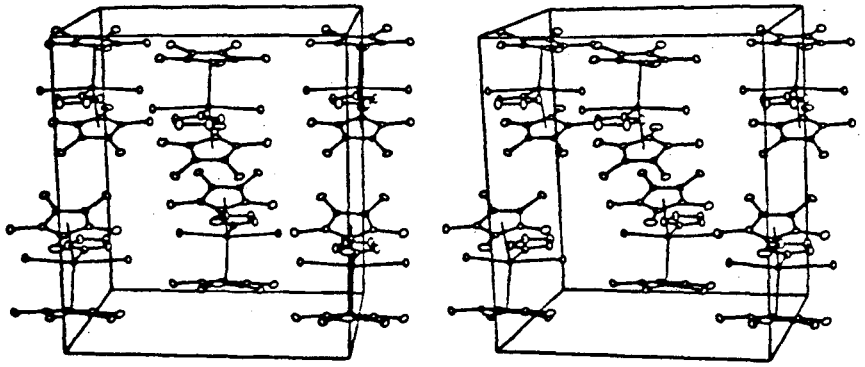

Figure 3. ORTEP drawing of the molecular unit of $UCp''_2Cl_2(pyrazole)$.

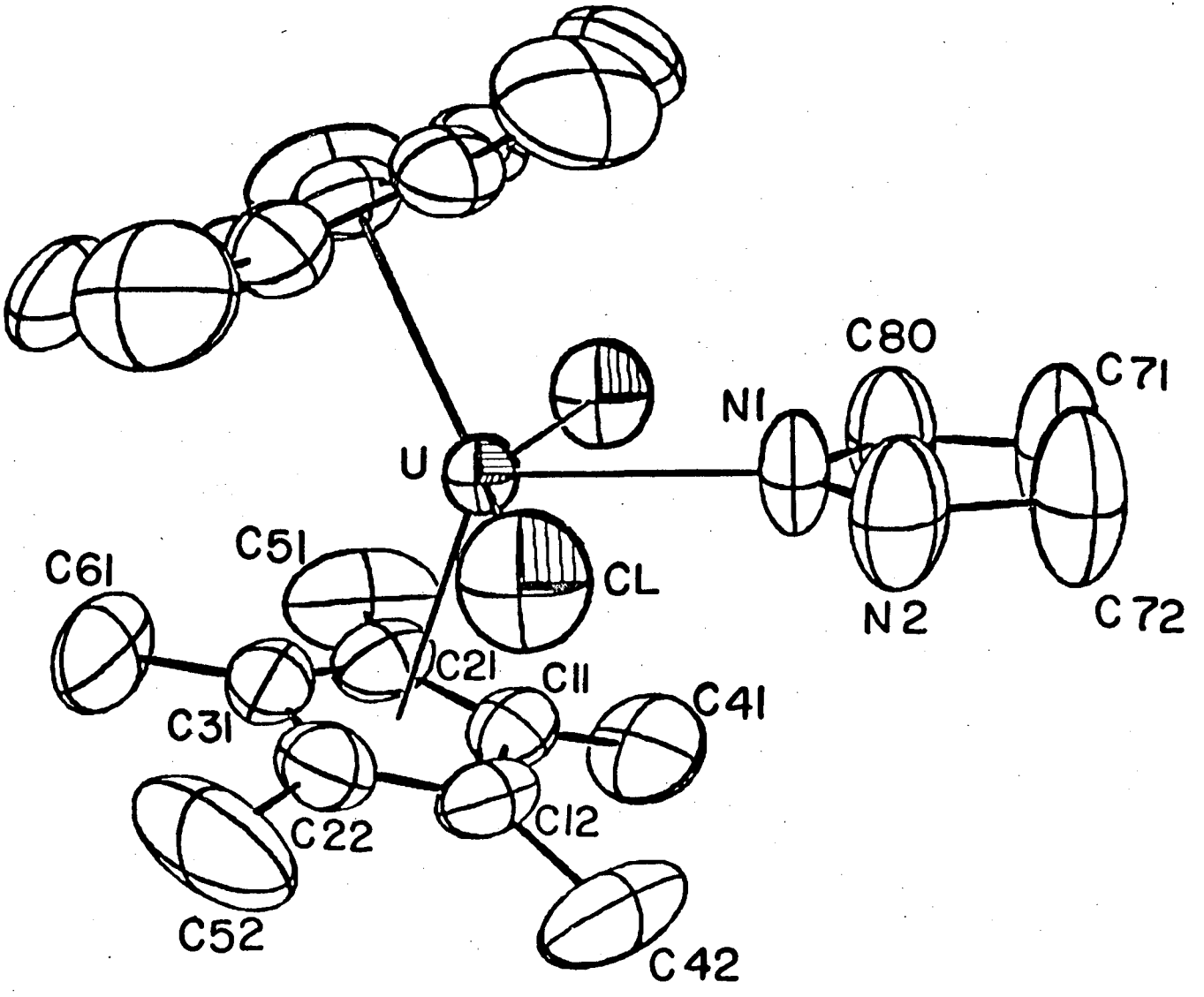

XBL 811-7793

Figure 4. Stereoscopic drawing of the unit cell of $UCp"_2Cl$(pyrazolate).

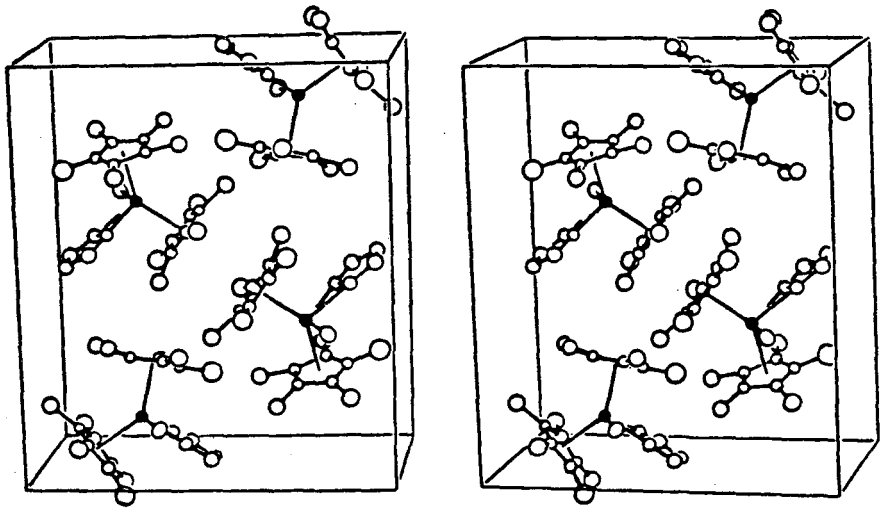

XBL 811-7789

Figure 5. ORTEP drawing of the molecular unit of $UCp"_2Cl$(pyrazolate).

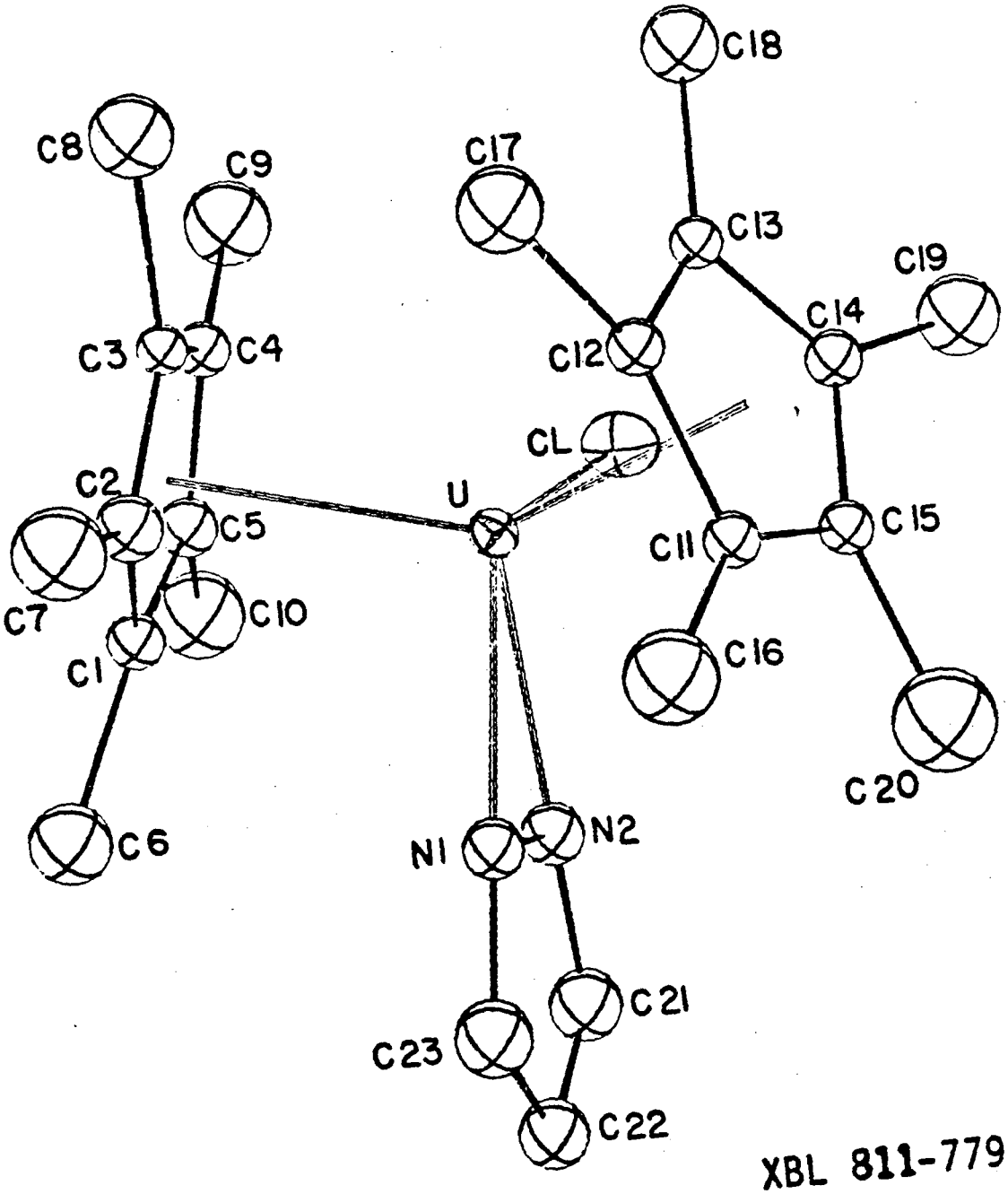
C18
C8
C9
C17
C13
C19
C3
C4
C12
C14
CL
C2
U
C5
C11
C15
C7
C10
C16
C1
C20
C6
N1
N2
C21
C23
C22

XBL 811-7795

Figure 6. Stereoscopic drawing of the unit cell of $UCp"_2(pyrazolate)_2$.

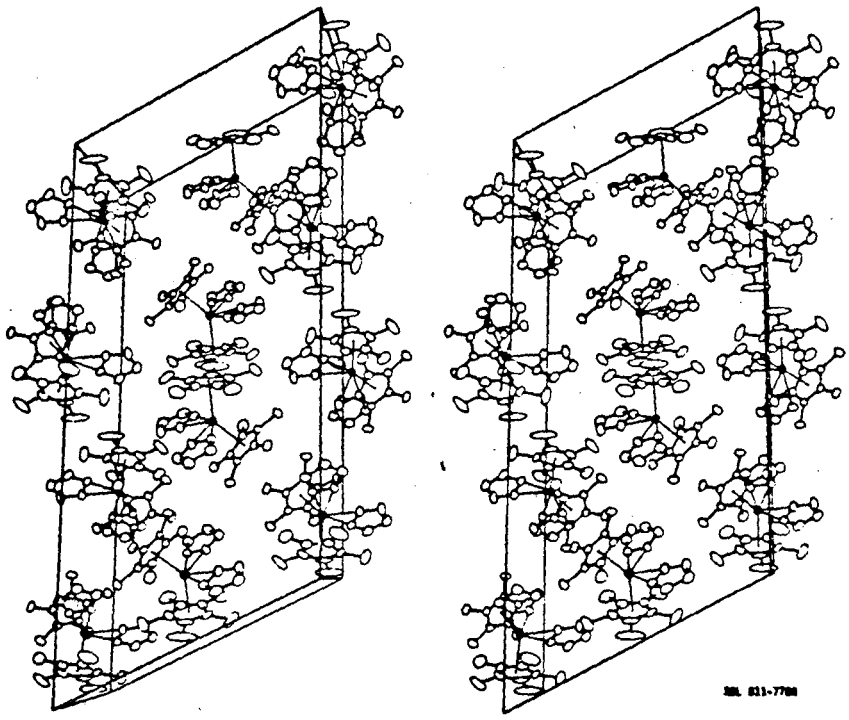

Figure 7. ORTEP drawing of the molecular unit of $UCp"_2(pyrazolate)_2$.

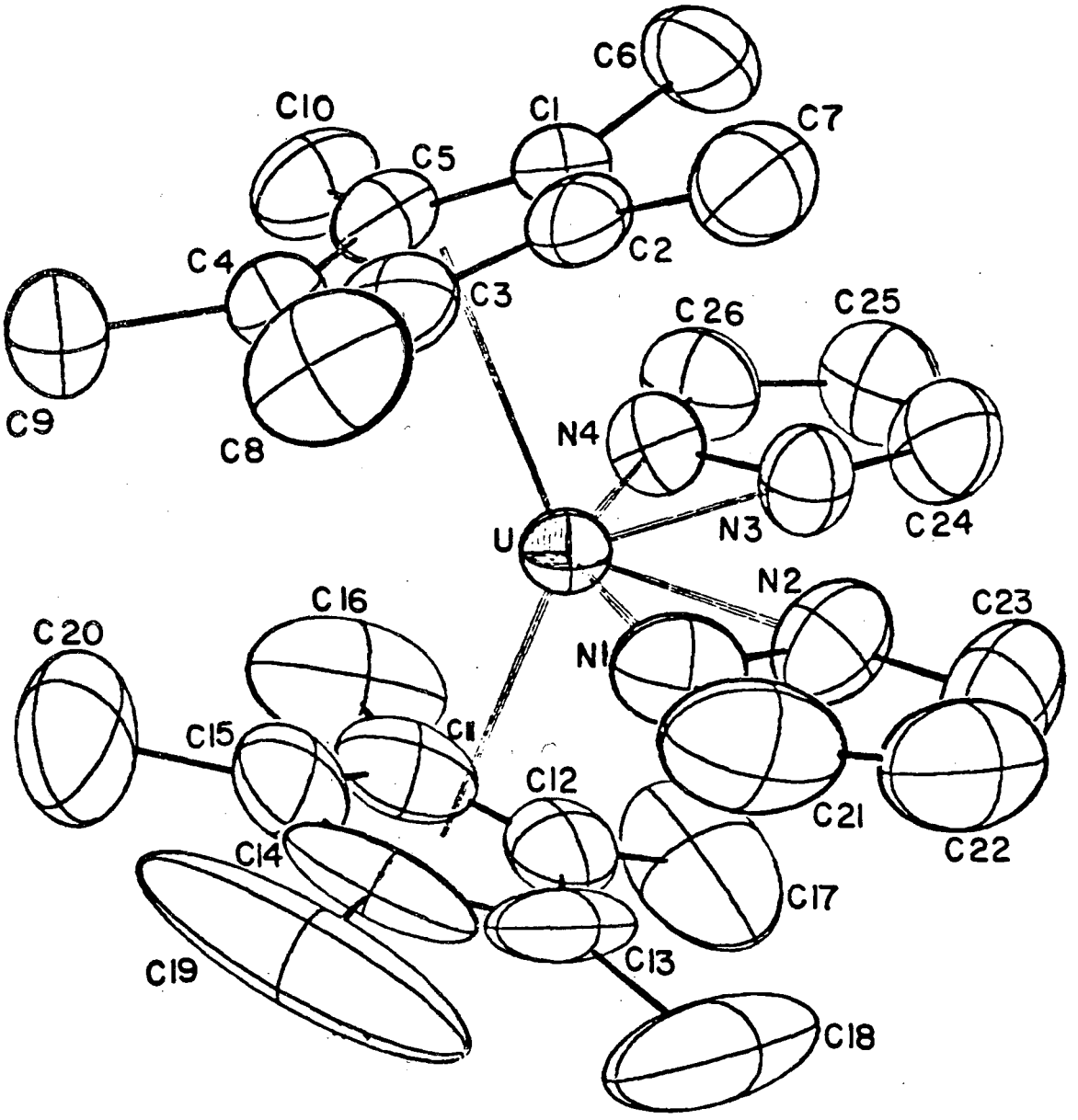
C6
C10
C1
C7
C5
C2
C4
C3
C26
C25
C9
N4
C8
N3
C24
U
N2
C23
C16
C20
N1
C15
C11
C12
C21
C22
C14
C17
C19
C13
C18

XBL 811-7794

References

1. Eigenbrot,C.W.,Jr.; Raymond,K.N.; Inorg.Chem. (1981), in press.

2. Fieselman,B.F.; Stucky,G.D.; Inorg.Chem. (1978), 17, 2074.

3. Manriquez,J.M.; Fagan.P.J.; Marks,T.J.; J.Amer.Chem.Soc. (1978), 100, 3939.

4. Manriquez,J.M.; Fagan,P.J.; Marks,T.J.; Vollmer,S.H.; Day,C.S.; Day,V.W.; J.Amer.Chem.Soc. (1979), 101, 5075.

5. Selwood,P.W.; "Magnetochemistry", 2nd Ed., Interscience, New York, (1956).

6. Breakwell,K.R.; Patmore,D.J.; Storr,A; J.Chem.Soc.Dalt.Trans. (1975), 749.

7. Hermann,J.A.; Suttle,J.F.; Inorg.Syn. (1957), 5, 143.

8. Molybdenum K_α radiation was used throughout. The intensity of three standard reflections was measured every 7200 seconds of X-ray exposure, and the position of three orientation standards was checked every 250 reflections.

9. Roof,R.B.; "A Theoretical Extension of the Reduced-Cell Concept in Crystallography", Publication LA-4038, Los

Alamos Scientific Laboratory, Los Alamos, New Mexico, 1969.

10. All calculations were performed on a PDP 11/60 equipped with 128 kilowords of memory, twin RK07 28 MByte disk drives, Versatec printer/plotter, and a TU10 tape drive using locally-modified Nonius-SDP[11] software operating under RSX-11M.

11. Structure Determination Package User's Guide, April 1980, from Molecular Structure Corporation, College Station, Texas, 77840.

12. The data reduction formulae are;

$$Fo^2 = \frac{\omega(C-2B)}{Lp}$$

$$Fo = (Fo^2)^{\frac{1}{2}}$$

$$\sigma o(Fo^2) = \frac{\omega(C + 4B)^{\frac{1}{2}}}{Lp}$$

$$\sigma o(Fo) = \frac{\sigma o(Fo^2)}{2Fo}$$

where C is the total count in the scan, B is the sum of the 2 background counts, ω is the scan speed in degrees per minute, and

$\frac{1}{Lp} = \frac{\sin 2\theta(1+\cos^2 2\theta_m)}{1+\cos^2 2\theta_m - \sin^2 2\theta}$ is the correction for Lorentz and polarization effects for a reflection with scattering angle 2θ and radiation monocromatized with a 50% perfect single-crystal monochromator with scattering angle $2\theta_m$.

13. $R = \frac{\Sigma||Fo| - |Fc||}{\Sigma|Fo|}$

$$wR = \left|\frac{\Sigma w(|Fo| - |Fc|)^2}{\Sigma wFo^2}\right|^{\frac{1}{2}}$$

$$GOF = \left|\frac{\Sigma w(|Fo| - |Fc|)^2}{(n_o - n_v)}\right|^{\frac{1}{2}}$$

where n_o is the number of observations and n_v is the number of variable parameters, and the weights w were given by $w = \frac{4Fo^2}{\sigma^2(Fo^2)}$, and $\sigma^2(Fo^2) = |\sigma o^2(Fo^2) + (pF^2)^2|$ where p is the factor used to lower the weight of intense reflections.

14. Atomic scattering factors are from Cromer,D.T.; Waber,J.T.; "International Tables for X-ray Crystallography," Vol. IV, The Kynoch Press, Birmingham, England, 1974, Table 2.2B, and Cromer,D.T; ibid., Table 2.3.1.

15. Instrumentation at the University of California Chemistry Department X-ray Crystallography Facility (CHEXRAY) consists of two Enraf-Nonius CAD-4 diffractometers, one controlled by a DEC PDP 8/a with an RK05 disk and the other by a DEC PDP 8/e with an RL01 disk. Both use Enraf-Nonius software as described in the CAD-4 Operation Manual, Enraf-Nonius, Delft, November 1977, updated January 1980.

16. Johnson,C.K.; Report ORNL-3794, Oak Ridge National Laboratory, Oak Ridge, Tenn., 1965.

17. Marks,T.J.; Manriquez,J.M.; Fagan,P.J.; Day,V.W.; Day,C.S.; Vollmer,S.H.; "Lanthanide and Actinide Chemistry and Spectroscopy," N.Edelstein, Ed., ACS Symposium Series 131, American Chemical Society, Washington,D.C.,pp 1,29.

18. Broach,R.W.; Schultz,A.J.; Williams,J.M.; Brown,G.M.; Manriquez,J.M.; Fagan,P.J.; Marks,T.J.; Science (1979), 203, 172.

19. Manriquez,J.M.; Fagan,P.J.; Marks,T.J.; Day,C.S.; Day,V.W.; J.Amer.Chem.Soc. (1978), 100, 7112.

20. Bruce,M.I.; J.Organomet.Chem (1978), 151, 313.

21. Bruce,M.I.; J.Organomet.Chem (1979), 167, 361.

22. Baker,E.C.; Halstead,G.W.; Raymond,K.N.; Stuct.Bonding(Berlin) (1976), 25, 23.

23. Leong,J.; Hodgson,K.O.; Raymond,K.N.; Inorg.Chem. (1973), 12, 1329.

24. Fronczek,F.R.; Halstead,G.W.; Raymond,K.N.; J.Amer.Chem.Soc. (1977), 99, 1769.

25. Burns,J.H.; Laubereau,P.J.; Inorg.Chem. (1971), 10, 2789.

26. Ernst,R.D.; Kennelly,W.J.; Day,C.S.; Day,V.W.; Marks,T.J.; J.Amer.Chem.Soc. (1979), 101, 2656.

Chapter 4

Crystal and Molecular Structure of $[Nd(tren)_2(CH_3CN)](ClO_4)_3$

Introduction

Lanthanide coordination chemistry is dominated by oxygen donor ligands, especially by chelate ligands like β-diketonates or EDTA. The number of well-characterized nitrogen-bonded complexes has been increasing recently, however. As with the oxygen donating ligands, amine complexes are generally more stable when they involve chelate ligands. For example, pyridine complexes exist only in solution, while complexes with ethylenediamine or 1,10-phenanthroline can be isolated[1]. As another example, Forsberg and coworkers have recently added compounds of the type $Ln(tren)X_3$ and $Ln(tren)_2X_3$ to the list of lanthanide amine complexes[2,3].

The other general characteristic of lanthanide coordination complexes is their kinetic lability, which results from the negligible contribution the crystal field stabilization energy makes to the free energy of activation. The work reported here expands the present knowledge of lanthanide amine complexes, while at the same time laying the groundwork for the isolation of substitutionally inert lanthanide complexes.

In addition to an interest in lanthanides and actinides

based on the chemical effects of their unique position in the Periodic Table, there has been a continuing interest in the use of lanthanide ions as shift reagents in nmr spectroscopy. During the last decade[4], lanthanide shift reagents have been actively investigated and utilized in simplifying complex nmr spectra. The effective use of these reagents, and subsequent assignments in the expanded spectrum, requires consideration of the shift reagent properties.

In general, lanthanide shift reagents operate through a predominantly dipole-dipole interaction between the paramagnetic lanthanide ion and certain nuclei on the substrate. The magnitude of the interaction, and hence of the induced shift, is a sensitive function of geometry. It is understood that intermittent coordination of a functional group on the substrate molecule (O or N donors) to an unsaturated coordination sphere around the lanthanide ion produces new perturbations on the magnetic environment at substrate nuclei, leading to altered chemical shifts. The sensitive radial and geometric functions of these lanthanide-induced shifts are responsible for simplifying the substrate spectrum. The most elegant applications require several assumptions to be made[5]. Typically they include;

1. the observed shifts are totally dipolar
2. only one lanthanide-substrate complex is in equilibrium
3. only one geometric isomer of the complex exists
4. the magnetic field of the complex is axially symmetric
5. the principal magnetic axis has only one, known orientation with respect to the ligands
6. there is one conformation per substrate or at least a time-averaged conformation.

As one might guess, the necessity of making some rather rough assumptions has hampered the development and popularity of lanthanide shift reagents. For this reason we have endeavored to design and synthesize lanthanide shift reagents that circumvent the geometry problem. We reasoned that a substitutionally inert lanthanide complex, once such a novelty were isolated, would prevent actual coordination of functional groups but still impart to the substrate an altered magnetic field. This research was undertaken to determine what, if any, advantages might result from this new type of shift reagent.

This chapter reports the crystal structure of a Nd^{3+} compound that will serve as the starting material for the

synthetic work. We analyzed a known N-bonded complex $[Nd(tren)_2(CH_3CN)](ClO_4)_3$ to determine the appropriate number of methylene units to use in linking the tren ligands, thereby encapsulating the metal ion.

Experimental

Manipulation of moisture-sensitive materials was accomplished with Schlenk techniques and the use of a Vacuum Atmospheres HE-93-A glove box with recirculating moisture free argon atmosphere. Elemental analyses were performed by the Microanalytical Laboratory, U.C.Berkeley. Infra-red spectra were obtained on a Perkin-Elmer 597 spectrophotometer (Nujol mulls, reported in wavenumbers).

Materials

Acetonitrile, CH_3CN, was distilled from P_2O_5, benzene from potassium benzophenone ketyl. The tren ($N(EtNH_2)_3$) was extracted from triethylenetetraamine[2]. Crystalline 16-cyclam was a generous gift from William Smith[6].

Neodymium perchlorate, $Nd(ClO_4)_3$, was prepared by addition of excess Nd_2O_3 to 70% $HClO_4$[7]. The excess Nd_2O_3 was filtered off and the solution evaporated to dryness. Residual H_2O was removed by heating to ~250°C under vacuum for three days. Some reversion to the oxide was evidenced by the presence of blue amongst the pink perchlorate. This contaminant was conveniently left behind during an extraction into acetonitrile. Evaporation of the solution left a compound of

formula $Nd(ClO_4)_3(CH_3CN)_4$.

Analysis: calculated-- %C, 15.83; %H, 1.98; %N, 9.27; %Nd, 23.78 : found-- %C, 16.23; %H, 2.26; %N, 9.23; %Nd, 24.88 .

$Nd(tren)_2(ClO_4)_3$ was prepared after Forsberg[3]. Crystals suitable for diffraction were obtained by the addition of benzene to a concentrated acetonitrile solution. After standing at room temperature for 2 days, the clear pink solution yielded several large, well-formed crystals. Infra-red spectroscopy revealed the presence of acetonitrile ($\nu_{CN} = 2262 cm^{-1}$).

Data Collection, Solution, and Refinement[8]

The absences identified with the precession camera (hkl, h+k =2n ; h0l, l =2n) indicated the space group was either Cc or C2/c. The cell parameters were determined using 25 automatically centered reflections with 2θ between 27 and 43 degrees. They are;

$$a = 15.0442(11)\ \text{Å}$$

$$b = 17.7290(14)\ \text{Å}$$

$$c = 11.0880(6)\ \text{Å}$$

$$\beta = 95.079(5)^{\circ}$$

These data, in conjunction with the measured density ($1.751 \frac{g}{cm^3}$), yield Z= 4 ($d_{calc} = 1.750 \frac{g}{cm^3}$).

The initial Patterson map confirmed space group Cc. The structure was then solved using heavy atom techniques. The model refined to weighted and unweighted R factors of 3.19 and 2.94% respectively[10]. (The initial polarity refined to 3.58 and 3.24%). Final positional and thermal parameters appear in Table I. Pertinent bond distances and angles appear in Table II.

Discussion

The crystal structure consists of discrete mononuclear cations at general positions in the unit cell (Fig. 1), and immersed in a three dimensional network of hydrogen bonds. The structure of the molecular cation (Fig. 2) consists of Nd coordinated by 8 tren nitrogens and an acetonitrile nitrogen, to form a tri-capped trigonal prismatic coordination geometry. The inclusion of two tetradentate tren ligands in the coordination sphere of one neodymium ion is a reflection of the lanthanide's relatively large size. Table IIb reveals that, as in other tren structures (vide infra), the intraligand bond angles indicate the ligand molecules are essentially unstrained. The capping nitrogens are the two tertiary tren nitrogens and that of the acetonitrile. Data on the various planes and their interrelationship can be found in Table III. These data confirm the tri-capped trigonal prismatic coordination geometry (Fig.2) and suggest a two-fold axis along the acetonitrile (Fig. 3). A two-fold axis was then defined as the vector from Nd to a point 'X'

whose coordinates were obtained by the summation of all pseudo-two-fold related atoms (C's and N's). Rotation by 180° about this axis and calculation of the difference between the new atom positions and the old ones yields the results tabulated in Table IV. Here we see that the average difference is 0.21 Å with a standard deviation of 0.16 Å, and that the major aberrations from the two-fold symmetry are the carbon atoms of the acetonitrile. The remaining atoms have an average difference of 0.16 Å with a standard deviation of 0.06 Å. When considering only the nitrogen atoms that constitute the coordination sphere, the average difference is 0.11 Å with a standard deviation of 0.03 Å.

Figure 4 illustrates the hydrogen bonding around a cation, between perchlorate oxygens and some of the primary amine nitrogen atoms. The lengths of these bonds are tabulated in Table V. Among the other metal tren stuctures published is another example of a perchlorate salt, $[Co(tren)(glycinato)]Cl(ClO_4)$, where a more extensive hydrogen bonding network was found[12]. The network in this compound involves the perchlorate oxygens, the chloride ion, and glycinato oxygen atoms. Of the remaining tren structures that have been reported, the majority are tetraphenyl borate salts reported by Hendrickson and coworkers. The compounds $[Ni_2(tren)_2(OCN)_2](B\phi_4)_2$[13] and $[Cu_2(tren)_2X_2](B\phi_4)_2$[14-16] have been characterized. The tren ligands in all the above compounds are tetradentate. In the Cu^{2+} systems, the ligand forms part of a trigonal bipyramidal coordination

environment, with the primary nitrogens in equatorial sites. In the Ni^{2+} and Co^{3+} structures, the tren contributes to an octahedral environment.

Although the past 10 years have seen a notable increase in the number of lanthanide amine complexes, very few of these involve nitrogen coordination exclusively. In addition to the $Ln(tren)_2X_3$ complexes analogous to that described here (vide supra), lanthanide tris-terpyridine complexes have been reported[1]. The structure of one of these, $[Eu(terpy)_3](ClO_4)_3$[17], is the only other lanthanide structure in which all coordination sites are occupied by nitrogen atoms. The M-N bond distances in lanthanide amine complexes are in general agreement with those predicted from the metal ionic radii, a reflection of the predominantly ionic bonding lanthanide complexes exhibit. While there are no strict analogues with which to compare such distances in the present compound, one may note that the M-N distances in $[Eu(terpy)_3](ClO_4)_3$ are about 0.05 Å shorter than those found in the present compound. This difference is about what one would expect for the difference between an sp^3 and an sp^2 hybridized nitrogen atom. In this light, we mention that the metal ionic radii in these compounds differ by about 0.04Å[18].

This crystal structure was carried out in part to determine the appropriate number of carbon atoms needed to bridge across the tren ligands in order to encapsulate the

metal ion. The proposed encapsulation would bridge N's 3 and 7, 6 and 4, and 2 and 8; Table VI reveals these are the closest ones. In the structure of 16-cyclam[6], non-bonded nitrogens are separated by 2.9 Å and bridged by propyl chains. Because such linkages are somewhat flexible, and because the present configuration is subject to adjustment, it appears a C_3 linkage would be appropriate in the encapsulating reaction.

Table Ia. Positional and Thermal Parameters ($\times 10^4$) for $[Nd(tren)_2(CH_3CN)](ClO_4)_3$

	x	y	z	β_{11}	β_{22}	β_{33}	β_{12}	β_{13}	β_{23}
ND	-.250000	-.235763(17)	0.	31.49(13)	22.12(8)	60.9(2)	-3.1(3)	11.22(12)	-.6(4)
CL(1)	-.16340(17)	-.36018(14)	-.5761(2)	66.7(14)	42.5(9)	98.(2)	-9.7(9)	-4.2(13)	16.7(11)
CL(2)	-.05706(16)	-.07716(15)	-.3868(3)	50.7(12)	49.4(10)	147.(3)	8.2(8)	27.7(15)	27.8(14)
CL(3)	-.38879(16)	-.15158(13)	-.4311(2)	57.3(12)	39.5(9)	98.(2)	-6.2(8)	-.5(13)	8.8(10)
N(1)	-.2653(4)	-.3781(3)	-.0893(6)	45.(3)	25.(2)	84.(6)	-2.(2)	9.(3)	-8.(3)
N(2)	-.4074(5)	-.2625(4)	-.1225(6)	43.(3)	40.(3)	97.(6)	2.(2)	1.(4)	4.(4)
N(3)	-.2009(5)	-.2504(4)	-.2184(6)	51.(4)	43.(3)	81.(6)	-6.(2)	20.(4)	-3.(3)
N(4)	-.1339(5)	-.3341(4)	.0931(6)	54.(4)	36.(3)	84.(6)	7.(2)	10.(4)	4.(3)
N(5)	-.3521(4)	-.1357(3)	.1090(5)	53.(4)	25.(2)	80.(6)	2.(2)	23.(4)	2.(3)
N(6)	-.1767(5)	-.1829(5)	.2069(7)	67.(5)	42.(3)	109.(8)	-7.(3)	-6.(5)	-15.(4)
N(7)	-.2668(5)	-.1045(4)	-.1092(6)	61.(4)	34.(3)	77.(6)	-2.(2)	18.(4)	7.(3)
N(8)	-.3470(5)	-.2967(4)	.1601(6)	47.(4)	32.(3)	83.(6)	-6.(3)	18.(4)	6.(3)
N(9)	-.0869(5)	-.1767(4)	-.0183(7)	44.(4)	35.(3)	109.(7)	-12.(2)	13.(4)	5.(3)
O(1)	-.1006(6)	-.3106(5)	-.6216(8)	119.(7)	68.(4)	171.(10)	-40.(4)	5.(6)	29.(5)
O(2)	-.2261(8)	-.3140(10)	-.5198(17)	92.(9)	191.(12)	435.(29)	29.(6)	-8.(13)	-159.(17)
O(3)	-.2144(7)	-.3573(5)	-.6718(7)	118.(6)	69.(4)	129.(8)	-26.(4)	-20.(6)	15.(4)
C(4)	-.1247(7)	-.4066(5)	-.4888(8)	149.(5)	58.(4)	164.(10)	-19.(5)	-51.(8)	29.(5)
O(5)	-.0450(8)	-.1462(8)	-.4427(13)	87.(7)	68.(5)	384.(25)	0.(5)	32.(10)	-75.(10)
O(6)	-.1082(6)	-.0882(6)	-.2891(7)	92.(6)	101.(5)	151.(9)	-25.(4)	63.(6)	13.(5)
O(7)	-.1003(6)	-.0294(6)	-.4732(8)	89.(6)	83.(5)	191.(11)	10.(4)	-16.(6)	55.(6)
C(8)	.0299(5)	-.0471(5)	-.3472(8)	68.(4)	67.(4)	173.(9)	-13.(3)	11.(5)	21.(5)
C(9)	-.4388(8)	-.1258(10)	-.5321(8)	94.(7)	174.(12)	74.(7)	30.(7)	15.(5)	24.(7)
O(10)	-.4169(9)	-.1141(9)	-.3288(8)	150.(12)	154.(9)	125.(10)	65.(8)	-35.(9)	-47.(8)
O(11)	-.4016(12)	-.2248(6)	-.4150(13)	272.(18)	53.(5)	309.(21)	-46.(7)	-43.(15)	47.(8)
O(12)	-.3019(7)	-.1364(10)	-.4381(16)	61.(6)	161.(10)	483.(29)	-14.(6)	0.(11)	127.(14)

Table 1a. continued

C(1)	-.2151(6)	-.3863(5)	-.1983(8)	64.(5)	38.(3)	92.(8)	2.(3)	22.(5)	-11.(4)
C(2)	-.1531(6)	-.3235(6)	-.2122(9)	52.(5)	50.(5)	97.(9)	3.(4)	33.(5)	-9.(5)
C(3)	-.3655(7)	-.3960(6)	-.1191(9)	55.(5)	33.(4)	108.(9)	-10.(3)	2.(6)	-4.(5)
C(4)	-.4132(6)	-.3352(6)	-.1904(8)	51.(5)	44.(4)	113.(9)	-14.(3)	-11.(5)	-12.(5)
C(5)	-.2343(8)	-.4307(4)	.0066(14)	54.(7)	25.(2)	119.(8)	9.(3)	9.(6)	-2.(6)
C(6)	-.1427(7)	-.4139(6)	.0534(10)	68.(6)	32.(3)	127.(11)	8.(3)	-2.(7)	2.(5)
C(7)	-.3000(7)	-.0938(5)	.2073(8)	85.(7)	30.(3)	96.(8)	-4.(3)	26.(6)	-14.(4)
C(8)	-.2025(10)	-.1043(7)	.2124(12)	114.(10)	51.(6)	161.(15)	-27.(6)	-1.(9)	-16.(7)
C(9)	-.3890(6)	-.0829(5)	.0147(8)	57.(5)	34.(3)	106.(8)	13.(3)	26.(5)	9.(4)
C(10)	-.3206(7)	-.0465(5)	-.0537(9)	51.(7)	26.(3)	111.(9)	3.(3)	27.(6)	10.(4)
C(11)	-.4256(6)	-.1766(5)	.1614(8)	45.(4)	37.(3)	113.(8)	8.(3)	39.(5)	7.(4)
C(12)	-.3550(7)	-.2431(5)	.2334(8)	67.(5)	39.(3)	98.(8)	0.(3)	46.(5)	9.(4)
C(13)	-.0226(6)	-.1446(5)	-.0283(7)	49.(4)	31.(3)	93.(8)	-2.(3)	11.(5)	0.(3)
C(14)	.0592(7)	-.1033(6)	-.0405(10)	93.(5)	47.(4)	132.(11)	-14.(4)	19.(6)	-7.(5)

Table Ib. Calculated Hydrogen Atom Positions[a] for $[Nd(tren)_2(CH_3CN)](ClO_4)_3$

	x	y	z
H(1A)	-.18764	-.43271	-.19302
H(1B)	-.26082	-.38673	-.26808
H(2A)	-.12453	-.33067	-.28414
H(2B)	-.10585	-.32322	-.14437
H(3A)	-.36991	-.44139	-.16444
H(3B)	-.39258	-.40258	-.04553
H(4A)	-.47405	-.34907	-.20644
H(4B)	-.38697	-.32913	-.26465
H(5A)	-.27123	-.42764	.07190
H(5B)	-.23648	-.48039	-.02523
H(6A)	-.10406	-.42249	-.00507
H(6B)	-.12572	-.44603	.11988
H(7A)	-.31226	-.04152	.19618
H(7B)	-.31543	-.10983	.26227
H(8A)	-.17636	-.08342	.28591
H(8B)	-.18079	-.07860	.14579
H(9A)	-.42098	-.04450	.05243
H(9B)	-.42897	-.10993	-.04082
H(10A)	-.26247	-.01641	-.00033
H(10B)	-.34882	-.01550	-.11570
H(11A)	-.45424	-.14289	.21231
H(11B)	-.46725	-.19275	.09709
H(12A)	-.44527	-.26793	.26153
H(12B)	-.35608	-.22720	.30063
H(13A)	-.44792	-.26290	-.07102
H(13B)	-.41836	-.22602	-.17401
H(14A)	-.24704	-.25210	-.27184
H(14B)	-.16592	-.21351	-.23618
H(15A)	-.08156	-.31863	.07690
H(15B)	-.13723	-.33375	.17109
H(16A)	-.19633	-.20769	.26701
H(16B)	-.11905	-.18683	.20995
H(17A)	-.21347	-.08624	-.11276
H(17B)	-.29123	-.11255	-.18214
H(18A)	-.38656	-.32568	.12132
H(18B)	-.31194	-.32363	.20926

[a] isotropic thermal parameters equal 7.0 $e^-/Å^2$.

Table IIa. Pertinent Bond Distances (Å) for $[Nd(tren)_2(CH_3CN)](ClO_4)_3$

Nd-N(1)	2.717(6)	Nd-N(6)	2.629(7)
Nd-N(2)	2.666(7)	Nd-N(7)	2.625(7)
Nd-N(3)	2.607(6)	Nd-N(8)	2.628(7)
Nd-N(4)	2.615(7)	Nd-N(9)	2.692(7)
Nd-N(5)	2.701(6)	Nd-N(ave)	2.65(4)
N(1)-C(1)	1.49(1)	N(5)-C(7)	1.49(1)
C(1)-C(2)	1.51(1)	C(7)-C(8)	1.47(2)
C(2)-N(3)	1.48(1)	C(8)-N(6)	1.45(1)
N(1)-C(3)	1.49(1)	N(5)-C(9)	1.47(1)
C(3)-C(4)	1.48(1)	C(9)-C(10)	1.48(1)
C(4)-N(2)	1.49(1)	C(10)-N(7)	1.48(1)
N(1)-C(5)	1.48(1)	N(5)-C(11)	1.48(1)
C(5)-C(6)	1.46(2)	C(11)-C(12)	1.48(1)
C(6)-N(4)	1.48(1)	C(12)-N(8)	1.48(1)
N(9)-C(13)	1.14(1)	C(13)-C(14)	1.45(1)
Cl(1)-O(1)	1.416(8)	Cl(2)-O(5)	1.391(11)
Cl(1)-O(2)	1.432(12)	Cl(2)-O(6)	1.396(7)
Cl(1)-O(3)	1.416(8)	Cl(2)-O(7)	1.396(8)
Cl(1)-O(4)	1.361(8)	Cl(2)-O(8)	1.444(8)
Cl(3)-O(9)	1.371(10)	Cl(3)-O(10)	1.412(10)
Cl(3)-O(11)	1.327(10)	Cl(3)-O(12)	1.344(10)

Table IIb. Ligand Bond Angles for $[Nd(tren)_2(CH_3CN)](ClO_4)_3$ ($\pm.2^o$)

C(1)-N(1)-C(3)	110.6	C(7)-N(5)-C(9)	110.1
C(3)-N(1)-C(5)	107.6	C(9)-N(5)-C(11)	109.9
C(5)-N(1)-C(1)	110.4	C(7)-N(5)-C(11)	108.7
N(1)-C(1)-C(2)	113.4	N(5)-C(7)-C(8)	115.1
C(1)-C(2)-N(3)	109.2	C(7)-C(8)-N(6)	112.9
N(1)-C(3)-C(4)	112.2	N(5)-C(9)-C(10)	113.9
C(3)-C(4)-N(2)	110.8	C(9)-C(10)-N(7)	110.0
N(1)-C(5)-C(6)	113.1	N(5)-C(11)-C(12)	113.3
C(5)-C(6)-N(4)	110.9	C(11)-C(12)-N(8)	111.1

Table III. Relationships Between Planes for $[Nd(tren)_2(CH_3CN)](ClO_4)_3$

plane no.	N's	ave. dev.(Å)	d-Nd (Å)	d-cap (Å)	angle with planes 1,2,3,4
1	2,3,7	--	1.83	--	--
2	4,6,8	--	1.80	--	12.58
3	2,3,4,8	.18	.95	1.75	84.79 91.91
4	3,4,6,7	.09	.90	1.79	84.27 96.75 62.68
5	2,7,6,8	.16	.96	1.72	89.63 93.86 54.44 62.88

Table IV. Results of a Two-Fold Rotation for $[Nd(tren)_2(CH_3CN)](ClO_4)_3$

related atom pairs	difference (Å)
Nd , Nd	.000
N(1) , N(5)	.156
N(2) , N(8)	.113
N(3) , N(6)	.105
N(4) , N(7)	.129
N(9) , N(9)	.064
average	.11
std. dev.	.03
X , X	.000
C(1) , C(7)	.152
C(2) , C(8)	.242
C(3) , C(11)	.173
C(4) , C(12)	.122
C(5) , C(9)	.242
C(6) , C(10)	.265
average	.16
std. dev.	.06
C(13) , C(13)	.304
C(14) , C(14)	.687
average	.21
std. dev.	.16

Table V. Hydrogen Bond Lengths for $[Nd(tren)_2(CH_3CN)](ClO_4)_3$ (Å)

N(2)-O(1)	3.18(1)	N(7)-O(6)	3.25(1)
N(4)-O(1)	3.19(1)	N(7)-O(10)	3.17(1)
N(4)-O(3)	3.17(1)	N(8)-O(3)	3.16(1)
N(6)-O(1)	3.11(1)	N(8)-O(5)	3.25(1)

Table VI. Interatomic Distances (Å) for $[Nd(tren)_2(CH_3CN)](ClO_4)_3$

nitrogens	distance
3,7	3.06
6,4	3.06
2,8	3.24
7,2	3.51
6,8	3.27
2,3	3.38
4,8	3.42
3,4	3.81
6,7	3.90

Figure 1. Stereoscopic drawing of the unit cell of $[Nd(tren)_2(CH_3CN)](ClO_4)_3$.

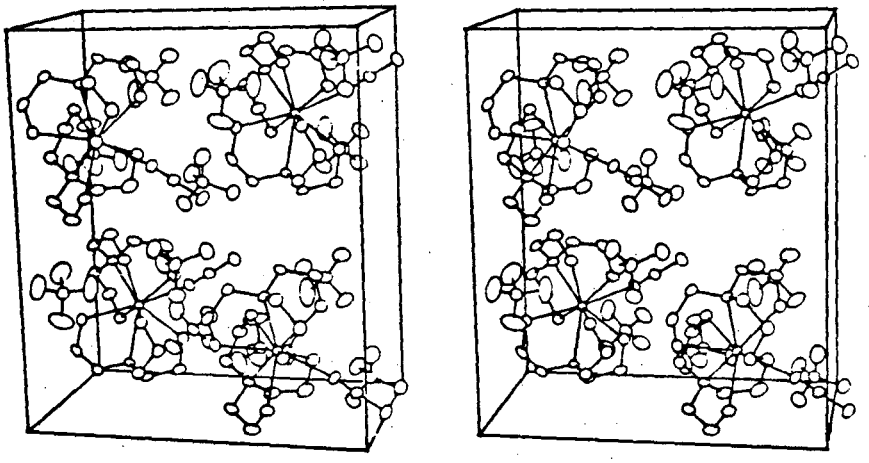

XBL 811-7790

Figure 2. ORTEP drawing of the molecular cation of $[Nd(tren)_2(CH_3CN)](ClO_4)_3$ emphasizing the pseudo-threefold symmetry. The nitrogen atoms are drawn at the 50% contour. For clarity, the carbon atoms are drawn at the 10% contour.

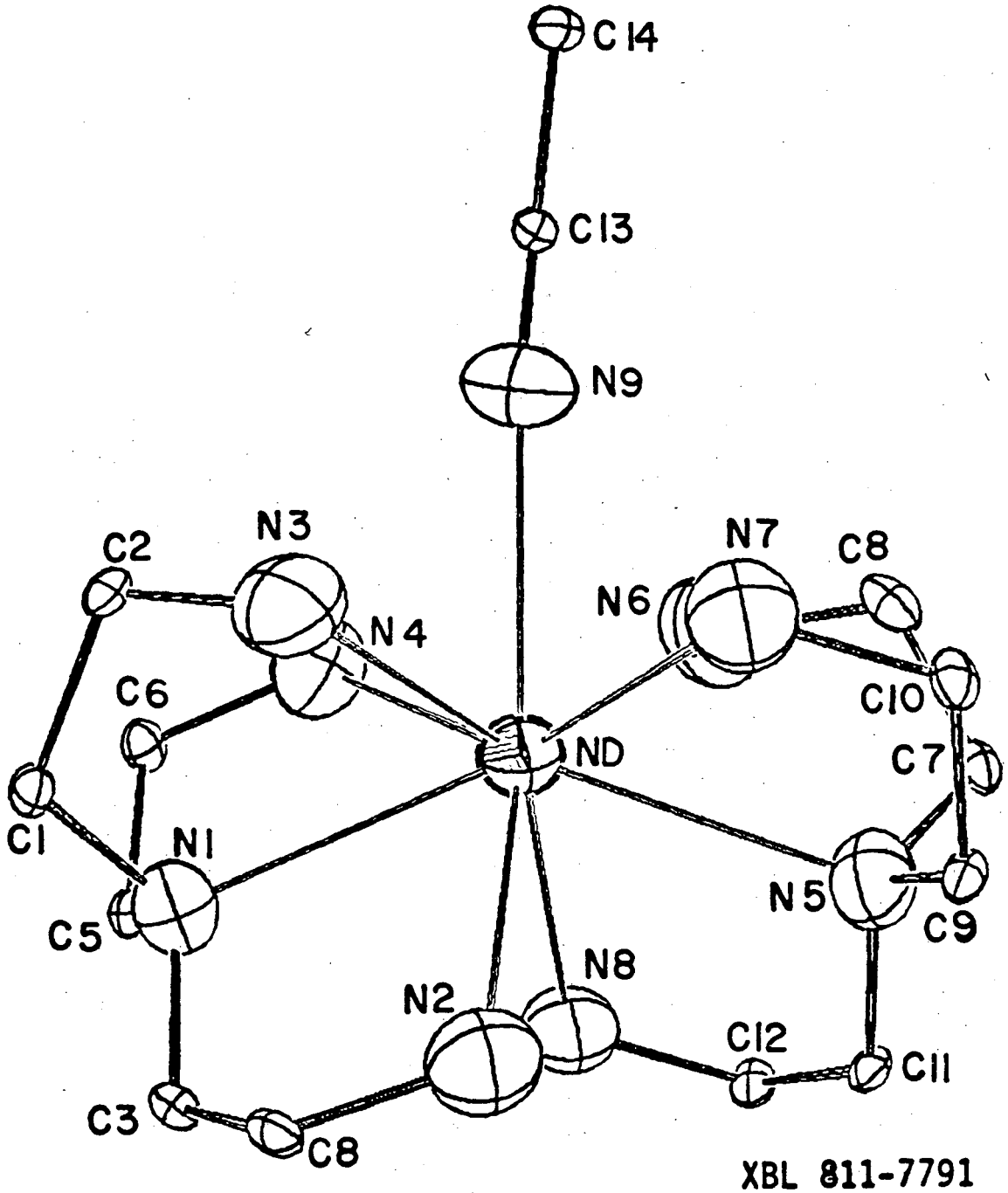
C14
C13
N9
N3
C2
N7
C8
N6
N4
C6
C10
ND
C7
C1
N1
N5
C5
C9
N8
N2
C12
C11
C3
C8

XBL 811-7791

Figure 3. ORTEP drawing of the molecular cation of $[Nd(tren)_2(CH_3CN)](ClO_4)_3$ emphasizing the pseudo-twofold symmetry. The nitrogen atoms are drawn at the 50% contour. For clarity, the carbon atoms are drawn at the 10% contour.

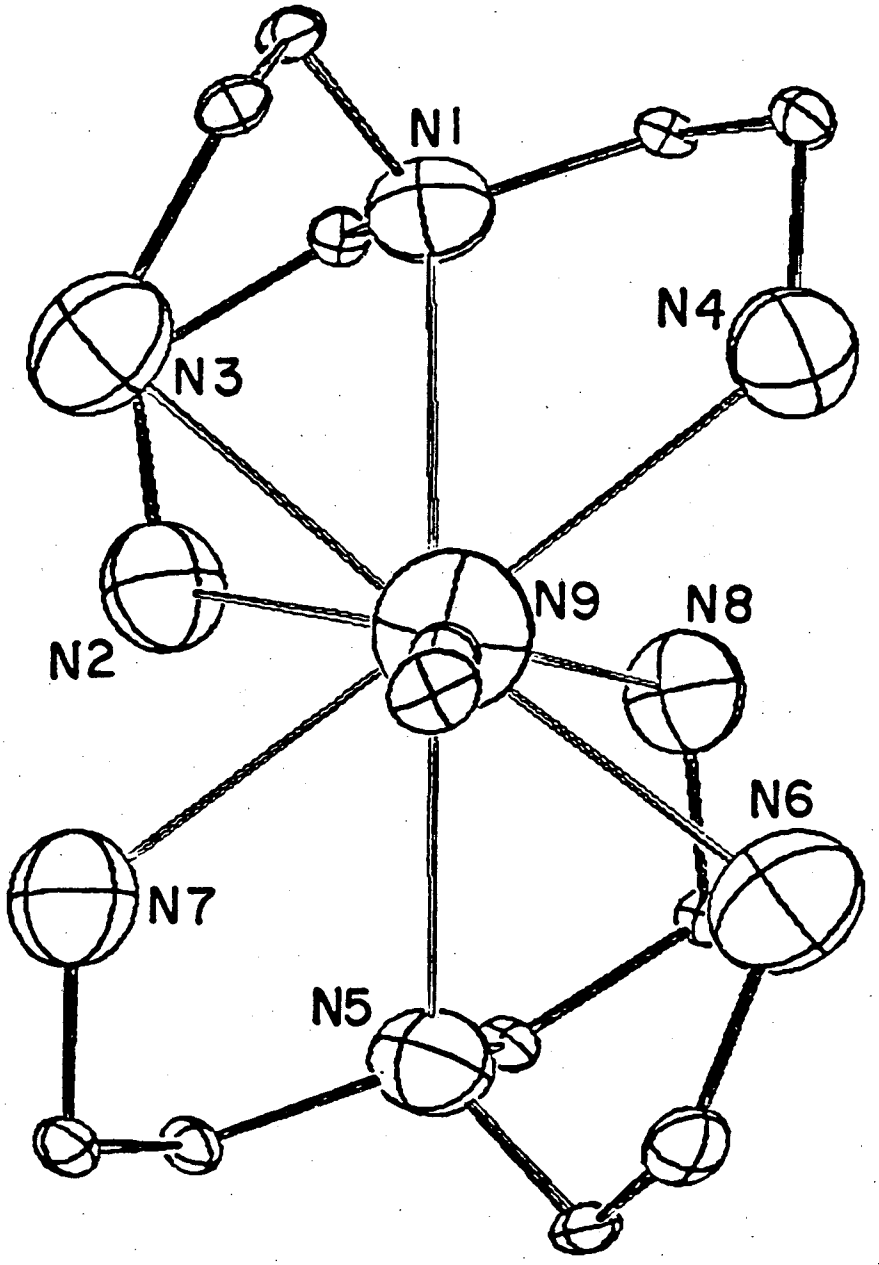

XBL 811-7792

Figure 4. ORTEP drawing of the hydrogen-bonding experienced by one molecular cation of $[Nd(tren)_2(CH_3CN)](ClO_4)_3$.

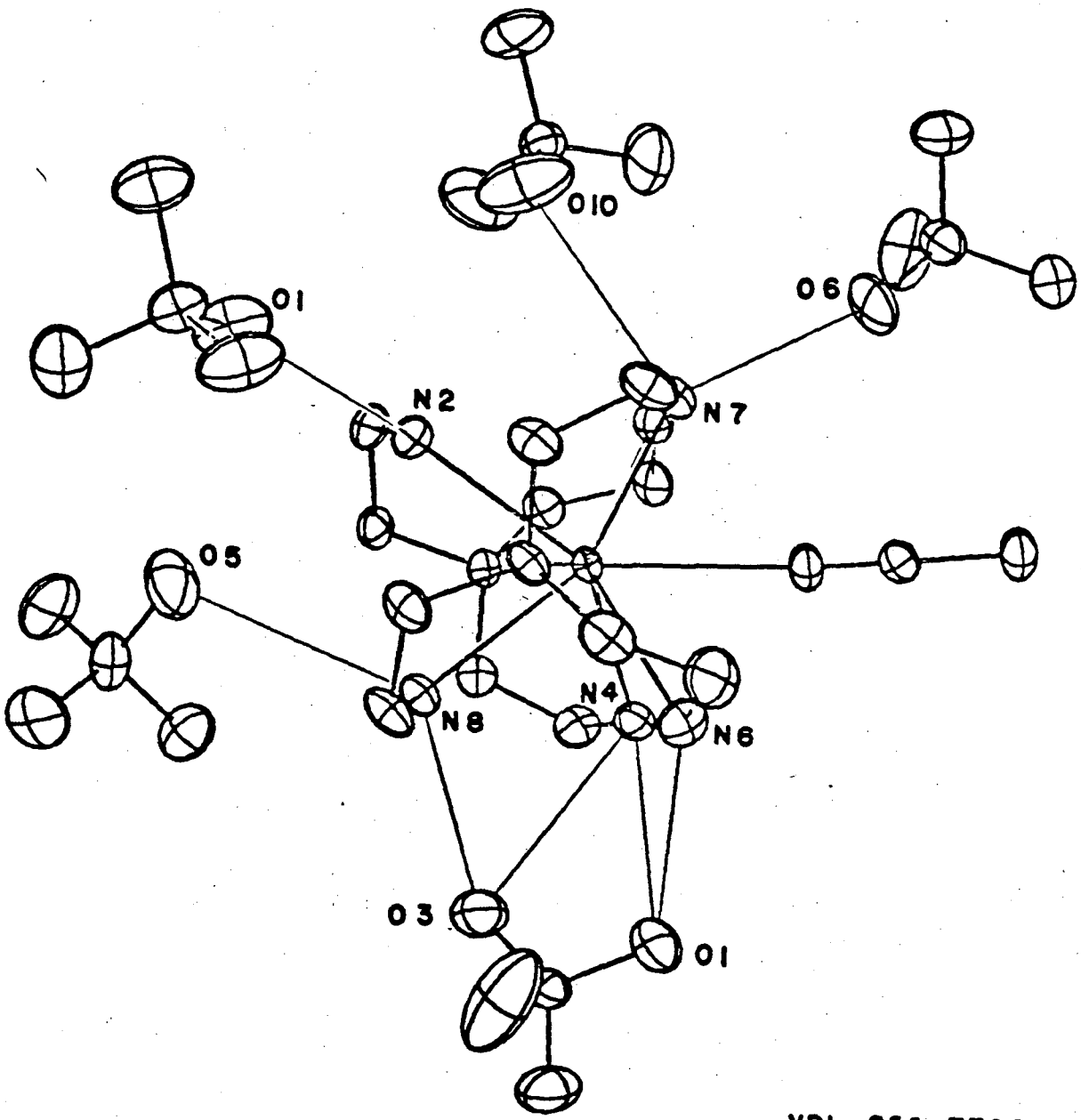

XBL 811-7796

References

1. Cotton,F.A.; Wilkinson,G.W.; "Advanced Inorganic Chemistry", 3rd ed., Interscience, New York, (1972), p 1069.

2. Forsberg,J.H.; Kubik,T.M.; Moeller,T.; Gucwa,K.; Inorg.Chem (1971), 10, 2656.

3. Johnson,M.F.; Forsberg,J.H.; Inorg.Chem (1976), 15, 734.

4. Wenzel,T.J.; Bettes,T.C.; Sadlowski,J.E.; Sievers,R.E.; J.Amer.Chem.Soc. (1980), 102, 5903., and references therein.

5. Horrocks,W.D.,Jr.; Sipe,J.R.; Science (1972), 177, 994.

6. Smith,W.L.; Ekstrand,J.D.; Raymond,K.N.; J.Amer.Chem.Soc. (1978), 100, 3539.

7. Forsberg,J.H.; Moeller,T.; Inorg.Chem (1969), 8, 883.

8. A total of 3819 hk±l data were collected between 4° and 56° in 2θ, monitoring three intensity standards every 7200 seconds of X-ray exposure, and checking three orientation standards every 250 reflections. Azimuthal scans were collected on 4 reflections with 2θ between 11 and 33 degrees. Data reduction and processing were carried out as described elsewhere[9]. The intensity

standards underwent decay of 14%, 14%, and 17% during data collection. A decay correction of 14% was applied. The six crystal faces were identified with the help of the diffractometer and their dimensions measured at 7X under a binocular microscope. The absorption correction (μ = 21.09 cm^{-1}) applied ranged between 1.212 and 1.498. The data were then averaged (R = 2.6%) to yield the 3553 independent reflections used in refinement.

9. Sofen,S.R.; Abu-Dari,K.; Freyberg,D.P.; Raymond,K.N.; J.Amer.Chem.Soc. (1978), 100, 7882.

10. After a difference Fourier revealed most of the hydrogens, their positions were calculated with a C-H distance of .95Å and an N-H distance of .87Å[11]. The temperature factors of all atoms were refined anisotropically except for those of the hydrogens, where the isotropic B's were set at 7.0 $Å^2$ and not refined. On the final least-squares cycle, all parameters shifted by less than 0.06 sigma. In the final difference Fourier, the largest peak at a grid point was .55$\frac{e^-}{Å^3}$ and the most negative electron density was -.38$\frac{e^-}{Å^3}$. The residuals showed no abnormalities.

11. Churchill,M.R.; Inorg.Chem (1973), 12, 1213.

12. Mitsui,Y.; Watanabe,J.; Yoshinori,H.; Sakamaki,T.; Iitaka,Y.; J.Chem.Soc.Dalt.Trans. (1976), 2095.

13. Duggan,D.M.; Hendrickson,D.N.; Inorg.Chem (1974), 13, 2056.

14. Duggan,D.M.; Jungst,R.G.; Mann, K.R.; Stucky,G.D.; Hendrickson,D.N.; J.Amer.Chem.Soc. (1974) 96, 3443.

15. Duggan,D.M.; Hendrickson.D.N.; Inorg.Chem (1974), 8, 1911.

16. Laskowski,E.J.; Duggan,D.M.; Hendrickson,D.N.; Inorg.Chem (1975), 14, 2449.

17. Frost,G.H.; Hart,F.A.; Heath,C.; Hursthouse,M.B.; J.Chem.Soc.Chem.Comm. (1969), 1421.

18. Raymond,K.N.; Eigenbrot,C.W.,Jr.; Acc.Chem.Res. (1980), 13, 276.

This work was supported by the Director, Office of Energy Research, Office of Basic Energy Sciences, Chemical Sciences Division of the U.S. Department of Energy under Contract Number W-7405-ENG-48.

TECHNICAL INFORMATION DEPARTMENT
LAWRENCE BERKELEY LABORATORY
UNIVERSITY OF CALIFORNIA
BERKELEY, CALIFORNIA 94720